Lineage Tracing of *Sca1*-expressing cells in the Heart and Skeletal Muscle

Inaugural Dissertation
submitted to the
Faculty of Veterinary Medicine **or** Faculty of Medicine
in partial fulfillment of the requirements
for the PhD-Degree
of the Faculties of Veterinary Medicine and Medicine
of the Justus Liebig University Giessen

by
De Gaspari, Piera
of
Dolo, Italy

Giessen, 2014

From the: Institute of Max Planck Institute for Heart and Lung Research
Director / Chairman: Thomas Braun
Of the Faculty of Veterinary Medicine **or** Medicine of the Justus Liebig University Giessen

First Supervisor and Committee: Member: Prof. Dr. Dr.Thomas Braun
Second Supervisor and Committee: Member: Prof. Dr. Adriaan Dorresteijn
Committee Members: Prof. Dr. Dr. Thomas Braun, Prof. Dr. Adriaan Dorresteijn, Prof. Thomas Brand, Ph.D. (Imperial College London), Prof. Dr. Klaus-Dieter Schlüter

Date of Doctoral Defense: 20-06-2014

1 TABLE OF CONTENTS

1 TABLE OF CONTENTS 1

2 ZUSAMMENFASSUNG (Deutsch) 4

3 ABSTRACT (English) 5

4 INTRODUCTION 6
4.1 Stem cells 6
4.1.1 Embryonic stem cells and induced pluripotent stem cells 8
4.1.2 Fetal stem cells 10
4.1.3 Adult stem cells 10
4.1.3.1 Resident adult stem cells and the concept of niche 11
4.2 Heart 12
4.2.1 Cardiac stem cells 14
4.3 Skeletal muscle 15
4.3.1 Muscle stem cells 15
4.4 SCA1 as marker for stem cells 16
4.5 Lineage tracing 17
4.5.1 Genetic recombination 19
4.5.1.1 The switch component 19
4.5.1.1.1 Doxycycline inducible Cre system (Tet-Off and Tet-On) 21
4.5.1.1.2 CreERT tamoxifen inducible system 22
4.5.1.2 The reporter component 23

5 MATERIAL AND METHODS 25
5.1 Transgenic mice 25
5.1.1 Sca1- tTA//LC1-Cre//Z/AP and Sca1- tTA//LC1-Cre//R26RConfetti 25
5.1.2 Sca1-GFP 26
5.1.3 Pax7-Cre//Z/AP 26
5.1.4 Sca1-tTA//LC1-Cre//Z/AP//mdx 27
5.1.5 Sca1-tTA//LC1-Cre//Z/AP//Pax7$^{loxGu/loxPGu}$ 27
5.2 Cell culture 29
5.2.1 Murine adult cardiomyocytes 29
5.2.2 Cardiac stem cells (CSCs) 30
5.2.3 Muscle derived stem cells (MDSCs) 30
5.3 Differentiation of cells 31
5.3.1 In vivo assays 31
5.3.2 Injections of BMP molecules 31
5.3.3 Injection of glycerol 31
5.4 Pathological models 31
5.4.1 Myocardial infarction and transverse aortic constriction 31
5.4.2 Muscle regeneration (cardiotoxin injection) 31
5.5 Histology 32
5.5.1 Isolation of organs 32
5.5.2 Cryosections 32
5.6 Immunohistochemistry 32
5.6.1 Detection of alkaline phospathase activity 32
5.6.2 Trichrome staining 32
5.6.3 Oil red O (OrO) 33
5.6.4 Alizarin red 33

5.7 Immunofluorescence analyses 33
5.7.1 Antibody staining 33
5.7.2 Immunofluorescence staining and cells counting 34
5.7.3 Confocal microscopy and three-dimensional (3D) reconstructions 36
5.7.4 Fluorescent in situ hybridization (FISH) 36
5.8 Fluorescence-activated cells sorting (FACS) 36
5.8.1 FACS 36
5.8.2 Cell populations isolated by FACS 37
5.8.3 Cytospin 37
5.9 Molecular biology and single cell analyses 37
5.9.1 Microarray analyses 37
5.9.2 Single cell analysis 38

6 RESULTS 41
6.1 Identification and analyses of resident cell populations in the heart and their contribution to cardiac tissue renewal 41
6.1.1 Sca1 progenitors cells are detected in vivo during normal physiological conditions 41
6.1.2 Sca1 progenitor cells contribute to cardiomyocyte renewal under pathological conditions 43
6.1.3 The presence in vitro of mononucleated cardiomyocytes reinforces the contribution of progenitor cells to heart self-renewal 45
6.1.4 Identification of newly regenerated cardiomyocytes not derived from fusion events 46
6.1.5 CSCs are located beneath the basal lamina suggesting the presence of a niche in the heart 48
6.1.6 $Sca1^+$-cell are a heterogeneous population in the heart 49
6.1.7 Molecular analyses of the $Sca1^+$-cells population 50
6.2 Identification and analyses of resident cell populations in the skeletal muscle and their contribution to muscle regeneration 53
6.2.1 Sca1 progenitor cells contribute to myofiber formation during aging and after injury 53
6.2.2 Sca1 progenitors cells contribute to the formation of myofibers in a model of Duchenne muscular dystrophy 56
6.2.3 Sca1 progenitors cells could differentiate into muscle tissue following different pathways 57
6.2.4 In vivo Sca1 progenitor cells seem to be multipotent stem cells whereas satellite cells are unipotent 60
6.2.5 Sca1 progenitors cells could contribute to adipocytes formation in vivo 65
6.2.6 Microarray Analyses of Satellite cells, FAPs and Sca1-expressing progenitor cells 66
6.2.7 Single cell transcriptomic analyses of muscle cell 68

7 DISCUSSION 75
7.1 Evidence of the presence of *Sca1*-expressing cardiac stem cells in the heart 75
7.2 Evidence that *Sca1*-expressing cells are a source of skeletal muscle renewal and regeneration 84

8 ABBREVIATIONS 95

9 LIST OF FIGURES AND TABLES 101
9.1 Figures 101
9.2 Tables 102

10 REFERENCES 103

11 DECLARATION 114

12 APPENDIX 115
12.1 Acknowledgments 115
12.2 Curriculum Vitae 117

2 ZUSAMMENFASSUNG (Deutsch)

Zur Aufrechterhaltung der Homöostase und der Regeneration von Geweben und Organen existieren im Säugetierorganismus verschiedene residente adulten Stammzellen. Der Herzmuskel besitzt nur eine geringe Selbstheilungsfähigkeit, welche durch lokale adulte Stammzellen ermöglicht wird. Diese sind in der Lage, glatte Muskelzellen, Endothelzellen oder auch beschädigte Kardiomyozyten zu ersetzen. Die Herkunft und die Identität dieser kardialen adulten Stammzellen sind nicht eindeutig definiert. In diese Arbeit ein genetisches Zellmarkierungssystem verwendet, das gezielt *Sca1*-exprimierende Zellen markiert und damit eine *in vivo* Verfolgung der genetischen Abstammung dieser Zellen ermöglicht. Sca1 ist einer der am häufigsten verwendeten adulten Stammzellmarker. Die Analyse der markierten Zellen im Herzen ergab, dass sowohl im Alterungsprozess als auch unter pathologischen Bedingungen die von *Sca1*-abstämmenden Zellen zu den drei wesentlichen kardialen Zelllinien differenzieren. Dies deutet auf eine Rolle von *Sca1*-exprimierenden Zellen bei der kardialen Selbsterneuerung hin. Sowohl *in vivo* als auch Transkriptomdaten zeigten, dass diese eine heterologe Zellpopulation bilden und eine spezifische Lokalisation im Herzen besitzen. Die Skelettmuskulatur besitzt hingegen ein hohes regeneratives Potential. Ermöglicht wird dies durch adulte Vorläuferzellen, die Satellitenzellen, welche zu Skelettmuskelfasern differenzieren können. Obwohl Satellitenzellen als grundlegende Stammzellquelle im Skelettmuskel gelten, wurden in den letzten Jahren alternative Quellen von multipotenten Zellpopulationen, die *Sca1* exprimieren, beschrieben. Mit Hilfe des *in vivo* Zellmarkierungsmodells konnten wir zeigen, dass *Sca1*-exprimierende Zellen an der Muskelregeneration, wenn auch in wesentlich geringerem Maße als Satellitenzellen, beteiligt sind. Darüber hinaus konnte nachgewiesen werden, dass eine kleine Population *Sca1*-exprimierender Zellen unabhängig von Pax7, in Muskelfasern differenzieren kann. Desweiteren wurde die Plastizität von Satellitezellen und *Sca1*- exprimierenden Zellen *in vivo* untersucht und durch Genexpressionanalysen bestätigt. Diese Daten belegten, dass Satellitenzellen eine unipotente Stammzellpopulation darstellen, die nur Muskelfasern regenerieren können. Dagegen zeigten sich *Sca1*-exprimierenden Zellen multipotent und waren in der Lage zu Adipozyten oder Osteoblasten zu differenzieren. Somit konnte ich darlegen, dass *Sca1*-exprimierende Zellen in der Lage sind, zu Regeneration von Myozyten beizutragen. Eine weitere Charakterisierung dieser *Sca1*-exprimierende Zellen wird wichtige Erkenntnisse über den molekularen Mechanismus, welcher Herz- und Muskelstammzellen im Menschen reguliert, liefern. Diese Erkenntnisse könnten hilfreich sein, um mögliche therapeutische Behandlungen für Herz- und Skelettmuskelerkrankungen zu entwickeln.

3 ABSTRACT (English)

Different types of resident adult stem cells exist in mammalian organs in order to maintain tissue homeostasis and organ repair.

Even though the heart has low regenerative capacity it has been demonstrated that resident adult stem cells exist and are able to replace smooth muscle cells, endothelial cells and damaged or lost cardiomyocytes. Currently, the origin and the identity of cardiac resident adult stem cells remain controversial. In this study, descendants of cells that have expressed *Sca1*, which is one of the most widely used adult stem cell markers, were traced. Their contribution to self-renewal in the heart during aging and under pathological conditions was characterized. In both conditions, *Sca1*-expressing cells could differentiate into three major cardiac lineages, providing evidence of their role in myocardial renewal. These cells appeared to be a heterogeneous population *in vivo* as well as at a transcriptomic level, showing a specific location in the heart.

Unlike the heart, skeletal muscle shows a high regenerative potential. It contains adult resident progenitor cells called "satellite cells", which are able to differentiate into mature muscle fibers. Although satellite cells are considered to be the principal stem cells in the skeletal compartment, recent works have identified alternative sources of multipotent stem cells that are positive for *Sca1*. In this study, an *in vivo* lineage tracing approach in skeletal muscle revealed that *Sca1*-expressing cells are involved in skeletal muscle regeneration, although their contribution is lower compared to satellite cells. It was also possible to identify a small population of *Sca1*-expressing cells able to differentiate into muscle fibers without expressing *Pax7*, a marker for satellite cells known to be involved in quiescence, proliferation and differentiation of myogenic cells. Furthermore, the plasticity of satellite cells and *Sca1*-expressing cells was tested *in vivo* and was confirmed by gene expression profiling analysis. The data obtained verified that satellite cells are unipotent stem cells only able to regenerate skeletal muscle fibers. In contrast to satellite cells, *Sca1*-expressing cells are revealed to be multipotent and have the ability to differentiate into adipocytes and osteoblasts.

In conclusion, this study confirmed the presence of *Sca1*-expressing cells that are able to contribute to myocyte regeneration in the heart and skeletal muscle. Further characterization of these *Sca1*-expressing cells will provide valuable insights into the molecular mechanisms regulating cardiac and muscle stem cells in humans. Importantly, this could aid the future development of therapeutic strategies for human cardiac and skeletal muscle diseases.

4 INTRODUCTION

4.1 Stem cells

In the last few decades, the idea of using embryonic and/or adult stem cells to treat degenerative diseases (e.g. Parkinson´s disease, Alzheimer´s disease, multiple sclerosis, muscle skeletal dystrophy) has gained momentum with the hope of improving the health and quality of life of many of these patients. Although the concept of stem cells has existed for more than a century, the current hype surrounding stem cells, both in the scientific and public community has undoubtedly arisen due to many recent major scientific discoveries and developments in this field.

Stem cells can be defined as primordial cells, which are able to divide and differentiate into other cell lineages in an organism as well as being able to maintain a pool of undifferentiated cells. By definition, the major properties defining the stemness of a cell are:

1. ***Self-renewal.*** The ability of a cell to renew through numerous and unlimited cell cycle divisions, while keeping an undifferentiated state. To do this a stem cell divides in two ways (Figure 1):
    - *Symmetric division*: a mother cell gives rise to two identical daughter cells that maintain the stemnness.
    - *Asymmetric division*: from the same cell, two types of daughter cells arise, where one keeps the stemness and another (called "progenitor cell") is able to terminally differentiate into distinct cell types.

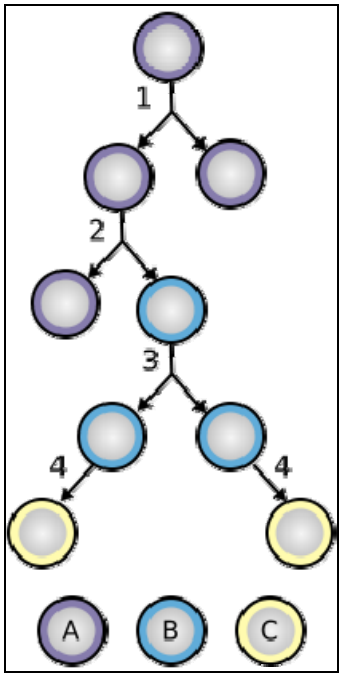

Figure 1. Symmetric and asymmetric cell division.
A: stem cell; B: progenitor cell; C: differentiated cell. (1) A stem cell can divide symmetrically into two identical daughter stem cells (called "symmetric division"). (2) Through asymmetric division, one stem cell gives rise to another stem cell and one progenitor cell. (3). Then, the progenitor cell divides into two daughter cells. (4) These daughter cells differentiate into mature cell types[1].

2. ***Potency***: defined as the capacity of a cell to differentiate into other lineages. As shown in Figure 2, potency is further defined as either:
    - *Totipotent* (e.g. morula cells): these stem cells are produced from the fusion of oocytes with sperm or are derived from the early divisions of the fertilized oocyte. They can differentiate into all the embryonic and extra-embryonic cells, including placenta.
    - *Pluripotent*: this type of stem cell includes embryonic stem cells from the inner cell mass of the blastocyst, which can differentiate into the cells of all three germ layers (ectoderm, endoderm and mesoderm). However, these pluripotent cells cannot contribute to the placenta.
    - *Multipotent*: these stem cells are able to differentiate into specific cell types only (e.g. hematopoietic stem cells differentiate into erythrocytes, leucocytes, platelets).
    - *Unipotent*: these cells can only differentiate into one cell type, but they are able to self-renew, which distinguishes them from lineage committed cells (e.g. neuronal cells, satellite cells).

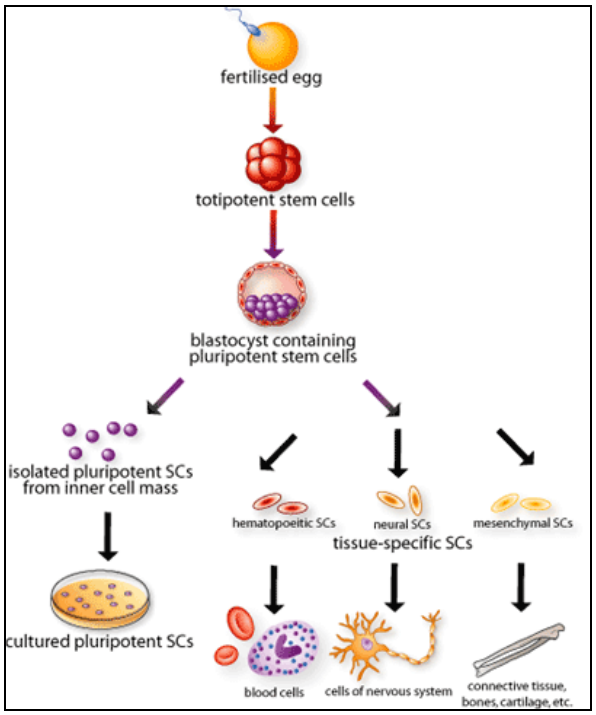

Figure 2. The potency of stem cells.
Totipotent cells are derived from fertilized oocyte and they are able to differentiate into all embryonic and extra-embryonic tissues. The pluripotent cells derived from the inner cell mass of blastocysts differentiate into all the cell types belonging to the three germ layers. Multipotent cells differentiate into several cell types, while unipotent cells are able to give rise to only one cell type but are able of self-renew[2].

Stem cells with different potency can be found in an organism throughout life. During adulthood, resident stem cells are confined to specific organs and function to ensure the maintenance of tissue homeostasis. Based on the time frame and the origin, a stem cell can be characterized as embryonic, fetal or adult.

4.1.1 Embryonic stem cells and induced pluripotent stem cells

Embryonic stem (ES) cells are derived from the epiblast of the inner mass of blastocysts, which consists of approximately 50-150 cells at embryonic stage day 4-5 after fertilization, or additionally, they are derived from the early embryonic stages of the morula. ES cells are pluripotent and are able to differentiate into all the cell types of the three germ layers: ectoderm, endoderm, mesoderm (Figure 3). ES cells do not contribute to the extra-embryonic membrane and placental formation. They can be identified by the presence of different transcription factors such as OCT4 (octamer binding protein 4), SOX2 (SRY, sex determining region Y-box 2) and GATA4 (binding the GATA DNA region). ES cells can also be characterized by the presence of specific surface markers although they are not universal, but rather species related. Human ES cells are positive for SSEA4 (Stage Specific Embryonic Antigens), TRA-1-60 and TRA-1-81 (Tumor rejection antigen)[3], while mouse ES cells present the antigen SSEA1 (Table 1)[4]. It is possible to cultivate ES cells by growing them on feeder cell layers of embryonic fibroblasts (e.g. murine embryonic fibroblasts, MEF) or in a conditioned medium that contains leukemia inhibitory factor (LIF), an inhibitor of differentiation. ES cells have high levels of telomerase activity[5], have a very short G1 cell cycle, and initiate DNA replication without external stimulation[6]**.** Mouse ES cells are the most well-studied, although ES cells have been derived from a number of different species[7] including human blastocysts[8]. Remarkably, ES cells display unlimited proliferation *in vitro* and an ability to differentiate into all the cell types of an organism. Due to these characteristics, ES cells have been extensively studied for their potential application in cell therapy in the hope of treating chronic and degenerative diseases (e.g. Parkinson´s disease)[9]. Stem cell therapy is based on injecting or transplanting stem cells into a damaged organ or tissue in order to repair the injury or treat the disease. This approach was first carried out in 1968[10] when the first bone marrow transplantation was achieved. ES cells, due to their multipotency and plasticity represent a perfect source for cell therapy. However, the use of ES cells raises ethical problems due to the generation of ES cells from human pre-implantation embryos. Furthermore, it often leads to oncogenic and immunogenic problems[11]. A possible solution to prevent the risk of immunological rejection is through the use of genetic engineering techniques to induce ES cells to express the hosts´ histocompatibility antigen or to produce ES cells that are genetically identical to the recipient of the transplantation[12]. Furthermore, induced pluripotent stem cells (iPS cells)[13] represent a possible alternative stem cell source compared to ES cells. IPS cells are stem cells obtained from culturing mouse embryonic or adult fibroblasts in the presence of four factors (OCT3/4, SOX2, C-MYC, and

KLF4) and these cells present properties similar to ES cells. Recent reports indicate that, although iPS cells showed no tumorigenic problems, certain genetic and epigenetic abnormalities still occur during their reprogramming and their maintenance in the cell culture[14]. ES and iPS cells are not the only sources of cell stem cells available for therapy. As mentioned before, bone marrow cells are most commonly used as well as stem cells from umbilical cord derived cells, placenta cells, adipose tissue cells[15], satellite cells[16], skeletal myoblasts[16] and resident cardiac stem cells[16]. To date, various studies have been performed using stem cells to treat brain damage[17], spinal cord injury[18], diabetes[19], Parkinson disease[20], baldness[21], blindness[22], cardiovascular diseases[23] and muscular dystrophies[24].

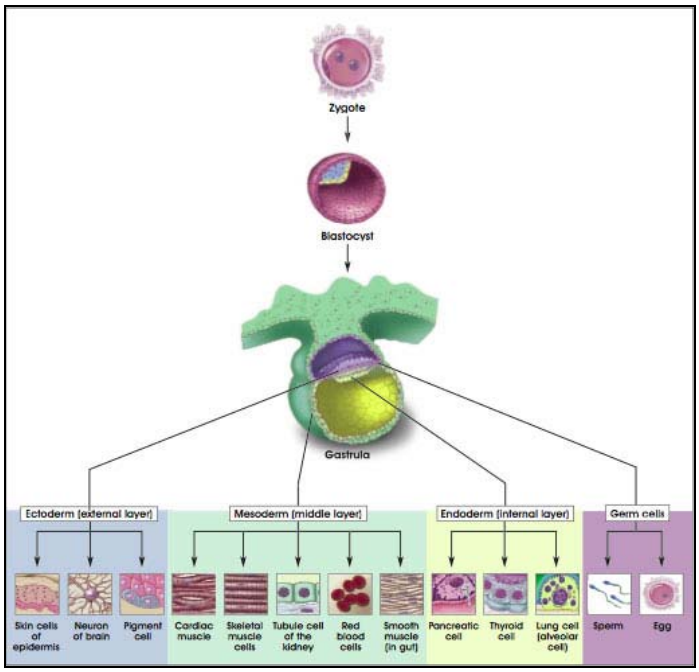

Figure 3. Pluripotency of embryonic stem cells[3].

marker	human	mouse	marker	human	mouse
OCT4	+	+	SSEA-3	+	+
SOX-2	+	+	SSEA-4	+	-
UTF-1	+	+	TRA1-60	+	-
REX-1	+	+	TRA1-81	+	-
TERT	+	+	BEX1	+	+
TRF-1	+	+	EMSD	+	-
TRF-2	+	+	HEB	+	-
FOXD3	-	+	HAND1	+	-
CX43	+	+	HIF-1b	-	+
CX45	+	+	GATA4	+	+
FGFR-4	+	+	AFP	+	-
ABCG-2	+	+	KTRL-14	+	-
GLUT-1	+	+	VIMENTIN	+	-
SSEA-1	-	+	betaIII-TUBULIN	-	+

Table 1. Markers for human and murine ES cells[4].

4.1.2 Fetal stem cells

Fetal stem cells are multipotent with characteristics between ES cells and adult cells. In particular, fetal stem cells show a phenotype similar to adult stem cells but with a more plastic phenotype compared to adult stem cell[25]. Fetal stem cells are characterized by high telomerase activity that allows for a greater replication potential and protects against aging. These cells are found in the cord blood, the placenta and the amniotic fluid. Although the umbilical cord is known for being the major reservoir of hematopoietic cells, recently, mesenchymal stem cells (MSCs) have also been isolated[26], which could be considered as fetal stem cells. Compared to the umbilical cord, the amniotic fluid and the placenta are easy to obtain. In these tissues, different stem cell populations (e.g. mesenchymal stem cells, hematopoietic stem cells, trophoblasts) have been found[27]. In the placenta, cells with high proliferative potential[28] or with immunomodulation properties that are implicated in fetal tolerance[29] have been identified. The amniotic fluid contains cells derived from all three germ layers[30,31]. These stem cells include MSCs[30,32] and CD117 (C-KIT)-positive subpopulations[33].

4.1.3 Adult stem cells

Adult stem cells are cells present in the adult organism which are able to divide in an asymmetric manner to give rise to identical cells and progenitor cells that are able to differentiate into alternative, more lineage-committed cell types. These adult stem cells are also called “somatic stem cells” (from greek Σωματικός, belonging to the body) as wells as “germ stem cells”. The majority of multipotent adult stem cells are usually defined by the name of the tissue they are originating from or associated with (e.g. mesenchymal stem cells, endothelial stem cells, etc.). The role of adult stem cells is to generate new cells that are able to maintain and repair the damaged tissue. The concept of adult stem cells was first suggested in 1990[34]. Researchers identified the presence of two different cell populations in the blood that were able to differentiate into a number of distinct cell types. These two populations of adult stem cells are: hematopoietic stem cells (forming all types of blood-related cells in the body[34]) and bone marrow stromal cells (generating bone, cartilage, fat, and fibrous connective tissue)[35]. The findings of adult stem cells in various tissues and the possibility of manipulating them resulted in increased focus and attention of researchers around the world, which led to the creation of a scientific field called “regenerative medicine”. A major goal of regenerative medicine is to stimulate and control the capacity of adult stem cells to differentiate into other cell types in order to use them as a source for cell therapies to treat serious common diseases.

4.1.3.1 Resident adult stem cells and the concept of niche

Through intensive research, it is now evident that resident adult stem cells are present in most of the organs in the human body to achieve tissue homeostasis and repair. Furthermore, each organ shows a different strategy in self-renewal using resident adult stem cells. Based on such strategies, it is possible to define organs with high cellular turnover and regenerative potential (e.g. gut, epithelium, epidermis), low cellular turnover but high regenerative potential (e.g. liver, pancreas) and low cellular turnover and regenerative potential (e.g. brain, heart)[36] (Figure 4).

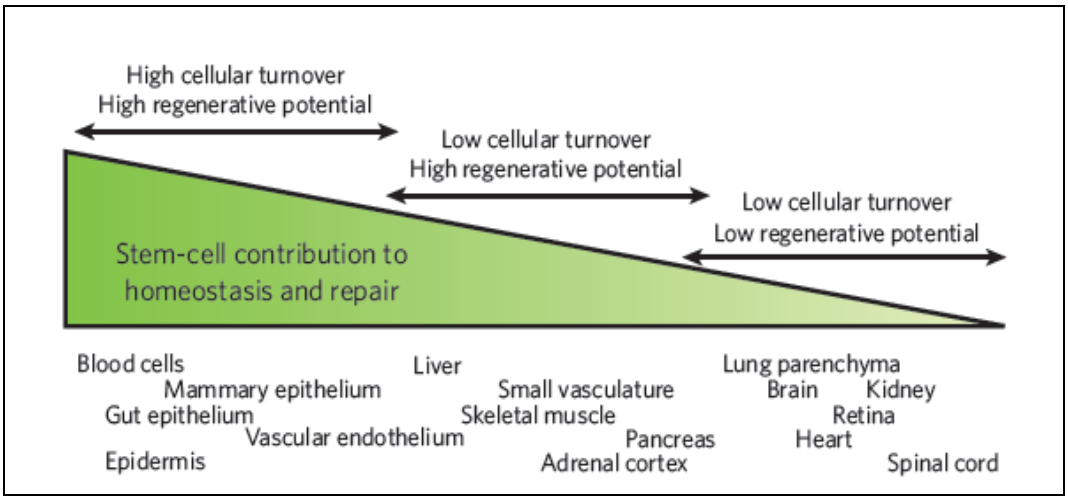

Figure 4. Scheme of potential regeneration and cellular turnover of different organs and tissues[36].

Hair follicles, blood and gut belong to the first category. These organs and tissues are constantly renewing and contain adult stem cells that are morphologically unspecialized. These adult stem cells have a low rate of division and are located in specific regions of the tissues called "niches", which regulate the behavior of adult stem cells (e.g. stemness)[37]. In the field of stem cells, the term "niche" first appeared in 1978. However, only after several studies reporting the presence of such locations in Drosophila, its concept was accepted by the scientific community. The niche is an environment that can control the quiescence and the activity of stem cells. It creates a particular surrounding that protects stem cells from external stimuli (differentiation stimuli, apoptotic stimuli, etc.) that could challenge their quiescence. At the same time, it controls the production of stem cells to avoid the development of cancer due to uncontrolled cell proliferation[38]. Furthermore, within the niche are secreted substances that allow stem cells to produce the so-called "transit amplifying (TA) daughter cells". TA daughter cells have a high rate of proliferation, can self-renew over a short term and give rise to precursors of all or many of the differentiated cell types of the organ that they are located in[39] (Figure 5).

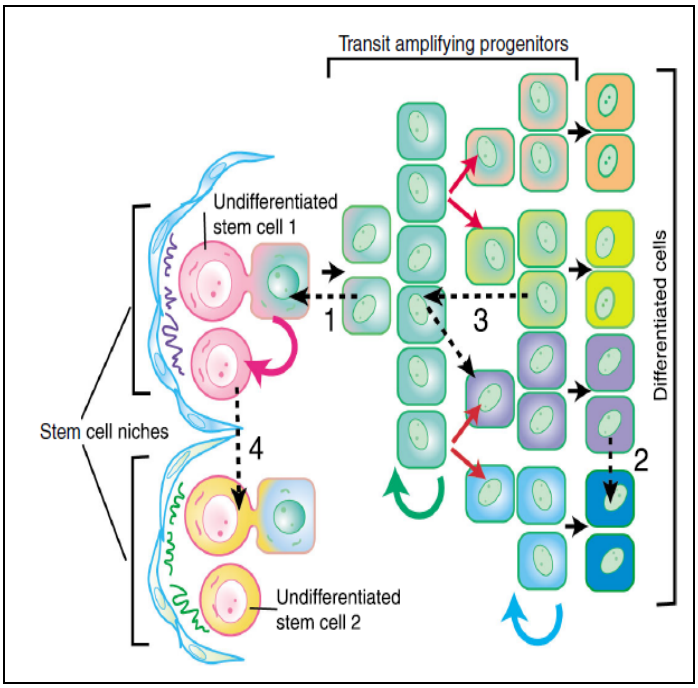

Figure 5. An example of classical hierarchy of adult stem cells in epithelial cells[39].
The model represents how undifferentiated epithelial stem cells, transit amplifying (TA) cells, progenitor cells and mature post mitotic differentiated cells are derived and controlled. The stem cell in its "niche" gives rise to different subclasses of TA cells, which can self-renew more rapidly than parental stem cells. (1) Early TA cells can replenish a stem cell pool; (2) A direct "transdifferentiation" of a differentiated cell into another cell type; (3) Dedifferentiation of more differentiated cells into more plastic TA cells, which creates distinct differentiated cells than the original ones; (4) Metaplasia or Transdetermination, where stem cells switch from one tissue-specific lineage to another.

The second group of organs and tissues, characterized by a low cellular turnover but a high regenerative potential, can maintain their tissue homeostasis without the need of undifferentiated adult stem cells. Instead, these organs and tissues contain so-called "facultative" stem cells, which are quiescent differentiated cells that behave like adult stem cells, with the potential to replicate themselves to replace the damaged tissues upon injury[36].
In the liver, for instance, upon hepatectomy (the surgical removal of the liver) the turnover and regeneration are acquired through hepatocyte differentiation[40]. In the muscle, regeneration is a result of proliferation and subsequent differentiation of resident progenitor cells called "satellite cells"[41].
In the third and last group, which shows a low cellular turnover and a low regenerative potential, lung, brain and heart are included. These are complex organs with a limited endogenous repair capacity following acute injuries; possibly due to the presence of resident adult stem cells with a limited potential of tissue repair.
Below, the two principal muscles present in an organism, cardiac and skeletal muscle will be further described together with their possible adult stem cell populations.

4.2 Heart

The heart is the first organ to become functional during embryonic development. It is composed of different cell types. Among them, the following four cell types are the most abundant: cardiomyocytes, endothelial cells, vascular smooth muscle cells and fibroblasts. It was previously accepted that a great part of the heart is represented by cardiomyocytes.

However, a closer look in the murine heart revealed a proportion of ~56% cardiomyocytes, 27% fibroblasts, 10% vascular smooth muscle cells and 7% endothelial cells[42]. In contrast, rat and human hearts show a similar composition in which fibroblasts (62.6%) are the major cell type[42,43]. Cardiomyocytes comprise only 26.4% in the rat and 20% in the human heart[44]. Given such similarity between the hearts of rats and humans compared to the mouse heart, rats clearly represent a better animal model for the study of cardiovascular diseases. However, until now, the difficulty in the genetic manipulation of rats[45], restricted the use of this experimental animal model. These limits and the possibility of purchasing reliable knockout mice favoured the mouse as the principal investigating model.

Cardiovascular disease (e.g. coronary heart disease, cardiomyopathy, heart failure, etc.) still remains one of the major causes of death around the world. This has increased the scientific interest in searching for ways to promote regeneration of cardiac tissue after damage. During the last century, the heart was considered a post-mitotic organ that is not able to regenerate during aging and upon damage. Although remodelling processes occur upon aging or damage, it was thought that such processes are due to cardiomyocyte hypertrophy rather than cardiomyocytes proliferation[46,47]. However, recent reports have suggested that the heart is an organ that is able to self-renew. In 2007 Hsieh and colleagues reported that upon cardiac injuries (i.e. myocardial infarction or pressure overload), cardiomyocyte turnover occurs in the murine heart, but not during normal aging[48]. In 2009, using carbon-14 (C14), Bergmann *et al.* confirmed the evidence of cardiomyocyte renewal in human hearts[49]. This isotope, released in the atmosphere after World War II nuclear bomb testing was absorbed by the human body resulting in a labeling of cardiomyocytes. This allowed the research group to estimate the age of cardiomyocytes and hence provided a way to measure renewal. According to their calculations, at the age of 25 years, approximately 1% of cardiomyocytes turnover annually, and the turnover rate decreases to 0.45% at the age of 75 years. Overall, it was estimated that approximately 50% of cardiomyocytes are exchanged during a normal life span[49]. However it is still not completely clear, what is the source of this renewal. It has been demonstrated that several types of somatic stem cells can contribute to the renewal of the heart: BMCs (bone marrow cells), HSCs (hematopoietic stem cells) and MSCs (mesenchymal stem cells). Although BMCs and HSCs showed a certain capacity to ameliorate cardiac function once injected, it was shown that they are not able to differentiate into cardiomyocytes[50]. MSCs are, indeed, able to contribute to heart regeneration due to their cardiomyogenic properties both *in vivo*[51] and *in vitro*[52]. Toma *et al.* proved *in vivo* that hMSC transplanted in mice were able to differentiate into cells, presenting a level of desmin, beta-

myosin heavy chain, alpha-actinin, cardiac troponin T comparable to those of the host cardiomyocytes. Makino *et al*., on the other hand, demonstrated that murine bone marrow stromal cells treated with 5-azacytidine, a hypomethylating agent, acquired *in vitro* myotube-like morphology and spontaneously started beating[52]. Another possible source of such renewed cardiomyocytes is the so called "cardiac stem cells" (CSCs)[53].

4.2.1 Cardiac stem cells

Cardiac stem cells (CSCs) (also known as "cardiovascular progenitor cells (CPs)) are resident adult stem cells in the heart that are able to give rise to different lineages (e.g. cardiomyocytes, endothelial cells, smooth muscle cells, etc.) *in vitro* and *in vivo*[54].

Whether these CSCs possess stemness and multipotency is still debatable. Furthermore, due to the lack of lineage tracing studies to uncover the origin and role of CSCs, the distinction between adult stem cells and progenitor cells in the heart is lacking in the field. To date, several molecular markers have been reported to identify CSCs. Based on their different profiles, six groups of CSCs can be defined as shown in table 2[55].The possibility of the existence of resident stem cells is favorable from the clinical point of view. A precise characterization of this population will be helpful in the future in terms of cell therapies because it will allow a higher accuracy regarding cell isolation and expansion and could thereby avoid the common problem of immune rejection.

Table 2. List of mouse and human resident CSCs based on the different markers expression[55].

Type of CSCs	Other Markers	References
$SCA1^+$ CSCs	$CD34^-$, $CD45^-$, $FLK1^-$, $C\text{-}KIT^{+/-}$, $GATA4^+$, $NKX2\text{-}5^{+/-}$, $MEF2C^+$	(Oh et al., 2003; Forte et al., 2008; Matsuura et al., 2004; Rosenblatt-Velin et al., 2005; Tateishi et al., 2007; Wang et al., 2006; Wu et al., 2006)
C-KIT+ CSCs	$CD34^-$, $CD45^-$, $SCA1^+$, $GATA4^+$, $NKX2\text{-}5^+$, $MEF2C^+$	(Bearzi et al., 2007; Beltrami et al., 2003; Dawn et al., 2005; Linke et al., 2005; Miyamoto et al., 2010; Tillmanns et al., 2008; Urbanek et al., 2003)
$ISL\text{-}1^+$ CSCs	$CD31^-$, $SCA1^-$, $C\text{-}KIT^-$, $GATA4^+$, $NKX2\text{-}5^+$	(Laugwitz et al., 2005; Moretti et al., 2006)
Side population (SP) cells	$CD34^+$, $CD45^+$, $ABCG2^+$, $SCA1^+$, $C\text{-}KIT^+$, $NKX2.5^-$, $GATA4^-$	(Martin et al., 2004; Liang et al., 2010; Oyama et al., 2007; Pfister et al., 2005)
Cardiospheres	$CD34^+$, $CD45^+$, $ABCG2^+$, $SCA1^+$, $C\text{-}KIT^+$, $NKX2.5^-$, $GATA4^-$	(Messina et al., 2004; Andersen et al., 2009; Cheng et al., 2010; Davis et al., 2010; Smith et al., 2007; Tateishi et al., 2007)
Cardiac mesangioblasts (EPCs)	$CD31^+$, $CD34^+$, $CD44^+$, $CD45^-$, $SCA1^+$, $C\text{-}KIT^+$	(Barbuti et al., 2010; Galvez et al., 2008; Gálvez et al., 2009)

4.3 Skeletal muscle

Skeletal muscle is a type of striated muscle tissue that is attached to the skeleton. Its contraction is under voluntary control, which differs from cardiomyocytes whose contraction is under involuntary control.

Skeletal muscle is composed of thousands of cylindrical muscle units called "myofibers", which are bound together by connective tissue and surrounded by vessels and nerves.

Myoblasts are the basic unit of cells in the skeletal muscle that are able to fuse together to give rise to the mature functional cells called "multinucleated myofibers". Each fiber contains several myofibrils, mitochondria and smooth endoplasmic reticulum (SER). The normal replacement of myoblasts and myofibers is acquired by the differentiation of so called "satellite stem cells", the muscle resident stem cells located between basal lamina and sarcolemma.

Due to the abundance of skeletal muscle in the body, satellite cells can be isolated and cultured, which allows for a convenient source of stem cells to be used in cellular and cell-mediated therapies. Recent reports show that beside satellite cells, other types of stem/progenitor cells in the skeletal muscle exist[56]. In the following subsections, different stem/progenitor cells present in the skeletal muscle are described in detail.

4.3.1 Muscle stem cells

Satellite cells are considered as the skeletal muscle stem cells *par excellence*.

They were described first in 1961 by Katz and Mauro[41]. The name "satellite" originated from their specific location within the fiber. Satellite cells reside between the sarcolemma and the basal lamina of the fiber but are separate from them. Their cellular origin is still unknown. Satellite cells are constituted by a heterogeneous population of mononucleated myogenic precursors that are quiescent and not proliferative. Upon injury, these satellite cells are activated and proliferate to regenerate the damaged muscle. It is known that during the normal lifespan of an organism, the capacity of the muscle to regenerate as well the number of satellite cells decreases with age[57,58]. Satellite cells can be identified by the expression of different molecular markers such as M-CADHERIN, C-MET, CD34, hepatocyte growth factor (HGF), myocyte nuclear factor (MNF) and PAX7, a paired box transcription factor[59].

Although satellite cells are considered *bona fide* muscle stem cells, recent reports reveal the presence of other populations of stem/progenitor cells in the skeletal muscle. These include PICs (Progenitor Interstitial Cells), mesangioblasts, pericytes, FAPs (Fibro-Adipogenic Precursor cells) and Muscle Derived Stem Cells (MDSCs).

PICS are muscle-resident stem cells, located in the interstitial space and express the cell stress mediator PW1 (or PEG3, paternally express 3). However, PICs do not express other typical skeletal stem cell markers such as PAX7. The presence or absence of these two genes (*PW1* and *Pax7*) accounts for the "P" in PIC. PICs are able to differentiate into muscle lineage *in vitro* and *in vivo*, are able to generate satellite cells and efficiently contribute to skeletal muscle regeneration but only in the presence of satellite cells[60].

Mesoangioblasts are cells related to the walls of large vessels. It has been shown that they possess the ability to differentiate into several types of mesodermal tissues (e.g. smooth, cardiac and skeletal muscle tissue, bone, fat). In contrast to pericytes, mesangioblasts are positive for the endothelial marker Flk-1[61].

Pericytes are myogenic precursor cells that are associated with micro-vascular walls in the human skeletal muscle[62]. They may be reminiscent of embryonic 'mesoangioblasts' present after birth and they appear to be positive for alkaline phosphatase but not for Flk-1.

FAPs (Fibro-Adipogenic Precursor cells), are another exclusive population of stem/progenitor cells that are able to interact with satellite cells to control the maintenance and regeneration of the skeletal muscle[63,64]. During regeneration, FAPs proliferate and produce different signaling molecules, including IL6, to stimulate satellite cells towards differentiation. During degeneration this secretion it is blocked and FAPs differentiate preferentially into adipocytes and fibroblasts, which inhibits proper myogenesis (the process of forming myofibers)[65].

MDSCs (Muscle Derived Stem Cells) may represent predecessors of satellite cells[66]. They are multipotent and can differentiate into bone, muscle, cartilage and adipose tissue. SCA1 has been consistently identified on the putative MDSCs as a marker[67].

All of the above-mentioned stem/progenitor cells express one common molecular marker, that is, Stem Cell Antigen 1 (SCA1).

4.4 SCA1 as marker for stem cells

In the field of stem cells, the most common way to isolate and identify stem cells is using molecular markers. These marker proteins are present on the surface of a cell. In general, to distinguish stem cells among the other cell types and to isolate them, instead of one marker, a combination of markers is used to achieve populations of target cells with a higher purity[3]. Among these markers, one of the most commonly used is Stem Cell Antigen 1 (SCA1).

SCA1 is an 18kDa glycosyl-phophatidyl-inositol-anchored cell surface protein and belongs to the *Ly6* gene family, which consists of at least 18 highly related genes present on mouse

chromosome 15. It was first identified on the surface of activated lymphocytes; thus SCA1 is also known as "Lymphocyte Activation protein-6". Its protein is encoded by two allelic genes "*Ly6E.1*" and "*Ly6A.2*"[68]. It is suggested that SCA1 acts as a co-regulator of lipid raft signaling, which influences the decision making processes of the fates of stem cells. It is expressed in hematopoietic stem cells (HSCs) as well as in stem/progenitor cells of different organs and tissues, including liver, skeletal muscle, heart, prostate and mammary gland.

In hematopoietic cells, SCA1 is involved in the down regulation of T-cell proliferation and in HSCs enrichment[69,70]. Concerning the heart, more than 93% of adult cardiac side population cells (SPs, one of the six different groups of CSCs) [71] express SCA1 while being negative for the hematopoietic cell marker CD45 and the endothelial marker CD34. Furthermore, *Sca1*-positive cells were reported to play an important role in tissue regeneration after myocardial infarction[72]. In skeletal muscle, the presence of SCA1 as a cellular marker seems to have a role in myoblast differentiation, proliferation, fusion and cell-cycle exit. In particular, *Sca1* expression contributes to keeping a pool of progenitor cells, leading to a down regulation of muscle proliferation[73,74].

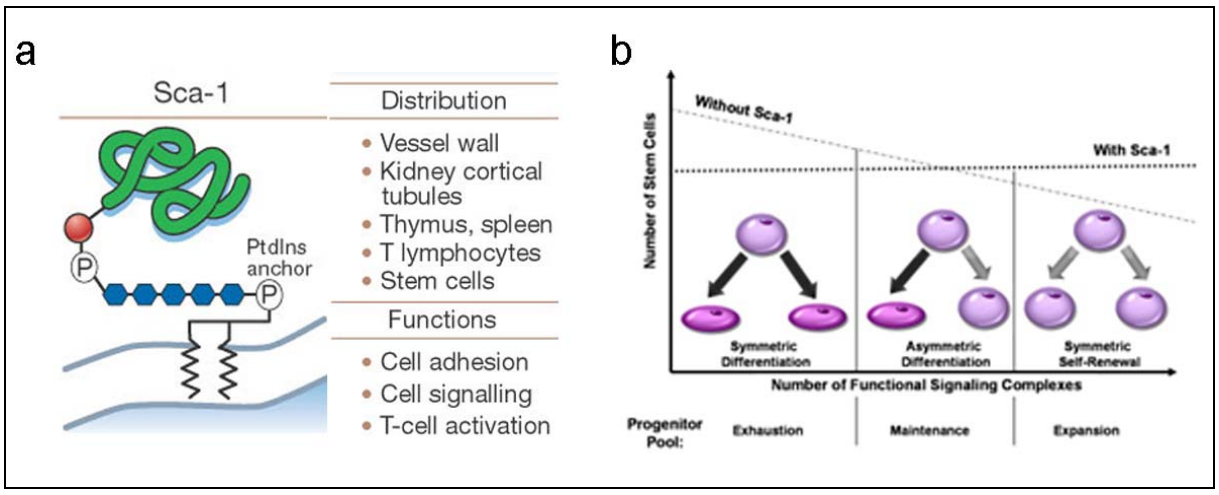

Figure 6. *Sca1* as a stem cell marker.
(a) Structure, distribution and function[75]. **(b)** A model in which the presence of *Sca1* maintains homeostasis and self-renewal of myogenic cells, while the absence of *Sca1* promotes differentiation of the myogenic cell pool[76].

4.5 Lineage tracing

As described in Section 4.1.3.1 and illustrated in Figure 4, tissues and organs show different abilities to maintain homeostasis and renewal upon damage. These processes, in most cases, are achieved through the division and differentiation of stem/progenitor cells, although the capacity to renew differs from one stem cell type to the other. Due to the lack of robust stem-cell-specific surface markers that can be used in various tissues and organs[77], various

approaches have been developed to identify stem-cell-specific markers. Although up until now, no gold standard in the field of stem cells exists, one of the most promising approaches is called "lineage tracing". Lineage tracing is a technique in which a cell is marked (e.g. with green fluorescence protein (GFP)). This mark should be transmitted to progenies of the target cell, if it is performed in a permanent lineage labeling manner[78]. Lineage tracing is an efficient tool to understand the characteristics of stem cells and their behaviors during normal development of an organism in their own environment (e.g. niches). Furthermore, when stem cells are labeled with a fluorescent protein (e.g. GFP) their fates can be monitored in real time even after isolation, transplantation into a host animal or when cultured *in vitro*.

Currently, the following techniques are available to lineage trace the fates of the labeled cells: direct observation (or time-lapse microscopy), cell labeling, genetic markers, transplantation, genetic mosaic, genetic recombination (constitutional or inducible) and multiple reporters.

- **Direct observation** is a non-invasive technique that is easy to handle and fast to establish. However, in the case of observing an entire organism, it is necessary to have only a small number of cells to be labeled in a transparent embryo or in a tissue that is easy to access. Commonly, this technique is used to follow cell division, motility and death of the cell *in vitro*[78].
- **Cell labeling** is used when it is not possible to perform direct observation. In this technique, the cells are labeled with vital dyes, such as carbocyanine dyes (indo/oxacarbocyanine e.g. Dil or DiO), or injected with fluorescein-conjugated dextran or horseradish peroxidase (HRP). With this technique, it is also possible to monitor the behavior of labeled cells, as was done in labeling DNA by C14 by Bergmann and colleague[49]. The disadvantages of this technique include the limitation of cell size and diffusion of dyes. When the cell is small for instance, it is difficult to inject the tracer. During cell division, the chemical compound will be diluted or diffused which is a problem for cells with high turnover if monitored for a long period of time as in the development of an organism.
- **Genetic markers** (e.g. green fluorescence protein (GFP), ß-galactosidase or alkaline phosphatase) provide an alternative method of avoiding the spread of the dye to neighboring cells since these genetic markers are relatively stable and can be inherited by the progeny if the promoter that drives the expression of such marker has not been turned off[79]. The cell to label can be chosen "*a priori*" because the insertion will be random and the labeling can be introduced to cells by direct injection, transfection or viral infection.

However, this technique also has some limitations such as low introduction efficiency and spontaneous retroviral silencing.

- **Transplantation** is suitable for clinical research which is mainly used to examine the fates of stem cells (e.g. bone marrow derived mesenchymal stem cells) in tissue like blood, muscle and skin[80].
- **Genetic mosaic** (e.g. chimeric mice) has been employed to investigate tissue organization[81] as well as to understand the molecular basis of intercellular communication (a mixture of cell population in the cell culture)[82].
- **Genetic recombination** is the most elegant and refined way to lineage trace cells and was first used in the 1990s. This technique will be described in details in the next subsection.

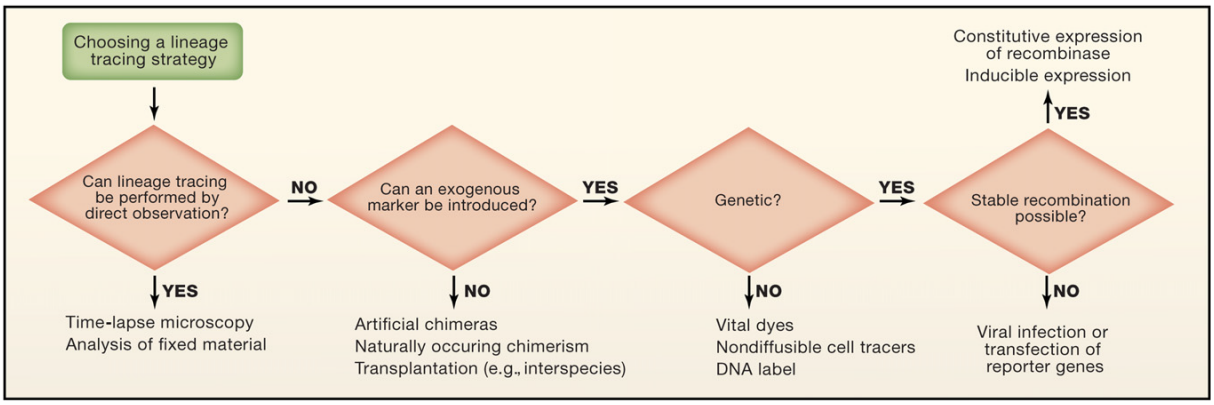

Figure 7. How to choose an appropriate lineage tracing strategy[78].

4.5.1 Genetic recombination

Genetic recombination technique marks a cell permanently to allow further labeling of the tagged cell. It is one of the most commonly used tools to manipulate the genome of a target organism and to create knockout, conditional knockout and reporter animals (e.g. mouse). In genetic recombination, the following components are required: a switch and a reporter.

4.5.1.1 The switch component

The switch is achieved by using a Cre-recombinase. The name of this enzyme derived from the locus where it is encoded originally defined as "Causes recombination" or "Cyclization recombinase"[83].

Cre-recombinase protein and *loxP* sites are the two basic elements of the site-specific recombination mechanism present in the P1 bacteriophage. This phage normally infects bacteria (e.g. *Escherichia coli*), without integrating in their genome but rather existing as a plasmid. During its replication long multimeric DNAs are processed by Cre-*loxP* system in

order to create a circular monomeric one. This system helps to circularize the genomic DNA of the phage and facilitates its replication (Figure 8a)[84]. The *loxP* site consists of a 34-base pair (bp) sequence in which two flanking 13-bp inverted repeats are separated by an 8-bp spacer region. Cre-recombinase recognizes the *loxP* site at their flanking regions[85] and in presence of two *loxP* sites promotes recombination generating free and catenated circular molecules[86] (Figure 8b & c). Cre and *loxP* are not commonly found in the genomes of higher organisms, but they can be introduced into the target genome by transgenic technology in order to promote specific recombination. Depending on the orientation of the *loxP* sites, this system can be used to obtain a specific translocation, a large deletion (or a set of deletions), duplication or inversion of a target sequence. When two *loxP* sites are in the same orientation on a single chromosome it is possible to delete the flanking sequences (e.g. gene). When this strategy is used in the homologous chromosomes, it is possible to obtain duplication of the sequences. Furthermore, when *loxP* sites are inserted in the genome in an opposite orientation it leads to inversion of the target sequence in one chromosome (e.g. dicentric or acentric chromosome). When used in different chromosomes, translocation of the target sequence will happen (Figure 8c).

The expression of Cre-recombinase can be controlled by targeting it to a specific promoter. For instance, promoters are often only active in a certain cell population (thus tissue-specific expression as in the case of *alphaMHC* in cardiomyocytes) or can be controlled using particular drugs (e.g. tetracycline (doxycycline)). The latter is very useful for controlling the expression postnatally by administration of the drug. Another possible system is based on the fusion of Cre-recombinase with the estrogen receptor responsive (ERT) element, which can be controlled by an injection of an estrogen receptor antagonist called “tamoxifen”. The latter system is called “Cre-ERT”[87]. The inducible systems mentioned above (with doxycycline or tamoxifen) will be clarified in the following paragraphs.

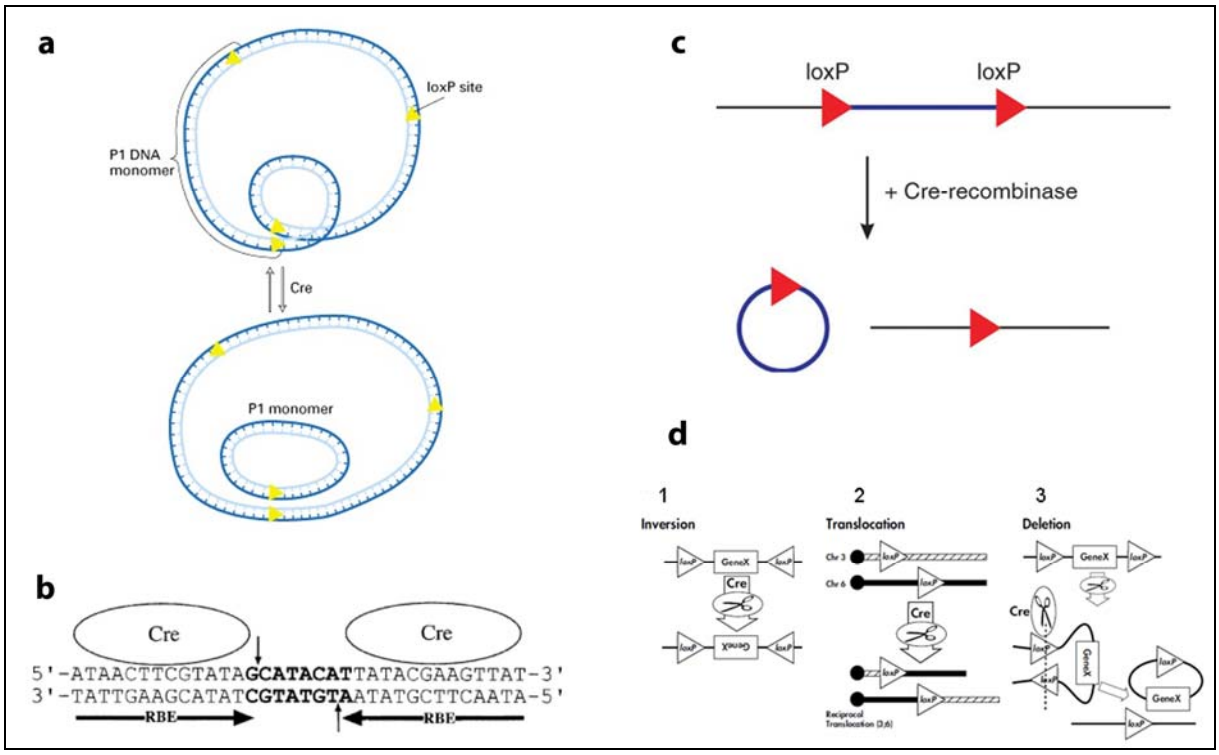

Figure 8. Cre-recombinase and *loxP* sites.
(a) Cre-recombianse protein and *loxP* system present in the P1 bacteriophage[84]. **(b)** A scheme of a *loxP* site underlying the flanking regions recognized by Cre-recombinase and the 8bp core sequence where the recombination occurs[85]. **(c)** A DNA region flanked by two *loxP* sites with the same orientation promotes Cre-mediated excision producing circular and linear fragments[86] . **(d)** Schemes of the different outcomes on the base of the *loxP* orientation[88].

4.5.1.1.1 Doxycycline inducible Cre system (Tet-Off and Tet-On)

There are two ways of achieving Cre-based recombination using tetracycline or doxycycline: (1) tetracycline transactivator protein (tTA) known as "Tet-Off" or (2) reverse tTA (rtTA), known as "Tet-On". In both cases, tTA is used to promote transcription of Cre-recombinase.

The tTA protein is derived from the fusion between the tetracycline repressor protein (TetR) found in the bacterium *Escherichia coli* and the activation domain of VP16 protein from Herpes simplex virus. The obtained tTA binds the tetO operator sequence present in the tetracycline response element (TRE), which is located upstream of a modified CMV (cytomegalovirus) minimal promoter ($P_{tet}1$ promoter).

In the Tet-Off system[89], tTA binds the TRE and activates transcription in absence of tetracycline or its homologues (e.g. doxycycline). In presence of the drugs, tTA is not able to bind the operator and the transcription is repressed. The opposite situation happens in the Tet-On system[90]. This system is based on rtTA protein (reverse tTA), that is derived from the modification of the amino acids sequence of the TetR present in tTA. The rtTA, different from tTA, depends on the presence of tetracycline or doxycline to be functional. The conformational change induced by the drugs, allows rtTA to bind TRE at the operator

sequence and promote transcription. In the Tet-On system, in the absence of drugs, transcription is repressed. Two other forms of Tet-On system exist: rtTA2s.M2 and Tet-On 3G or rtTA-V10. They were developed by modifying the amino acids sequence of tTA which results in increased stability and sensibility for doxycycline by a factor of 10 and 100 respectively[91].

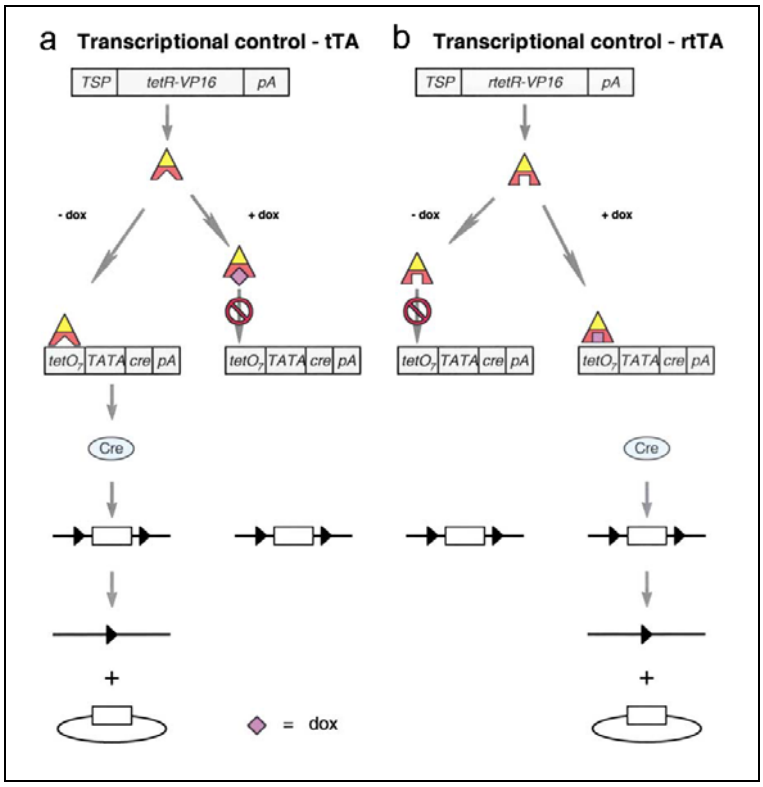

Figure 9. Tet-Off and Tet-On systems[92].
(a) Tet-Off system. In the absence of doxycycline, tTA can bind the tetO operon, which allows for the transcription of Cre-recombinase to mediate recombination. In the presence of doxycycline, tTA changes its conformation, which is unable to bind the tetO sequences and to promote recombination. **(b)** Tet-On system. Only in the presence of doxycycline, rtTA can bind the tetO operon to allow for the transcription of Cre-recombinase to mediate recombination**.**

4.5.1.1.2 CreERT tamoxifen inducible system

Another way to control Cre-mediated recombination is using "Cre-ERT" system. This system was derived from the fusion of Cre-recombinase to a modified version of the human estrogen receptor (ER)[93]. With this approach, it is possible to control the expression of Cre-recombinase in the temporal manner by injection of an activator, the estrogen receptor antagonist tamoxifen. Cre-ERT complex is normally sequestered in the cytoplasm by heat shock proteins (HSPs) in an inactive form. In the presence of tamoxifen or its active metabolite 4-hydroxy-tamoxifen (4-OHT), the drug binds Cre-ERT leading to conformational changes and consequently the release of HSPs. This modification allows Cre-ERT translocation into the nucleus, where Cre-recombinase can recombine *loxP* sites and induce

the excision of the floxed gene. Since this system is very useful in controlling the expression of Cre-recombinase in a time- and tissue-dependent manner, various modifications of this system are available: mouse ER^{TM} [94], human CreER^{T} [95] and human CreER^{T2} [96]. Among these modifications, CreER^{T2} is more sensitive to tamoxifen regarding the nuclear translocation and shows a stronger recombinase activity, approximately ten times higher than CreER^{T} [97].

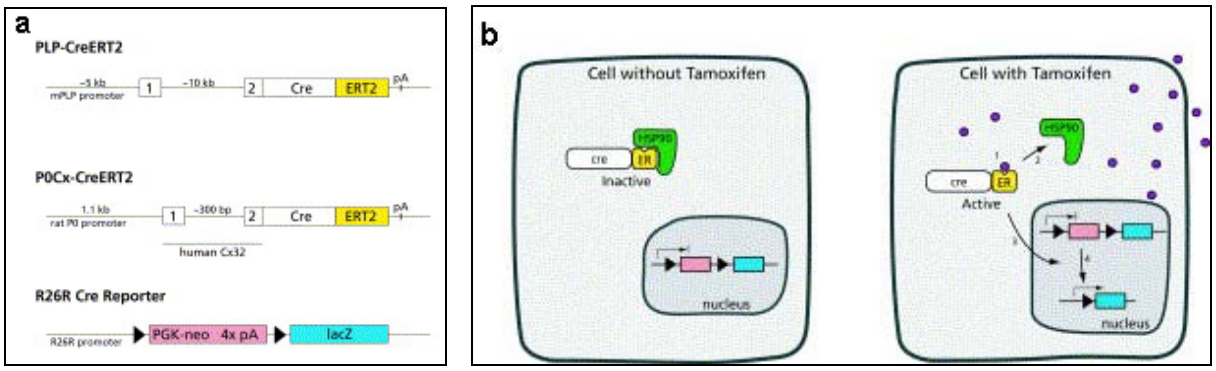

Figure 10. Cre-ERT system.
(a) Schemes of the constructs used and the modified locus R26R; *loxP* sites are indicated by triangles. **(b)** In the absence of an appropriate ligand, the CreERT fusion protein (indicated as "Cre-ERT2" in the figure, which is the improved version of CreERT[98]) is bound to the heat shock protein. When tamoxifen (violet circles) is present, HSP90 dissociated from Cre-ERT and this causes the translocation of Cre-ERT into the nucleus, where it mediates the recombination using the *loxP* sites[99].

4.5.1.2 The reporter component

The reporter component is a gene used as marker (e.g. beta-galactosidase) to determine the activity of another gene. In the Cre-*loxP* system, the reporter allows the visualization of Cre activity and the accuracy of the cell labeling. Two main approaches exist to follow reporter gene expression using Cre-mediate recombination technology. The first consists of a floxed stop cassette sequence (*loxP-STOP-loxP*) fused with an active promoter, that is upstream of the reporter gene. In this situation, in the absence of Cre-recombinase or when it is inactive, the transcription of the gene cannot occur and the cells will not be labeled. The presence of Cre-recombinase will recombine *loxP* leading to the excision of the stop cassette sequence. This removal allows the transcription of the reporter gene and the cells will be labeled.

The second strategy is the possibility of switching the reporter line using Cre-recombinase in combination with a double-reporter system. In this case, a specific reporter gene (e.g. LacZ) followed by the stop cassette sequence are floxed and they are fused to a second reporter gene (ex GFP/ alkaline phosphatase). In normal conditions the cells express the first reporter but in the presence of Cre-recombinase the entire cassette, containing also the stop sequence is excised, allowing the expression of the second reporter gene (e.g. EGFP in Z/EG mice[100]). Different systems have been developed using either enzymes such as human alkaline phosphatase (e.g. Z/AP mice[101]) or fluorescence proteins (e.g. EGFP[100], RFP[102], tdtomato[103])

that are more suitable for three-dimensional confocal imaging. Furthermore, to follow the lineages of labeled cells with more than one reporter gene, multicolor reporters are available. (Brainbow[104] or *R26R-Confetti* mouse[105]). These models are currently used in the research field to understand the origin and contribution of different cell types during the maintenance and repair of tissue[105,106].

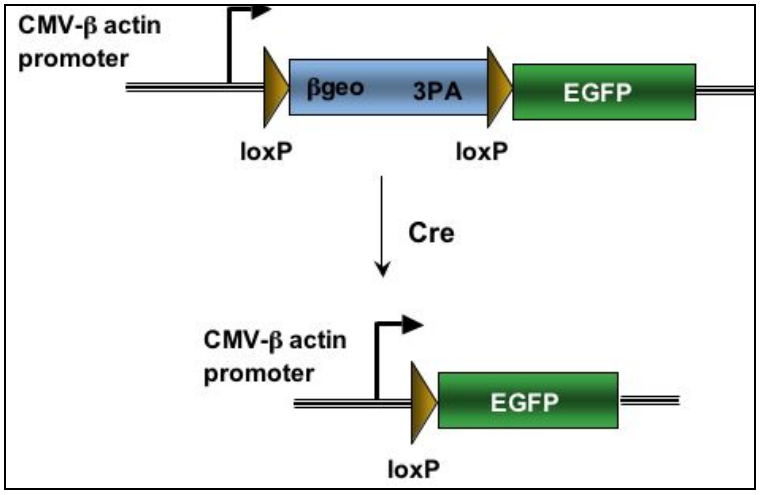

Figure 11. An example of a reporter mouse.
A representative scheme of a Z/EG[100] reporter mouse. In this mouse two reporter gene are present: the floxed lacZ gene fused to a stop-codon cassette (ßgeo-3PA) and the enhanced GFP (EGFP) gene. The expression of both reporter genes is based on the activation of CMV-ß actin promoter. In absence of Cre-recombinase the cell is labeled with lacZ whereas the expression of Cre leads to the excision of the floxed lacZ. This recombination will remove the fused stop codon cassette allowing the expression of EGFP.

The lineage tracing techniques mentioned above are not only useful in tracing the fates of labeled cells but are also important in understanding the regulatory pathways that control the proliferation and differentiation of resident stem cells.

Understanding these mechanisms will be not only help to ameliorate the manipulation or stimulation of resident stem cells but also to obtain reliable sources for stem cell therapy. However, in order for this to be possible a clear definition of the origin and status of resident stem cells is needed.

5 MATERIAL AND METHODS

5.1 Transgenic mice

All animal experiments in this study were performed with approval of the local animal care committee.

5.1.1 Sca1- tTA//LC1-Cre//Z/AP and Sca1- tTA//LC1-Cre//R26RConfetti

Triple transgenic mice were obtained by breeding *Sca1*-tTA with LC1[107] and Z/AP[101] or *R26R-Confetti*[105] reporter mice (Figure 12). *Sca1*-tTA mice were generated by pronucleus injection using standard procedures. Construction of the transgene was based on insertion of the tetracycline transactivator (tTA)-IRES-GFP-polyA cassette (~2.6Kb) into the ClaI cloning site of pPOLYIII-Ly6A in the first untranslated exon of *Ly6a* (*Sca1*) genomic region[108]. Genotyping was performed by PCR on tail DNA using the primers for *tTA*, *Cre*, *R26RConfetti* (Table 1). DNA was subjected to an initial five-minute denaturation at 94°C followed by 35 cycles of denaturation (1 minute at 94°C), annealing (30 seconds at 55°C for tTA and Cre, 30 seconds at 58°C for Confetti), and elongation (2 minutes at 72°C). LacZ staining of a tail was performed to reveal the presence of Z/AP allele.

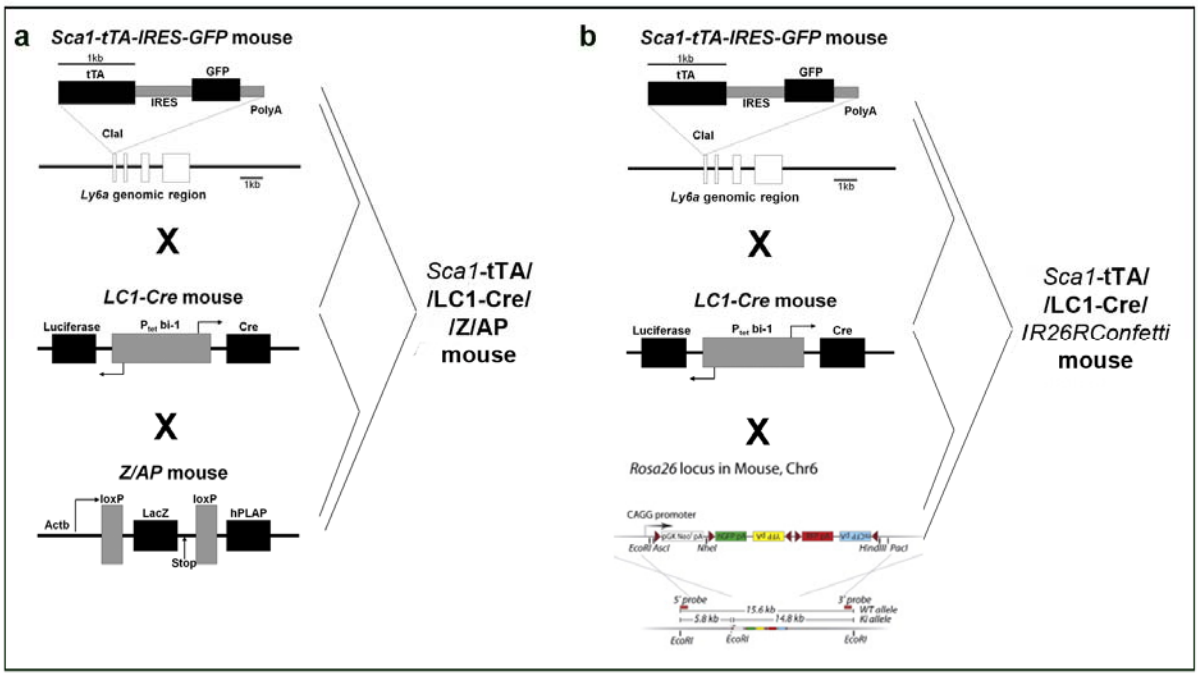

Figure 12. Mouse transgenic constructs.
(a) *Sca1*-tTA//LC-1-Cre//Z/AP**. (b)** *Sca1*-tTA//LC-1-Cre//*R26RConfetti*.

5.1.2 *Sca1-GFP*

Sca1-GFP (*Ly-6A*-GFP) mice were obtained as previously described[108]. Briefly, to create this mouse line, an enhanced GFP gene was inserted in the ClaI cloning site in the first untranslated exon of the Ly6a (Sca1) gene (Figure 2). Genotyping was performed by PCR on tail DNA using the GFP primers (Table 1). DNA was subjected to an initial five-minute denaturation at 94°C followed by 30 cycles of denaturation (1 minute at 94°C), annealing (2 minutes at 55°C), and elongation (2 minutes at 72°C).

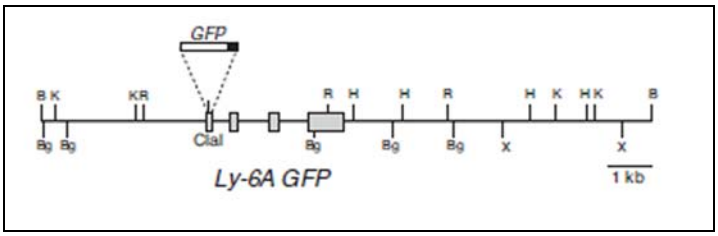

Figure 13. *Sca1*-GFP transgenic mouse.
Scheme of the 14-kb BamH1 fragment of the *Ly-6A* and the insertion of the GFP gene into the Cla1 cloning site; the following are the restriction site: B: BamH1; BG: BgIII; K: Kpn1; R: EcoR1, H: HindIII; X: Xba1[108].

5.1.3 *Pax7-Cre//Z/AP*

The mice were obtained by breeding *Pax7*-Cre[109] with Z/AP[101] reporter mice. *Pax7*-Cre was created by using a targeting vector containing an IRES-*Cre*-FRT-*Neo*-FRT cassette within the 3′-untranslated region of the *Pax7* gene following the stop codon in exon 10 in the ClaI. Genotyping was performed by PCR on tail DNA using the primers for *Pax7* and *Cre*, (Table 1). For genotyping of Z/AP allele, LacZ staining of a tail was performed. DNA was subjected to an initial 5 minute denaturation at 94°C followed by 35 cycles of denaturation (1 minute at 94°C), annealing (2 minutes at 58°C), and elongation (2 minutes at 72°C).

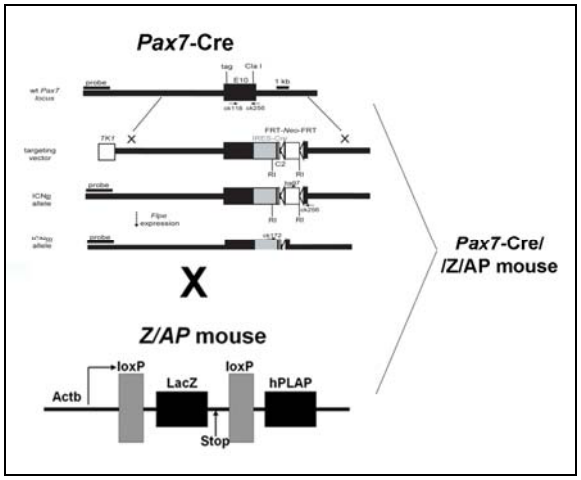

Figure 14. *Pax7*-Cre//Z/AP transgenic mouse.

5.1.4 *Sca1-tTA//LC1-Cre//Z/AP//mdx*

Mice were obtained by breeding *Sca1*-tTA//LC1-Cre//Z/AP with "X chromosome-linked muscular dystrophy" (*mdx*) mice[110] (C57BL/10ScSn-*Dmd*^{mdx}), a Duchenne dystrophy mouse model. Genotyping was performed by PCR on tail DNA using the primers for *mdx* (Table 1). DNA was subjected to an initial 3 minute denaturation at 94°C followed by 39 cycles of denaturation (1 minute at 94°C), annealing (1 minute at 50°C), and elongation (2 minutes at 72°C). This procedure creates a new recognition site for the restriction enzyme *MaeIII* in the wild type but not in the mutant. The PCR products were then digested with 4 units of *MaeIII* at 54°C for 4 hours and separated on 4% agarose gel.

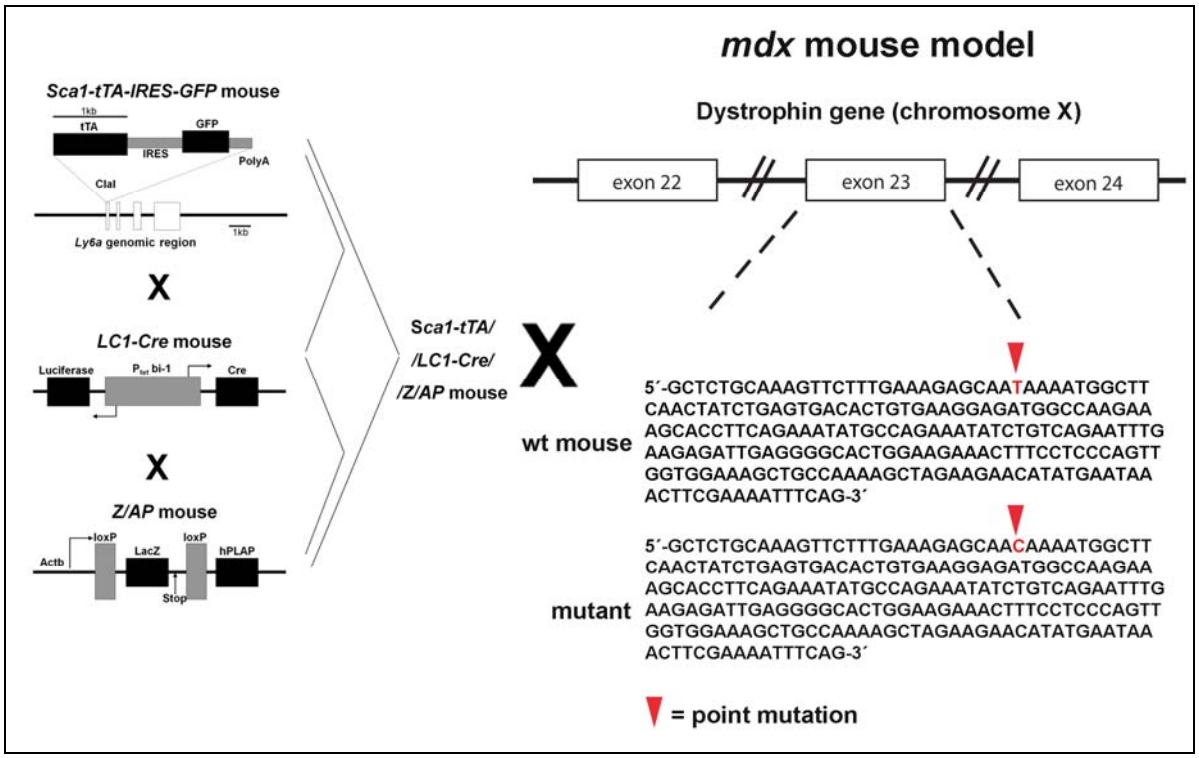

Figure 15. *Sca1*-tTA//LC1-Cre//Z/AP//*mdx* transgenic mouse.
Sca1-tTA//LC-1-Cre//Z/AP mouse was crossed with *mdx* mouse carrying a mutation in the dystrophin gene. The point mutation is in the exon 23 of the Chromosome X, in the mutant a T (Timine) base is exchange with a C (Citosine).

5.1.5 *Sca1-tTA//LC1-Cre//Z/AP//Pax7*$^{loxGu/loxPGu}$

Mice were obtained by breeding *Sca1*-tTA//LC1-Cre//Z/AP with *Pax7*$^{loxPGu/loxPGu}$ (resulting in the deletion of exon1, 2 ,3 in the Pax7 locus[111]). Genotyping was performed by PCR on tail DNA using the following primers: *tTA*, *Cre*, *Pax7*^{loxPGu} (Table 1) and Z/AP was checked as previously described (see section 5.1.1). For the *Pax7*^{loxPGu} primers, DNA was subjected to an initial 3 minute denaturation at 94°C followed by 35 cycles of denaturation (30 seconds at 68°C), annealing (1 minute at 50°C), and elongation (2 minutes at 72°C).

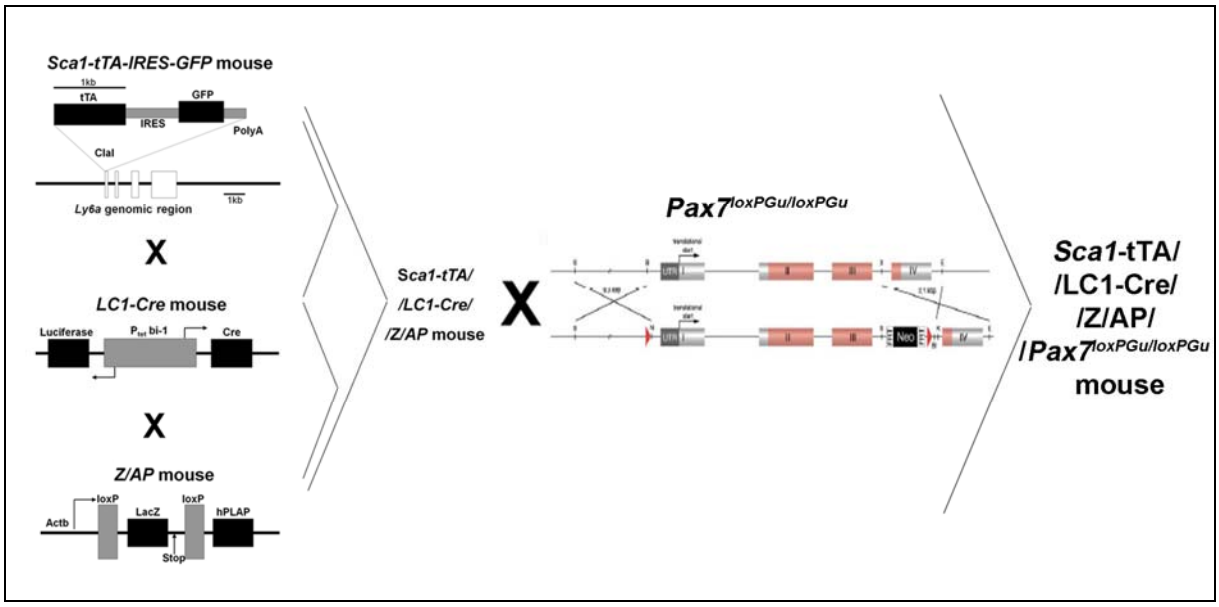

Figure 16. Sca1-tTA//LC1-Cre//Z/AP//*Pax7*$^{loxPGu/loxPGu}$ scheme.
The neomycin-selection cassette presents in the scheme in *Pax7*^{loxPGu} was deleted *in vivo* using a mouse strain expressing FLP-recombinase.

Table 3. List of Primers used for genotyping.

PRIMERS	STRAND	SEQUENCE
tTA	**forward**	5'-GGACGAGCTCCACTTAGACG-3'
	reverse	5'-AGGGCATCGGGTAAACATCTG-3'
Cre	**forward**	5'-AGGCTAAGTGCCTTCTCTACAC-3'
	reverse	5'-GACCAGGTTCGTTCACTCATGG-3'
R26RConfetti	**forward**	5'-GAATTAATTCCGGTATAACTTCG-3'
	reverse	5'-CCAGATGACTACCTATCCTC-3'
GFP	**forward**	5´-CTGGTCGAGCTGGACGGCGACGTAAAC-3´
	reverse	5´-ATGTGATCGCGCTTCTCGTTGGGG-3´
Pax7	**forward**	5'-CTGCGTTTCTCCGAGCTGCAG-3'
	reverse	5'-GCCCGCTGTGTAGGAAAGCC -3'
mdx	**forward**	5´-CTCTGCAAAGTTCTTTGAAAGAGTAA-3´
	reverse	5´-GAAGTTTATTCATATGTTCTTCTAGC-3´
***Pax7*^{loxPGu}**	**forward**	5'-CTGCGTTTCTCCGAGCTGCAG-3'
	reverse	5'-GCCCGCTGTGTAGGAAAGCC -3'

5.2 Cell culture

5.2.1 Murine adult cardiomyocytes

Cardiomyocytes were isolated as previously published[112]. Briefly, mice were injected intraperitoneally with 0.5ml heparin diluted in phosphate buffered saline (PBS) to 100 IU/ml and anesthetized with isoflurane. After, the peritoneal cavity and chest were open with small scissors, the rib cage was carefully peeled back to expose the heart. Pulmonary vessels and aorta were dissected and the heart was collected in a 60-mm dish containing perfusion buffer (calcium free buffer: NaCl 113mM, KCl 4.7mM, KH_2PO_4 0.6mM, Na_2HPO_4 0.6mM, $MgSO_4x7H_2O$ 1.2mM, $NaHCO_3$ 12mM, $KHCO_3$ 10mM, Hepes 10mM, Taurin 30mM, 2,3-Butanedionemonoxime 10mM (B0753), Glucose 5.5mM) at room temperature. The heart was then attached to a burette, tying the aorta to the bottom of the column in order to start the perfusion. After 20 minutes of perfusion, the burette was re-filled with another 10ml of dissociation buffer (calcium free buffer, Liberase DH 0.14mg/ml (#5401089001, Roche), trypsin 0.14mg/ml, $CaCl_2$ 12.5µM). The perfusion was stopped once the heart became pale and no cardiomyocytes were visible in the flow through. The heart was collected in a 10mm dish containing 2.5ml of dissociation buffer and minced using forceps. The tissue was harvested in 2.5ml MC1 stop buffer (dissociation buffer, FCS 10%, $CaCl_2$ 12.5µM) and allowed to settle for 5 minutes. The supernatant was centrifuged at 300rpm for one minute. The supernatant was either collected as a non-cardiomyocyte fraction or discarded. Ten ml of MC2 stop buffer (dissociation buffer, FCS 5%, $CaCl_2$ 12.5µM) were added to the pellet. The calcium content was adjusted, every 4 minutes, with $CaCl_2$ solutions at different concentrations (2 times 50µl 10mM, 100 µl 10mM, 30µl 100mM and 50µl 100mM). The cells were filtered with a cell strainer (Cell Strainer, 100µm Nylon, #352360, BD Falcon) and centrifuged at 300rpm for one minute. The supernatant was either collected with the previous non cardiomyocytes fraction or discarded while the pellet containing the cardiomyocytes fraction was re-suspended in culture medium (M199 w Earle Salt (3113, Gibco), CreatininexH_2O 5mM (C3630, Sigma), L-CarnitinexHCl 2mM (C0283, Sigma), Taurin 5mM (T8691, Sigma), Hepes 25mM, 1% Penicillin/Streptomicyn, 10% FCS, 1% Insulin/Transferrin/Selenium (I1884, Sigma)). Isolated cardiomyocytes were left to attach to chamber slides coated with laminin overnight at 37°C. The plates were coated with laminin at the concentration of 10µg/ml (BD Bioscience, cat. no. 354232) and incubated at 37°C for 2 hours. Attached cardiomyocytes were processed for staining.

5.2.2 Cardiac stem cells (CSCs)

Cardiac Stem Cells were isolated based on density gradient centrifugation using a commercial isolation kit (Millipore, Catalog #SCR061) following the manufacturer's protocol. Briefly, 5 hearts from 2-3 month old C57BL/6 mice were washed in 10ml of cardiac stem cell isolation buffer (Millipore, Catalog #SCR061). The atria were dissected and discarded. The ventricles were minced into small pieces (approximately 1-2 mm in diameter) and collected in a 50ml centrifuge tube containing 6ml of dissociation buffer. The digestion of the tissue was performed for 45 minutes at 37°C at 150 rpm in Cardiac Tissue Dissociation Buffer. Tissue was subsequently dissociated using a 1000µl pipette for 2-5 minutes and further incubated for 10 minutes at 37°C at 150rpm. The digestion was stopped using 24ml of Cardiac Stem Cell Maintenance Medium (Millipore, Catalog #SCR061). Cells were filtered using a Steriflip filter unit, centrifuged at 300g for 5 minutes and suspended in 945µl Cardiac Stem Cell Maintenance Medium. The re-suspended cell suspension was transferred to a new centrifuge tube and 2.055ml of Gradient Solution 1 was added. The suspension was carefully overlaid with 3ml of Gradient Solution 2 and subsequently centrifuged at 1500g for 10 min at room temperature. The upper phase of the cell mixture containing CSCs, was used for further experiments.

5.2.3 Muscle derived stem cells (MDSCs)

Mice (4-8 weeks old) were sacrificed by cervical dislocation. The hind limb muscles were dissected from the bones and collected in medium kept on ice. Tendons and ligaments were carefully detached under the microscope. The muscles were minced using scissors until homogeneous slurry was obtained. The muscle were enzymatically dissociated in DMEM low glucose containing dispase (Art.Nr.354235, BD Biosciences) for 30 minutes, followed by a digestion with 0.2% of collagenase-type I (Art.Nr.4176, Worthington Biochemicals) for 30 minutes. The digestion was performed in a shaker chamber at 37°C with a speed of 500rpm. The muscle suspension was centrifuged at 1200rpm for 5 minutes and the tissue was mechanically dissociated using a 5ml pipette. To obtain a homogeneous cell suspension, the cells were filtered with 40µm cell strainer and centrifuged at 1200rpm for 5 minutes. Cells were suspended in DMEM low containing glucose, 10% FCS and 1% penicillin/streptomycin (P/S).The cell mixture contained muscle derived stem cells (MDSCs), which were used for further experiments.

5.3 Differentiation of cells

5.3.1 In vivo assays

5.3.2 Injections of BMP molecules

The following bone morphogenetic proteins (BMP) molecules were used: hBMP4 (Recombinant Human BMP-4 Heterodimer, R&D Systems, #314-BP/CF), hBMP7 (Recombinant Human BMP-7 Heterodimer, R&D Systems, #354-BP/CF), hBMP4/7 (Recombinant Human BMP-4/BMP-7 Heterodimer, R&D Systems, #3727-BP/CF). Proteins were reconstituted in 4mM HCl to a final concentration of 100µg/ml. In total, a volume of 50µl of the suspension was used. BMP solutions were injected in the left anterior tibialis muscle of 3 month old *Pax7*-Cre//Z/AP and *Sca1*-tTA//LC1-Cre//Z/AP mice. The mice were sacrificed one month after injection and both anterior tibialis muscle (right and left) were collected and used for further experiments.

5.3.3 Injection of glycerol

To induce lipid formations[63,64], a volume of 50µl of 50% (v/v) glycerol (Glycerol, Roth, 7533) was injected in the left anterior tibialis muscle of the mice as previously described[63,64].

5.4 Pathological models

5.4.1 Myocardial infarction and transverse aortic constriction

Myocardial infarction was achieved by permanent ligation of the left anterior descending coronary artery as described previously[113]. Transverse aortic constriction was accomplished by applying a haemoclip (Weck) to the proximal aorta resulting in an acute left-ventricular pressure overload[114].

5.4.2 Muscle regeneration (cardiotoxin injection)

To induce skeletal muscle regeneration, mice were injected with 50µl of 0.06µg/µl cardiotoxin snake venom (cardiotoxin from Naja mossambica mossambica, Sigma, C9759) into the left anterior tibialis muscle. The muscle was injected with cardiotoxin once per month for a total of three times. The injection was always performed in the left leg (tibialis anterior left, TAL) with the right one (tibialis anterior right, TAR) taken as control. Transverse cryosections were prepared and stained for alkaline phosphatase and laminin.

5.5 Histology

5.5.1 Isolation of organs

Mice were sacrificed by cervical dislocation.

The peritoneal cavity was opened and the diaphragm was punctured collapsing the lung. The chest was cut and the heart was quickly collected, washed in 1X PBS to remove excess blood. Then, the heart was directly snap frozen in liquid nitrogen.

The anterior tibialis muscle was collected by cutting the skin of the leg above the heel. The skin was pulled over the hips to expose the muscles. The muscles were collected carefully by cutting the tendons at the extremities. The isolated skeletal muscle was frozen in pre-cooled 2-methylbutane prior to embedding in tissue tek. For *Sca1*-GFP and *R26R-Confetti* mice, the tissues were fixed overnight with 4% paraformaldehyde (PFA). Tissues were kept in -80°C until further usage.

5.5.2 Cryosections

Sections of 6~8µm thickness were prepared on a cryostat (Leica CM3050). After air drying for 30 minutes, sections were kept at -80°C for further usage. To avoid degradation of proteins, sections were processed within one week.

5.6 Immunohistochemistry

5.6.1 Detection of alkaline phospathase activity

Cells or cryosections were fixed with 0.4% glutaraldehyde at room temperature for 5 minutes, washed two times with PBS, heated at 70°C for 30 minutes in PBS, and incubated in NTMT buffer (100mM NaCl, 100mM Tris-HCl pH 9.5, 50mM $MgCl_2$, 1% Tween-20 and 2mM Levamisol) at room temperature for 30 minutes. The color was developed using ready-to-use NCT/BCIP tablet (ref.11697471001, Roche) or a staining solution (168mg 4-Nitroblue tetrazolium (NBT) and 84.5mg 5-Bromo-4-chloro-8-indolilphosphate (BCIP) for each ml of NTMT) at 37°C for at least 2 hours. The reaction was quenched by washing with PBS. A negative control was included in all the stainings.

5.6.2 Trichrome staining

Cryosections were let dry for 30 min at RT. The section were stained using the Trichrome Masson kit (Trichrome stain (Masson) Kit, HT15, Sigma). Briefly, they were rinsed in ddH_2O for 1-2 minutes to remove the OCT in excess and incubated at 56 °C for 15 minutes in preheated Bouin's Solution. After the incubation, the slides were washed first in running tap

water for 20-25 minutes and then 3 seconds in ddH_2O. They were then subsequentially incubated in the following solutions: 1) 5 minutes in Mayer's hematoxylin (Haemalaun) to stain the nuclei; 2) 5 minutes in Biebrich Scarlet-Acid Fuchsin solution; 3) 5 minutes in working Phosphotungstic/Phosphomolybdic acid/ddH_2O solution (1:1:2); 4) 5 minutes in Anilin Blue solution; 2 minutes in acetic acid 1%. Between each step the slides were washed with running tap water for 5 minutes and for three seconds in ddH_2O. The sections were then dehydrated in different alcohol solutions: 90% ethanol for 2 seconds; 96% ethanol for 2 seconds; two times 100% ethanol, each time 2 minutes. As last step the sections were fixed 2 times in xylene for 10 minutes and mounted with Entellan (Entellan®, 107960, Merk).

5.6.3 Oil red O (OrO)

To detect triglycerids, lipids and lipoproteins, Oil red O was used.

Oil red O was dissolved in isopropanol (0,5%). Six ml of this solution were then diluted with 4ml of ddH_2O and left at room temperature for one hour to obtain the working solution. To peform Oil red O staining, cryosections were fixed one hour with 4% PFA at 4°C. After washing with tap water, the sections were incubated in Oil red O staining solution for 15 minutes at room temperature. The nuclei were counterstained with hematoxilin for one minute at room temperature.

5.6.4 Alizarin red

To detect calcium deposits, Alizarin red was used at the concentration of 2% suspended in distilled water. Cryosections were fixed with 4% PFA at 4°C for one hour.

After washing with tap water, the sections were stained with the Alizarin red solution at room temperature for one minute. Tap water was used to stop the reaction. The sections were then rinsed in acetone/xylene 1:1 for 15 seconds and in xylene one minute.

5.7 Immunofluorescence analyses

5.7.1 Antibody staining

Cells or cryosections were fixed in 4% PFA at room temperature for 5 minutes. The sections were washed 3 times with PBS, followed by a permeabilization step with 0.1% or 0.5% Triton X-100/PBS at room temperature for 5 minutes, when necessary. A primary antibody was diluted in PBS and incubated at room temperature for one hour or at 4°C overnight. The list of the antibodies used is provided below (Table 4). After incubation with primary antibody, the sections were washed three times with PBS, followed by incubation with the relative secondary antibody at room temperature for one hour. The dilutions of secondary antibodies

with PBS were as follows: 1:100 when coupled with FITC, GFP, CY2 (green), biotinylated antibodies, anti-streptavidin-Alexa633 (far red) and 1:300 when with TRITC, PE, CY3 (red). The nuclei were counter stained with DAPI (D1306, Molecular Probes, Invitrogen) diluted 1:1000 in PBS. The coverslip was mounted with Mowiol (Mowiol® 4-88, Art.-Num. 0713, Carl Roth) and left dry at 4°C before proceeding to microscopy. Counting and pictures were done using a Leica LEITZ DM RB, Camera: Leica DFC 300FX, Axioplan2, HBO100 Zeiss and Leica SP2-AOBS confocal microscope.

5.7.2 Immunofluorescence staining and cells counting

For the heart, at least 10 slides containing serial sections were prepared. Slides were incubated with antibodies against BS-1, dystrophin, α-smooth muscle actin, *Triticum vulgaris* lectin TRITC conjugate, and with NBT/BCIP staining solution (to check the specificity and efficiency of anti-human alkaline phosphatase placental (hPLAP) antibody staining). Cell-type-specific antibody labeling was performed together with anti-hPLAP antibody and the nuclei were counterstained with DAPI. To calculate the percentage of cell types, the number of $hPLAP^+$/cell-type-marker-positive cells was divided by number of $hPLAP^+$/ lectin-positive cells. To derive P-values, the Wilcoxon Mann-Whitney Test was applied in R. Results are presented as mean ± s.e.m.

For muscle, at least 16 consecutive cross sections were made. In addition to anti-hPLAP antibody, the muscle tissue was stained with dystrophin, laminin and the nuclei were counterstained with DAPI. The number of cells/mm^2 was obtained by measuring the area of each section with ImageJ. The percentage of the fibers was calculated by using “2088” as a total number of fibers present in an anterior tibialis muscle of a mouse[115]. To derive P-values, the Wilcoxon Mann-Whitney Test was applied in R. Results are presented as mean ± s.e.m.

Table 4. Table of antibodies.

Target	Company	Catalog	Application	Dilution	Source
alpha -smooth muscle actin -Cy3 conjugated	Sigma-Aldrich	C6198	ICH/IF	1:300	mouse
BCRP/Abcg2	Abcam	ab24115	Cytospin/IF	1:100	rat
CD45 - PercP conjugated (30-F11)	BD biosciences	553081	FACS	1:100	mouse
CD45.2 -FITC conjugated (clone 104)	eBioscience	11-0454-85	FACS	1:100	mouse
CD31 -PercP conjugated (30-F11)	eBioscience	46-0311	FACS	1:100	mouse
Collagen Type I -Biotin conjugated	Rockland	600-406-103	ICH/IF	1:100	mouse
Dystrophin (clone S8 mandy)	Sigma-Aldrich	D8168	ICH/IF	1:50	mouse
Fc block (CD16/CD32, clone 2, 4G2)	BD-Pharmigen	553142	FACS	1:100	rat
GATA4	Abcam	ab84593	Cytospin/IF	1:100	rabbit
GFP	Abcam	ab6556	Western Blotting	1:10000	rabbit
GFP -AlexaFluor488 conjugated	Life Technology	A21311	IF	1:100	rabbit
human placental Alkaline Phosphatase (hPLAP)	Accurate Chemical & Scientific Corp.	YSRTAHP537	ICH/IF	1:50	rabbit
IgG2a APC (eBR2a)	eBioscience	17-4321-41	FACS (isotype control)	1:100	rat
IgG2a FITC (eBR2a)	eBioscience	553929	FACS (isotype control)	1:100	rat
IgG2a PE (eBR2a)	BD Biosciences	553930	FACS (isotype control)	1:100	rat
IgG2a PercP (eBR2a)	eBioscience	46-4321-82	FACS (isotype control)	1:100	rat
Laminin	Thermo Scientific Labvision	RT-795-P	ICH/IF	1:100	rat
Lectin from Bandeirae simplicifolia -TRITC conjugated (BS-1)	Sigma-Aldrich	L5262	ICH/IF	1:20	
Lectin from Tricicum vulgaris -TRITC conjugated (Lectin)	Sigma-Aldrich	L5266	ICH/IF	1:40	
Ly-6A/E	BD Pharmigen	553333	ICH/IF	1:100	rat
Ly-6A/E	BD Pharmigen	557403	ICH/IF	1:100	rat
Ly-6A/E -APC conjugated (Sca1, clone D7)	eBioscience	17-5981	FACS	1:100	mouse
Ly-6A/E -PercP conjugated (Sca1, clone D7)	eBioscience	12-5981-82	FACS	1:100	mouse
Nanog	Abcam	ab80892	Cytospin/IF	1:100	rabbit
Oct4	Abcam	ab19857	Cytospin/IF	1:100	rabbit
Pan-Actin	Cell Signaling Technology	4968	Western Blotting	1:1000	rabbit
PDGFRalpha (anti-mouse CD140a, clone APA)	eBioscience	17-1401	FACS	1:100	mouse
Phalloidin -AlexaFluor633	Life Technologies	A22284	ICH/IF	1:300	
SM/C2.6 -Biotin conjugated	gift from profesor Soichiro Fukada, Department of Immunology, Graduate School of Pharmaceutical Science, Osaka University, Osaka 565-0871, Japan		FACS	1:50	rat
Sox2	Abcam	ab97959	Cytospin/IF	1:100	rabbit
Streptavidin -APC conjugated	BD Biosciences	554067	FACS	1:100	

5.7.3 Confocal microscopy and three-dimensional (3D) reconstructions

Sections were examined by laser scanning confocal microscopy (Leica TCS SP2, AOBS). After data acquisition, the images were transferred to Silicon Graphics Indy workstation (Silicon Graphics) for three-dimensional (3D) reconstruction using Imaris, the 3D multi-channel image processing software (Bitplane, Zürich, Switzerland) as described by Kostin *et al.*[116].

5.7.4 Fluorescent in situ hybridization (FISH)

Isolated cardiomyocytes were stained with mouse IDetect™ Chromosome Y FISH Paint Probe Red (Labs Inc Biotechnology) as described previously[117]. Briefly, slides were fixed in 4% PFA and dehydrated in 70, 80, and 100% ethanol for one minute each. The mouse paint probe and hybridization mixture were mixed at a ratio of 3:7. The mixture was applied to the cells, covered with a plastic coverslip, glued with rubber cement, and denatured at 69°C for 2 minutes and allowed to re-anneal for 16 hours at 37°C. The next day two post hybridization washes were done, using the following solutions: 2X SSC and 0.2% Tween at room temperature, 0.4X SSC and 0.2% Tween at 73°C for 2 minutes, and 2X SSC at room temperature for one minute. Immunofluorescence staining of FISH-hybridized cells was performed as described above. The following antibodies were used: rabbit human placental alkaline phosphatase (1:50, Axell), goat anti rabbit CF™488 (1:100, Biotium), AlexaFluor633 phalloidin (1:300, Invitrogen). Nuclei were stained with DAPI at room temperature for 5 minutes. Pictures were taken using a Leica SP2-AOBS confocal microscope. 10 randomly selected fields were examined and counted.

5.8 Fluorescence-activated cells sorting (FACS)

5.8.1 FACS

Cells were isolated and contaminating red blood cells were removed by incubating the single cell suspension in sterile filtered de-ionized water at 25°C for one minute followed by two washing steps with PBS. The resulting cell suspension was pre-incubated with blocking rat-mouse antibodies to the FcRγ III/II receptor (clone 2.4G2; BD Biosciences, Catalog #553141) before staining with primary antibodies. The following conjugated primary antibodies were used: fluorescein isothiocyanate mouse CD45.2 (anti-CD45.2; clone 104; eBioscience, Catalog #11-0454), phycoerythrin-conjugated anti-CD45 (30-F11; BD Biosciences, #553081), peridinin chlorophyll protein-eFluor710 conjugated anti-CD31 (clone 390; eBioscience, Catalog #46-0311), allophycocyanin-conjugated anti-SCA1 (Ly-6A/E, clone D7;

eBioscience, Catalog #17-5981), SM/C2.6 biotinylated (gift from professor Soichiro Fukada, Japan), allophycocyanin-conjugated anti-Streptavidin (BD Bioscience, Catalog #554067), PDGFRalpha (anti-mouse CD140a, clone APA, eBioscience, Catalog#17-1401) (Table 4). Cells were analyzed and sorted as single cells into a 96-well plate using a MoFlo-cytometer (BeckmanCoulter). Data were analyzed with FlowJo software (TreeStar).

5.8.2 Cell populations isolated by FACS

In the heart $SCA1^{+}CD31^{-}CD45^{-}$ cells were isolated**.**

In the skeletal muscle different populations were considered: $SM\text{-}C2.6^{+}SCA1^{+}CD31^{-}CD45^{-}$, $SM\text{-}C2.6^{+}SCA1^{-}CD31^{-}CD45^{-}$, $PDGFRalpha^{+}SCA1^{+}CD31^{-}CD45^{-}$, $PDGFRalpha^{+}SCA1^{-}CD31^{-}CD45^{-}$, $SM\text{-}C2.6^{-}SCA1^{+}CD31^{-}CD45^{-}$ and $PDGFRalpha^{-}SCA1^{+}CD31^{-}CD45^{-}$ cells.

5.8.3 Cytospin

After sorting, cells were cyto-centrifuged at 700rpm for 5 minutes using a Shandon Cytospin 2 Centrifuge (Block Scientific). Slides were fixed with 4% PFA for 5 minutes and air-dried at room temperature. The slides were stored at -80°C until further usage.

5.9 Molecular biology and single cell analyses

5.9.1 Microarray analyses

RNA was isolated using TRIzol reagent (Life Technologies) and processed for microarray experiments as described previously[118]. After scanning of the arrays, CEL files were up loaded to previously described web interfaces: (1) "Exon Array Analyzer (EAA)" (http://eaa.mpi-bn.mpg.de/)[119] for GeneChip® Exon 1.0 ST Arrays (Affymetrix) (called "exon array"); and (2) "Gene Array Analyzer (GAA)" (http://gaa.mpi-bn.mpg.de/)[118] for GeneChip® Gene 1.0 ST Arrays (Affymetrix) (called "gene array"). Multi-Array Average (RMA)[120] normalized values were utilized for further analyses using R (http://cran.r-project.org/) for statistical analyses, MultiExperiment Viewer (MeV)[121] for hierarchical clusterings as well as heatmaps and TreeGraph 2[122] for visualization of clustering trees.

For comparison of gene arrays, the following datasets deposited at the Gene Expression Omnibus (GEO) were used: (1)GSE14414: "**eCardio.1**", "**eCardio.2**", "**eCardio.3**" for murine embryonic cardiomyocytes and "**eCFibro.1**", "**eCFibro.2**", "**eCFibro.3**" for murine embryonic cardiac fibroblasts[123]; (2) GSE20991: "**eKEndo.1**", "**eKEndo.2**", "**eKEndo.3**" for endothelial cells from kidneys of Tie2-GFP transgenic mice[124]; (3) GSE22292: "**nCardio.1**", **nCardio.2**" , "**nCardio.3**" for murine neonatal cardiomyocytes and "**nCFibro.1**" , "**nCFibro.2**" , "**nCFibro.3**" for murine neonatal cardiac fibroblasts[125]; (4) GSE20991:

"**aCFibro.1**", "**aCFibro.2**", "**aCFibro.3**" for murine adult cardiac fibroblasts[124]; (5) GSE21324: "**aKEndo.1**", "**aKEndo.2**", "**aKEndo.3**" for glomerular endothelial cells from adult Tie2-GFP mice[124]; (6) GSE34948: "**Endo.N.1**", "**Endo.N.2**" for endothelial cell lines derived from murine embryonic stem cells expressing N-cadherin; "**Endo.VE.1**", "**Endo.VE.2**" for endothelial cell lines derived from murine embryonic stem cells expressing VE-cadherin; and "**Endo.VE+N.1**", "**Endo.VE+N.2**" for endothelial cell lines derived from murine embryonic stem cells expressing both N-cadherin and VE-cadherin[126]. Furthermore, (7) sample data sets of murine adult hearts ("**aHeart.1**", "**aHeart.2**", "**aHeart.3**") were downloaded from Affymetrix[118]. The followings data sets generated in our laboratory were added: (8)Undifferentiated murine ES cells: "**ES.1**" and "**ES.2**"[118]; and (9) Adult bone marrow-derived multipotent mesenchymal stem cells (BM-MASCs): "**MASC.1**" for clone #1 and "**MASC.2**" for clone #2[113]. All data sets were analyzed at once using the GAA web interface to minimize biases.

5.9.2 Single cell analysis

To perform single cell quantitative RT-PCR experiments the BioMarkTM HD System (Fluidigm Inc.) was utilized.

Different populations were considered in heart and muscle based on SCA1 expression. In the heart $SCA1^{+}CD31^{-}CD45^{-}$ cells were used. In the muscle $SM\text{-}C2.6^{+}SCA1^{+}CD31^{-}CD45^{-}$, $SM\text{-}C2.6^{+}SCA1^{-}CD31^{-}CD45^{-}$, $PDGFRalpha^{+}SCA1^{+}CD31^{-}CD45^{-}$, $PDGFRalpha^{+}SCA1^{-}CD31^{-}CD45^{-}$ populations were sorted. Single cells from each population were sorted into individual wells of a 96-well plate containing 5µl of Cells Direct 2X Reaction Mix (Life Technologies, Catalog # PN11753) with 0.05 units of RNase inhibitor. Care was taken to deliver only single cells into individual wells. Plates were centrifuged after sorting and immediately frozen on dry ice and stored at -80°C until further usage. Frozen plates were thawed on ice before reverse transcription according to the Fluidigm manual with the following modifications. In the heart, for pre-amplification, a primer mix consisting of 436 primer pairs (263 genes and one non-coding RNA (ncRNA) (*Airn*)) was used, in the muscle 576 primer pairs (288 genes) were used. The final concentration of each primer was 437nM for CSCs and 1052nM for skeletal muscle populations. All primers were designed to span two exons to prevent amplification of contamination genomic DNA. All primers were tested for the presence of single PCR products on agarose gels and for a single peak in the melting curve analysis using cDNA as templates using an iCycler (BioRad) in the presence of SYBR Green I for 40 cycles of amplifications. The cDNA was obtained from murine adult heart and murine adult skeletal

muscle. The number of cycles for the Reverse Transcription (RT)-Specific Target Amplification (STA) (STA-RT) was 20.

The following control samples were prepared: undifferentiated ES[118], P19CL6[127], CSCs and C2C12. To assess the performance of the reaction, 100, 10 and 1 cells were prepared from each of the above mentioned cell types. The buffer without cells was used as a negative control. For $SCA1^+CD31^-CD45^-$ CSCs sorted cells, 96 single cells were prepared. For the muscle samples 182 single cells were chosen among the following different populations: SM-$C2.6^+SCA1^+CD31^-CD45^-$ (32 cells), SM-$C2.6^+SCA1^-CD31^-CD45^-$ (32 cells), $PDGFRalpha^+SCA1^+CD31^-CD45^-$ (31 cells), $PDGFRalpha^+SCA1^-CD31^-CD45^-$ (23 cells). After pre-amplification, samples were treated with exonuclease I to remove possible unincorporated primers and diluted 10-fold. For quality control, 1µl of each of the diluted samples was used for real-time RT-PCR reactions in the iCycler (Biorad) using EvaGreen DNA binding dye (Biotium, Catalog #PN31000) and primer pairs against *Ly6a, Pax7, Pdgfralpha* were considered to monitor successful samples preparation. All samples passed this quality check and were used for each 96.96 Dynamic Array IFC.

After the data were generated of data, samples with no Ct value for endogenous control genes (*Actb* and *Gapdh*) and with high variation in Ct values, among three independent measurements of *Actb*, were excluded from further analysis. As a result, 74 heart samples and 106 muscle samples [SM-$C2.6^+SCA1^+CD31^-CD45^-$ (29 single cells), SM-$C2.6^+SCA1^-CD31^-CD45^-$ (29 single cells), $PDGFRalpha^+SCA1^+CD31^-CD45^-$ (31 cells), $PDGFRalpha^+SCA1^-CD31^-CD45^-$ (17 single cells)] were selected for further analyses.

The data were normalized as previously described[128]. Briefly, all the Ct values were converted into relative expression levels by subtracting the values obtained from the assumed baseline 40 (number of cycles used in the PCR reaction). Samples without Ct value were set to "0". The gene values were then normalized to the endogenous control by subtracting the *Actb* expression level to derive geometric means on a linear scale[128]. Finally, these normalized values were used to calculate "delta delta Ct (*ddCt*)" values.

The following filter was applied to uncover the heterogeneity of $SCA1^+CD31^-CD45^-$ single cells: if for a certain gene the Ct value was detected in less than 7 cells (10% of 74 $SCA1^+CD31^-CD45^-$ single cells), the gene was removed from analysis. This filtering step left a total number of 103 genes, which was used to create a matrix of 74 $SCA1^+CD31^-CD45^-$ single cells x 103 genes.

In order to understand the molecular signatures of single cells, *ddCt* of internal controls were derived and were used for further normalization. The following cell types consisting of 100

cells were used as internal controls: undifferentiated ES cells, P19CL6 cells, and CSCs for CSCs and C2C12 cells and MDSCs for the muscle. Furthermore, in the case of skeletal muscle, the populations SM-C2.6^{+}SCA1^{-}CD31^{-}CD45^{-}(A), SM-C2.6^{+}SCA1^{+}CD31^{-}CD45^{-}(B), PDGFRalpha^{+}SCA1^{-}CD31^{-}CD45^{-}(D), PDGFRalpha^{+}SCA1^{+}CD31^{-}CD45^{-}(E) were compared using the student T test (2 tails and 2 sample unequal variance) to distinguish if the presence of SCA1 could mark a separation at the gene expression level.

The hierarchical clustering and heatmaps were generated using the MultiExperiment Viewer (MeV)[121]. The data were analyzed using the nine different clustering algorithms (Hierarchical, K-means, DIANA, PAM, CLARA, FANNY, SOM, mclust and SOTA) present in the R package clValid.

6 RESULTS

6.1 Identification and analyses of resident cell populations in the heart and their contribution to cardiac tissue renewal

6.1.1 Sca1 progenitors cells are detected in vivo during normal physiological conditions

The presence of resident stem cells in the heart and in other organs and tissues has become apparent over the past years. Different populations of cardiac resident stem cells have been described in the literature based on the expression of different markers[55]. One population among them has been defined as being positive for stem cell antigen 1 (Sca1/Ly6A)[71,129]. However, to date, its contribution *in vivo* has not been clearly elucidated.

In order to investigate the role of these resident stem cells and in particular the contribution of *Sca1* progenitor cells in heart regeneration *in vivo*, the *Sca1*-tTA//LC-1-Cre//Z/AP triple transgenic mouse system was utilized (Figure 12a). In *Sca1*-tTA//LC-1-Cre//Z/AP mice, the cells that have expressed and express *Sca1* were labeled with human alkaline phosphatase (hPLAP). Briefly, in this mouse model, tetracycline transactivator (tTA) is under the control of the *Sca1* (*Ly6a*) promoter. Once expressed, tTA can interact with the P_{tet}bi-1 promoter, present in the LC1-Cre locus, consisting of a bidirectional transcription unit able to encode for Cre and the luciferase genes. The recruitment of tTA to the P_{tet}b-1 promoter stimulates the transcription of Cre-recombinase. The Cre will recombine the *loxP*-sites present on the Z/AP locus. In this reporter mouse the lacZ gene, fused with a stop codon cassette, is floxed by two *loxP* sites and is upstream of the human placental alkaline phosphatase gene (hPLAP). In the absence of Cre, the lacZ gene is transcribed, and due to the stop codon the expression of hPLAP does not take place. When Cre is transcribed from LC1 allele, the recombination of the *loxP* sites can take place leading to the excision of lacZ together with the stop cassette and allowing the expression of hPLAP.

In order to address whether in cardiac tissue a population of cells derived from *Sca1* progenitor cells is present, the hearts of mice from 2 to 18 months old were subjected to immunohistochemistry to detect alkaline phosphatase activity (Figure 17a). Furthermore, immunofluorescence staining was performed to detect the type of cells *Sca1* progenitors are able to give rise to. Human placental alkaline phosphatase antibody (AP) was combined with BS-1 to detect interstitial cells, with alpha smooth muscle actin for smooth muscle cells or with dystrophin for cardiomyocytes (Figure 17b). The percentage of the different *Sca1*-derived cells types was calculated by normalizing the number of *Sca1*-derived cells positive for lectin (from *Triticum Vulgaris*), a marker labeling all cellular membranes and

consequently all the AP^+-cells present in the sections. Counting revealed a constant proportion in the distribution of the three major cell types present in the heart during aging. The great part of cells expressing AP was constituted by endothelial/interstitial cells (an average of 87.48%), whereas a small portion by cardiomyocytes (2.97%) and smooth muscle cells (1.65%). When the number of counted cells was normalized to the area of a section (cells per mm^2) a linear increase in the number of AP^+-cardiomyocytes was observed from the age of 2 months to 18 months (Figure 17c & d). The presence of endothelial cells, smooth muscle cells and cardiomyocytes positive for AP confirms that *Sca1* progenitor cells can give rise to these lineages. Furthermore, the increased number of AP^+-cardiomyocytes during aging suggests that *Sca1* progenitor cells contribute to heart regeneration.

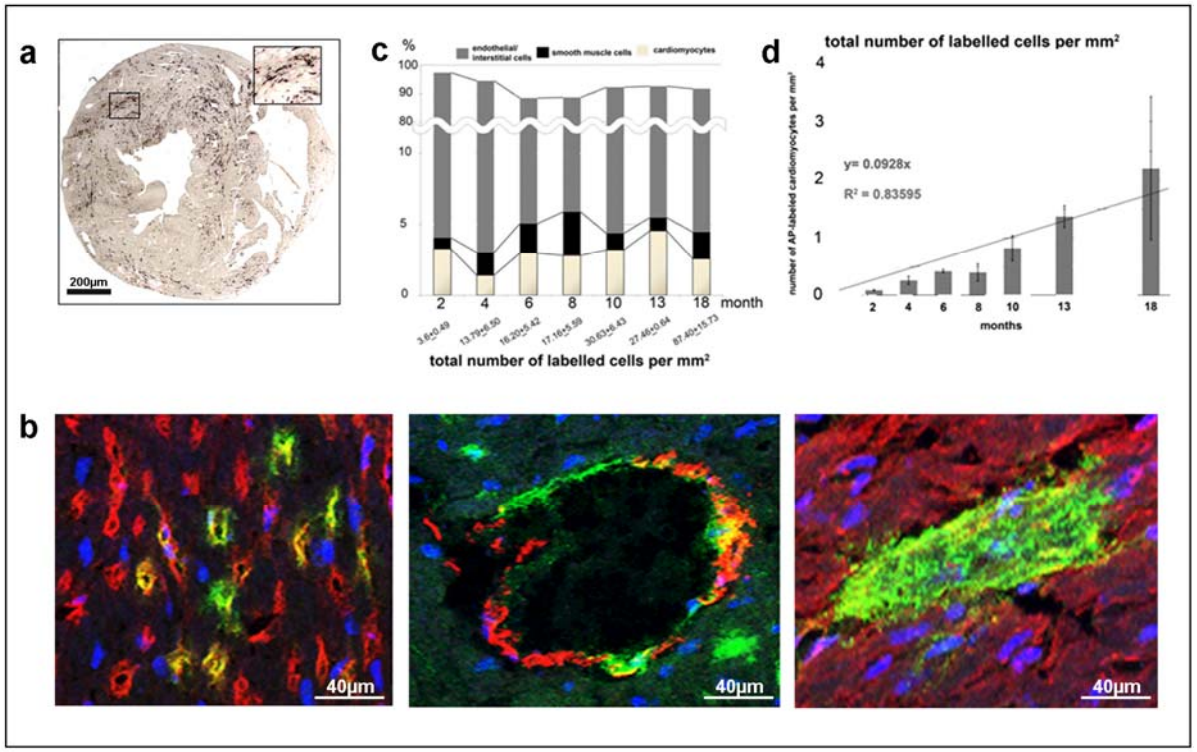

Figure 17. *Sca1* progenitor cells *in vivo*.
(a) Alkaline phosphatase staining of 2 months old *Sca1*-tTA//LC1-Cre//Z/AP murine heart. The staining shows a broad and random distribution of the *Sca1*$^+$ progenitor cells and their descendants. **(b)** Examples of immunofluorescence staining of endothelial/interstitial cells (BS1 in red), smooth muscle cells (alpha smooth muscle actin in red) and cardiomyocytes (dystrophin in red). The AP^+-labeled cells were shown in green. **(c)** Distribution of labeled cells in the three different cells types: about 87.48% were endothelial cells, 2.97% cardiomyocytes and 1.65% smooth muscle cells. The percentage was obtained counting the number of cells in consecutive sections of mice with an age between 2 and 18 months. Markers specific for endothelial cells, smooth muscle cells and cardiomyocytes were considered. **(d)** The number of cardiomyocytes per mm^2 presents a linear increase during the aging.

6.1.2 Sca1 progenitor cells contribute to cardiomyocyte renewal under pathological conditions

During aging in the heart of *Sca1*-tTA//LC-1-Cre//Z/AP mice, it was possible to detect AP^+-cells belonging to the all three major lineages as well as an increased number of cardiomyocytes expressing AP. These results suggest the possibility that a *Sca1*-expressing cell population contributes to the maintenance of cardiac homeostasis under normal physiological conditions. However, recently it was reported that cardiac stem cells play an important role in cardiac regeneration in response to damage[48]. Therefore the contribution of endogenous *Sca1*-expressing cells to myocardial regeneration was investigated under pathological conditions. For this purpose, the following two injury models were used: myocardial infarction and transverse aortic constriction (TAC).

In the first model, 3 month old mice were subjected to permanent ligation of the left anterior descending coronary arteries (LAD) to induce myocardial infarction (MI). Although a relative decrease of AP^+-cells in the infarcted area and in the border zone was observed (Figure 18a & b), clusters of AP^+-BS-1 expressing endothelial/interstitial cells were found in the septum. Overall, the number of AP^+-cardiomyocytes remained constant in the post-MI heart (Table 5).

In the second model, pressure-induced cardiac hypertrophy was induced by performing transverse aortic constriction (TAC). This strategy was used to test whether this damage could promote the generation of new *Sca1*-derived cardiomyocytes. First, AP staining was performed to obtain an overview of the AP^+-cells distribution within the heart of *Sca1*-tTA//LC1-Cre//Z/AP mice after the damage (Figure 18c). All mice were challenged by TAC at the age of 3 months. Four weeks after TAC-operation, despite the fact that the total number of AP-labeled cells did not change significantly (18.68±6.40 cells/mm^2 for TAC-operated hearts and 13.79±6.50 cells/mm^2 for the aged matched hearts; P=0.74), the number of AP^+-cardiomyocytes increased more than three-fold (0.17±0.06 cells/mm^2 and 0.57±0.10 cells/mm^2 for the aged-matched and TAC-operated hearts, respectively; P=0.03) (Figure 18d). Five months after TAC-operation, the number of AP^+-cardiomyocytes increased two fold compared to the sham operated mice (0.84±0.49 cells/mm^2 for TAC-operated hearts and 0.4±0.15 cells/mm^2 for the aged matched hearts; P=0.5) and the total number of AP^+-cells (compared to the age-matched 8-month old hearts) increased three fold (45.15±7.46 cells/mm^2 for TAC-operated hearts and 15.23±2.94 cells/mm^2 for the aged matched hearts; P=0.05).

These data suggest that the *Sca1*-expressing cells are involved in myocardial regeneration after damage and the type of damage might influence the fate decisions of *Sca1*-expressing cells in heart regeneration.

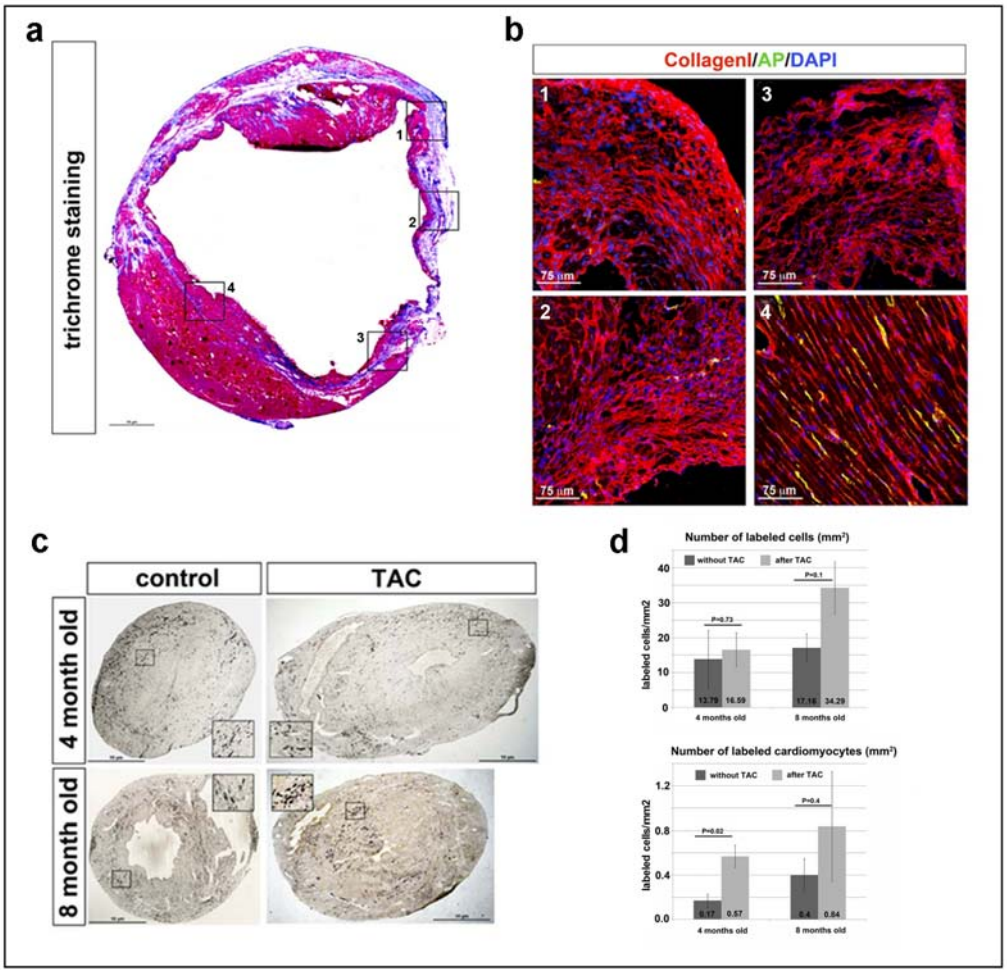

Figure 18. *Sca1* progenitor cells contribution *in vivo* under pathological conditions (myocardial infarction and transverse aortic constriction).
(a) Trichrome staining of a representative section of four month old *Sca1*-tTA//LC1-Cre//Z/AP mice, one month after LAD ligation. **(b)** Triple labeling of areas from different regions of post-infarcted hearts stained for collagen I (red), AP (anti-hPLAP antibody, green), and nuclei (DAPI, blue). The numbers indicate the different regions of the operated heart as indicated in the picture (**b**). Areas bordering the scar (1, 4) identified by massive deposition of collagen I or within the scar (3), show a reduction of *Sca1*-derived cells. An increase in *Sca1*-derived cells (green) was found in areas showing a compensatory hypertrophy (4). **(c)** AP-staining of cross-sections of 4 and 8 months old *Sca1*-tTA//LC1-Cre//Z/AP sham operated mice (**control**) and relative age-matched mice subjected to TAC at 3 months old (**TAC**). **(d)** Numbers of total AP^+-cells and AP^+-cardiomyocytes per mm^2 in hearts of TAC-operated and control mice at 4 and 8 months of age.

Table 5. Distribution of labeled cells after myocardial infarction.

	AP/BS1	AP/Dystrophin	AP/alpha-SM-actin
4 months control	87.67% 92.33% 94.03%	1.37% 1.59% 1.24%	2.05% 1.32% 1.49%
	91.34±1.90%	1.4±0.1%	1.62±0.22%
4 months after myocardial infarction	90.84% 81.48% 84.29% 92.75% 96.31% 93.03%	2.29% 5.56% 2.14% 0.86% 0.89% 1.07%	3.82% 5.56% 4.29% 1.23% 1.77% 3.22%
	89.78±2.33%	2.14±0.73%	3.32±0.66%

Percentage of *Sca1*-derived (AP^+) endothelial/interstitial cells ($BS\text{-}1^+$), cardiomyocytes, (dystrophin positive), and smooth muscle cells (alpha smooth muscle positive) at 4 months of age without and after myocardial infarction. LAD was performed at 3 months of age. Percentages were calculated by dividing the number of specifically labeled cells (e.g. dystrophin-positive cells) by the number of lectin-positive/ AP^+-cells, representing the total number of AP-labeled cells in the heart. SEM values and sample numbers are indicated. All labeled cells in the respective sections were counted.

6.1.3 The presence in vitro of mononucleated cardiomyocytes reinforces the contribution of progenitor cells to heart self-renewal

The heart has long been considered a post mitotic organ unable to self-renew. However, recently it has been shown that, although at a low rate, the heart exhibits a certain turnover[36]. Two hypotheses have been proposed to explain the possible cellular source responsible for this renewal. The first sustains the presence of common resident precursor or stem cells (called "cardiac progenitor/stem cells (CSCs)")[130-132], that are able to differentiate and give rise to new cardiomyocytes. The second claims that existing cardiomyocytes are able to re-enter the cell cycle, divide again and originate new cardiomyocytes[133,134]. Cardiomyocytes are defined to be terminally differentiated cells presenting more than one nucleus[135]. However, the presence of cardiomyocytes with one nucleus in the heart, could lead to the assumption that these mononucleated cells are derived from CSCs rather than from pre-existing multinucleated cardiomyocytes. In order to understand if mononucleated cardiomyocytes are present in the mouse heart and their distribution during aging, cardiomyocytes were isolated from the hearts of 3, 6, 18 and 21 month old C57BL/6 mice. The number of mice considered for each group was a minimum of three. The cells were stained with phalloidin, which provides a general overview of the myocardial morphology whereas DAPI was used to visualize the nuclei (Figure 19a). Ten random pictures were taken from different fields of the slides to achieve an unbiased, statistically-sounds analysis. In each field, the number of nuclei present in each cardiomyocyte was counted. As shown in Figure 19b, from the age of 3 to 21 months, the majority of cardiomyocytes were found to be binucleated (3 months: 73.91%±4.05; 6 months: 68.90%±5.61; 9 months: 63.05%±3.66; 21 months: 59.54%±4.86). In comparison mononucleated cardiomyocytes were detectable at a constant level until the age of 6 months, while they increased approximately 17% in 6 to 9 month old mice, (3 months: 21.48%±2.22; 6 months: 21.34%±1.96; 9 months: 34.19%±3.01; 21 months: 33.97%±3.54). A small percentage of cardiomyocytes, of about 4.71%, were trinucleated (3 months old: 2.81%±1.35; 6 months old: 7.15%±1.15; 9 months old: 2.39%±0.68; 21 months old: 6.49%±1.52), while tetranucleated cardiomyocytes were found in 3 and 6 month old mice (3 months old: 1.79%±0.71; 6 months old: 2.44%±0.69) (Figure 19b). These data suggest the presence of a constant number of mononucleated cardiomyocytes *in vitro* during aging.

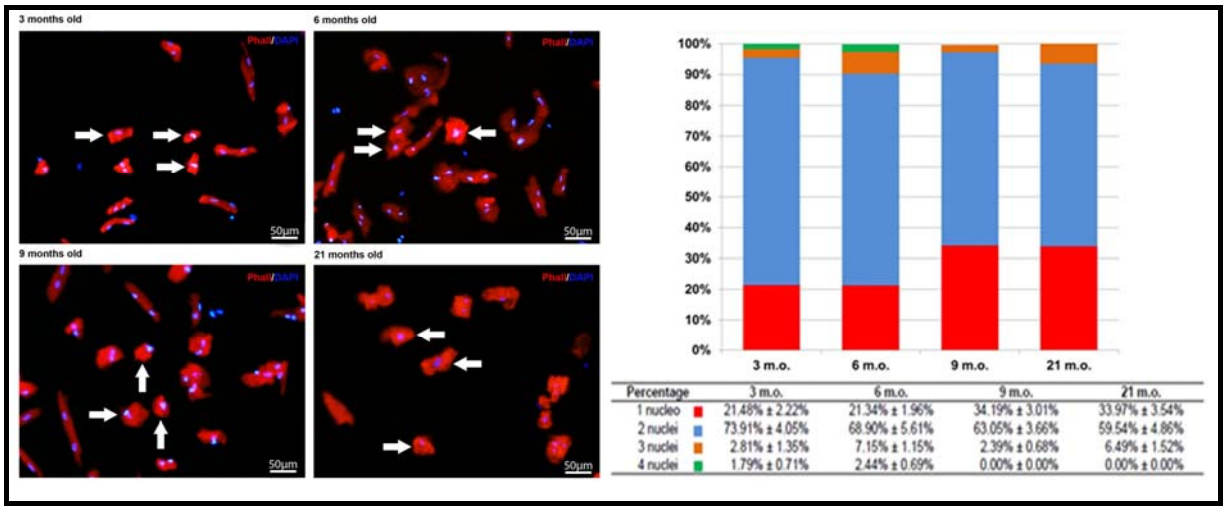

Percentage	3 m.o.	6 m.o.	9 m.o.	21 m.o.
1 nucleo	21.48% ± 2.22%	21.34% ± 1.96%	34.19% ± 3.01%	33.97% ± 3.54%
2 nuclei	73.91% ± 4.05%	68.90% ± 5.61%	63.05% ± 3.66%	59.54% ± 4.86%
3 nuclei	2.81% ± 1.35%	7.15% ± 1.15%	2.39% ± 0.68%	6.49% ± 1.52%
4 nuclei	1.79% ± 0.71%	2.44% ± 0.69%	0.00% ± 0.00%	0.00% ± 0.00%

Figure 19. Number of nuclei in cardiomyocytes.
(a) Cardiomyocytes were freshly isolated from 3, 6, 9, 21 month old C57BL/6 mice. After overnight culture, they were stained with Phalloidin TRITC (in red) and the nuclei counterstained with DAPI (in blue). **(b)** Summary of the number of cardiomyocytes counted at different ages discriminating on the base of the number of nuclei detected. Although a majority of cardiomyocytes turned out to be binucleated, a substantial increase in the number of mononucleated cardiomyocytes from the age of 6 to 9 months was observed.

6.1.4 Identification of newly regenerated cardiomyocytes not derived from fusion events

The identification of mononucleated cardiomyocytes and their increase during aging suggest the possibility of the existence of newly generated cardiomyocytes. However, it is known that cardiomyocytes as well as hepatocytes, present polyploidy (more than one set of chromosomes)[136], although this event is generally rare in mammals. Polyploidy normally derives from cell to cell fusion events, although it has been stated that this phenomenon might also occur during physiological and pathological conditions either in response to aging (e.g. cell senescence) or to stress (e.g. oxidative and mechanical insults)[136]. If one assumes that cardiomyocytes are polyploid then, the mononucleated fraction identified in the previous section must present only one set of chromosomes, in order to suggest that these cells do not originate from cell fusion events but rather come from precursor cells able to differentiate into this cell type. In order to examine the polyploidy of their nuclei, cardiomyocytes were isolated from 2 month old *Sca1*-tTA//LC1-Cre//Z/AP male mice. Using FISH (Fluorescence *in situ* hybridization) against the Y chromosome, cardiomyocytes were counted based on the number of nuclei and their Y chromosome. As shown in Figure 20, 18.88±2.97% of isolated AP^+-cardiomyocytes contained one nucleus with one Y-chromosome, while 8.06% of all mononucleated cells were AP^+. 73.50% contained more than one nucleus but still had only one Y-chromosome per nucleus (68.28±14.27, 3.55±6.60 and 1.67±1.67 for 2, 3 and 4 nuclei, respectively) and 7.83±5.65% contained two nuclei with more than one Y-chromosome in at least one nucleus. These data are comparable to the number of cardiomyocytes found in the

AP-negative fraction. In this case, 25.60±6.02% had one nucleus and one Y-chromosome and 71.98% had more than one nucleus but one Y-chromosome per nucleus (64.38±7.85, 3.62±2.11 and 3.98±2.30 for 2, 3 and 4 nuclei, respectively). Furthermore, the AP-negative fraction revealed a slight decrease in the number of cardiomyocytes with two nuclei but more than one Y-chromosome in at least one nucleus (2.41±1.67%). In general, in both the AP^+ (derived from *Sca1* progenitor cells) and AP^- cardiomyocytes, it was possible to find a similar pattern regarding the number of nuclei. Although the majority was constituted by one Y-chromosome-binucleated cardiomyocytes, still a percentage of one Y-chromosome-mononucleated cardiomyocytes was detected. These data highlight that, cardiomyocytes with one nucleus and only one Y-chromosome could not derive from cell fusion events, but rather are newly generated. In the case of the AP^+-cardiomyocytes, the one Y-chromosome-mononucleated fraction possibly represents the outcome of *Sca1*-derived cardiac stem/progenitor cells (CSCs) differentiation.

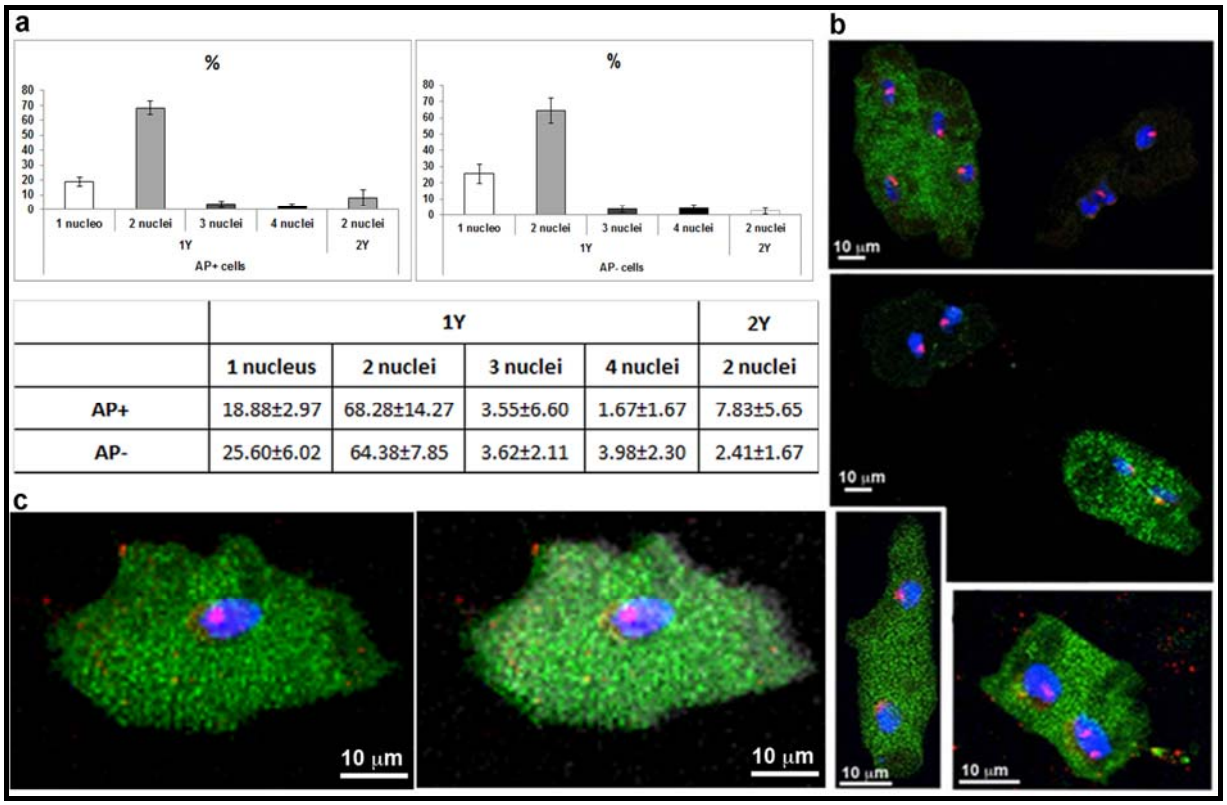

	1Y				2Y
	1 nucleus	2 nuclei	3 nuclei	4 nuclei	2 nuclei
AP+	18.88±2.97	68.28±14.27	3.55±6.60	1.67±1.67	7.83±5.65
AP-	25.60±6.02	64.38±7.85	3.62±2.11	3.98±2.30	2.41±1.67

Figure 20. Cardiomyocyte regeneration and polyploidy.
Adult cardiomyocytes were isolated from 2 month old *Sca1*-tTA//LC1-Cre//Z/AP male mice. After overnight culture, FISH was performed using Y-chromosome probe (in red), in combination with AP (anti-hPLAP antibody in green) and nuclei were counterstained with DAPI (blue). **(a)** Representative graphs and relative table evaluating the number of nuclei and presence of Y chromosome in the AP^+ and AP-negative cardiomyocytes fractions. **(b)** Examples of binucleated AP^+-cardiomyocytes with different numbers of Y-chromosomes. **(c)** An example of mononucletated AP^+-cardiomyocyte (green) with one Y-chromosome red, DAPI (in blue) (left picture) and stained also with Phalloidin-633 (in gray) (right picture).

6.1.5 CSCs are located beneath the basal lamina suggesting the presence of a niche in the heart

During the experiments performed in section 6.1.4, the presence of small, round shape cells attached to cardiomyocytes was observed. Although a strong dissociation method was used, it seemed that these small cells were tightly attached to isolated cardiomyocytes. In order to characterize these cells and to understand whether they belong to a *Sca1* subpopulation of cells, immunostaining with an antibody against SCA1 was performed.

Only these small round cells were positive for SCA1 surface marker, whereas cardiomyocytes never showed expression of this marker (Figure 21b). To confirm this observation, cardiomyocytes were isolated from *Sca1*-GFP mice. In this mouse strain the GFP expression is under the control of *Sca1* promoter, therefore each cell presenting an active *Sca*1 promoter will be GFP positive. As shown in Figure 21a, small, round shaped GFP^+-cells were observed right next to the isolated cardiomyocytes. A quantitative analysis revealed that 8.55% cardiomyocytes owned an attached $SCA1^+$-cell. To identify the structural position of the above identified small cells, laminin immunostaining was performed (Figure 21c). The co-staining of SCA1 together with laminin revealed the possible location beneath the basal lamina, which resembles the location of skeletal progenitor muscle cells called "satellite cells"[41]. This result highlights the possible presence of a niche where *Sca1*-expressing cells are confined.

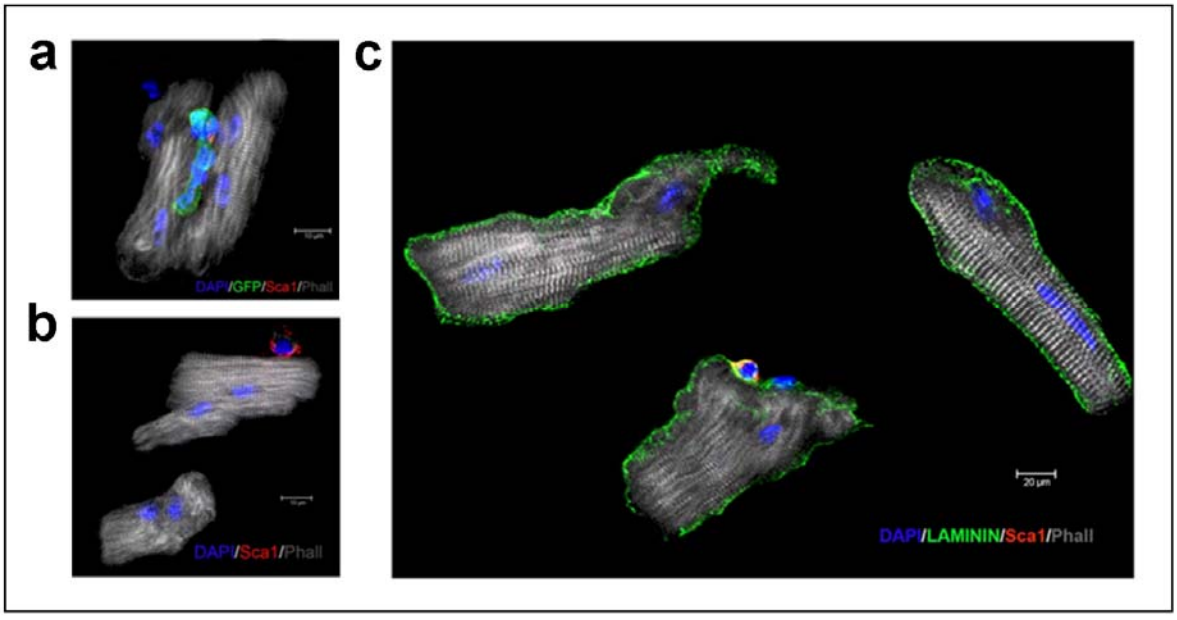

Figure 21. Possible niche of CSCs.
(a), (b) Adult cardiomyocytes were isolated from *Sca1*-GFP and wild type (C57BL/6) mice. The presence of small, round shaped cells attached to the cardiomyocytes was clearly visible. Immunofluorescence staining was performed for GFP (in green), SCA1 (in red), phalloidin (in grey) and nuclei were counterstained with DAPI (in blue). **(c)** Laminin staining (in green) was performed to check the position of *Sca1*-positive cells (in red) attached to the cardiomyocytes in wild type mice.

6.1.6 Sca1$^+$-cell are a heterogeneous population in the heart

Although *Sca1*-derived cells in the heart seem to give rise to all the three major lineages as shown in the previous section (6.1.1), it is not clear whether these cells derive either from a common progenitor cell or from various cell populations expressing *Sca1*. To address this, *Sca1*-tTA//LC1-Cre mice were crossed with *R26R-Confetti* reporter line[105]. This mouse consists of a floxed neomycin resistance roadblock fused with the floxed Brainbow 2.1 construct[104] and is inserted into the Rosa26 locus under the CAAG promoter. The Brainbow 2.1 construct encodes four different fluorescent reporter proteins flanked by variant *loxP* sites: mCFP (blue), nGFP (green), YFP (yellow) and RFP (red). Upon Cre expression, the *loxP* sites recombine, the roadblock cassette will be removed and randomly one of the four fluorescence proteins will be located under the control of the CAAG promoter and therefore expressed. As a consequence, if the cells are derived from the same progenitor it will be labeled by only one color. The presence of cells with different colors will indicate the heterogeneity of cell populations and the existence of cell clones with different origins. In the case of *Sca1*-tTA//LC1-Cre//*R26R-Confetti* mice, the expression of Cre is under the control of the *Sca1* promoter and whenever a cell expresses *Sca1*, it will be labeled with one of the 4 fluorescence proteins. In this mouse, the presence of cells with different colors is a sign of the presence of distinct clone population of *Sca1*-derived cells. As shown in Figure 22a, a random activation of specific fluorescent reporter protein in different areas of the myocardium was observed in the heart of 2 months old *Sca1*-tTA//LC1-Cre//*R26R-Confetti* mice. Immunofluorescence stainings with Phalloidin-633 and alpha smooth muscle actin-FITC were performed to characterize the cell type of the labeled cells. The staining revealed the presence of labeled *Sca1*-derived cardiomyocytes and smooth muscle cells (Figure 22b & c). All the four colors were detected in the heart section indicating that *Sca1*-derived cells are composed of different cells populations. Furthermore, it was possible to find in a precise area cells belonging to the same lineage having different colors (e.g. cardiomyocytes either in red, or yellow, or blue). Due to the fact that each color represents a different *Sca1*-derived cell clone, a possible conclusion is that the color is not specific for a certain lineage (e.g. the red clone gives rise only to cardiomyocytes). In this regard, the color variety of the differentiated cells (e.g. cardiomyocytes and smooth muscle cells) reflects the capacity of each clone to give rise to different lineages (Figure 22d). Furthermore, the colors distribution was evaluated in 10 random areas of heart sections derived from three different mice. This quantitative analysis revealed that there is an unequal distribution of the four fluorescence proteins among all marked cells, cardiomyocytes and non-cardiomyocytes (Figure 22e). These data indicate that

Sca1-derived cells represent a highly heterogeneous population able to give rise to both non-cardiomyocytes (such as smooth muscle cells) and cardiomyocytes but not in equal number and fixed proportion.

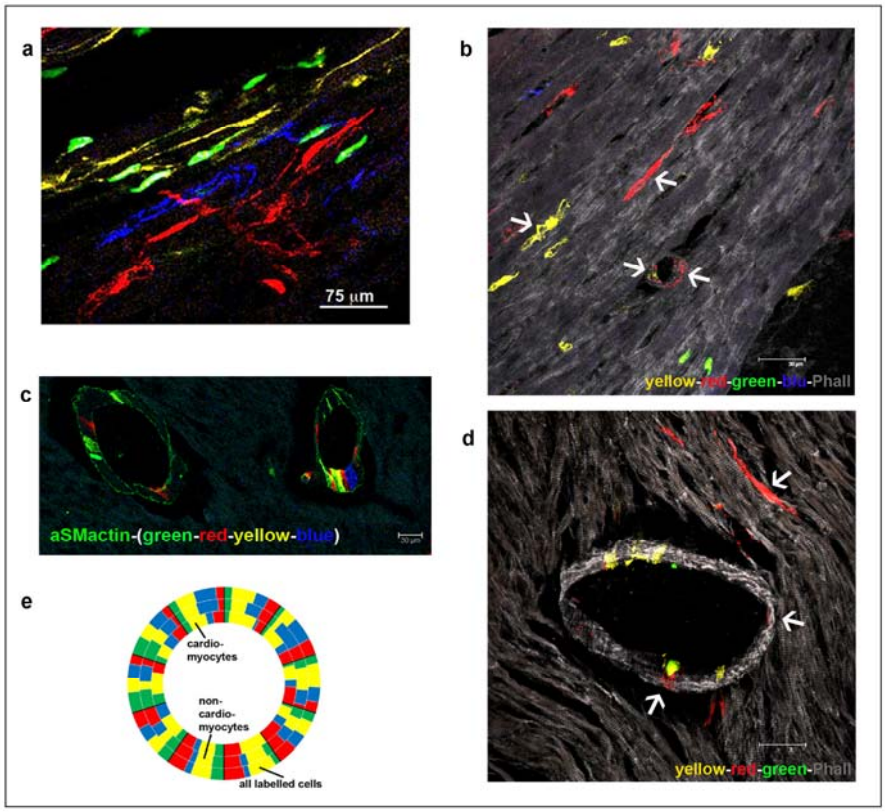

Figure 22. Heterogeneity of *Sca1*-derived progenitor cells *in vivo*.
Representative images of *Sca1*-tTA//LC1-Cre//*R26R-Confetti* mice heart (2 months old). In this mouse model, the expression of *Sca1* will lead to Cre-*loxP* recombination with consequent random activation of one out of the four fluorescent reporter proteins (GFP, YFP, RFP and CFP). Each color represents a different clone coming from *Sca1* progenitor cells. The presence of different colors indicates the cellular heterogeneity of *Sca1*-derived population. **(a)** Cells belonging to the same lineage but with different colors were detected in the same area. **(b & d)** *Sca1*-derived cardiomyocytes with different colors were detected by phalloidin staining. **(c)** A representative image of blood vessels with cells with different colors identified by an antibody against alpha smooth muscle actin (green). **(e)** A multilevel pie chart summarizing the counting of cardiomyocytes and non-cardiomyocytes cells in ten different regions of different heart sections.

6.1.7 Molecular analyses of the Sca1$^+$-cells population

The results obtained from *Sca1*-tTA//LC1-Cre//*R26R-Confetti* mice suggest the existence of heterogeneity in *Sca1* progenitor cells. This heterogeneity could indeed reflect differences at the transcriptional level of the *Sca1*-derived cells´ subpopulations. To investigate this, microarray analyses were performed to characterize the transcription profile of *Sca1*-expressing cells. CSCs were isolated using Millipore kit (as described in section 5.2.2). The kit guarantees an enrichment of SCA1$^+$-cells with a purity of 33 to 50%. After isolation, total RNA extracted from CSCs was hybridized to Affymetrix gene arrays. Comparison to gene array data sets from other cell types including ES cells, mesenchymal stem cells, endothelial cells, cardiomyocytes and different types of fibroblastoid cells, revealed that the

transcriptional profile of CSCs is more similar to adult cardiac fibroblasts than any other cell type analyzed (Figure 23a). Recently, Ieda *et al.*[125] have shown that the concomitant expression of three different cardiac developmental transcriptional factors (*Gata4*, *Mef2c*, and *Tbx5*), can efficiently reprogram cardiac fibroblasts into differentiated cardiomyocyte-like cells which show a gene expression profile similar to neonatal cardiomyocytes. The similar transcription profile between *Sca1*$^{+}$-enriched CSCs and cardiac fibroblasts could support the hypothesis that CSCs give rise to cardiomyocytes. CSCs however represent a mixed population and the transcriptomic profile was not specific for a pure population of *Sca1*$^{+}$-cells. Therefore, the second step was to focus on SCA1-expressing cells to obtain a specific gene profile of this cell population. From the total heart, individual SCA1^{+}CD31^{-}CD45^{-} CSCs were isolated by FACS (Figure 23b) and single cell real-time RT-PCR was performed on Dynamic Arrays^{TM} using the BioMark HD system (Fluidigm Inc.). The primers used were designed against 263 coding mRNAs and one non-coding RNA (ncRNA) (*Airn*), which were chosen on the basis of their expression in different stem cell types as well as during cardiac development. Samples with no Ct value for endogenous control genes (*Actb* and *Gapdh*) and with high variation in Ct values among three independent measurements of *Actb* for each sample were excluded from further analysis. As a result, 74 samples were selected for further analyses. The gene values were then normalized to the endogenous control by subtracting the *Actb* expression level to derive geometric means on a linear scale[128]. Furthermore, genes with Ct value detected less than in 7 cells were excluded from analysis. The remaining 103 genes were used to create the array matrix together with the 74 SCA1^{+}CD31^{-}CD45^{-} single cells. Furthermore, the expression of each gene in SCA1^{+}CD31^{-}CD45^{-} cells was compared to other cells such as ES[118], P19CL6 [127] and unsorted CSCs, used as internal positive controls.

From these analyses, more than 80% of individual SCA1^{+}CD31^{-}CD45^{-} CSCs expressed *Sirt7*, *Stat5a*, *Stat2*, *Nestin*, *Lin28a*, *Hes3*, *CD79a*, *Axin1*, *Il1r1*, *Crabp2* and *Pdgfrbeta*, while the remaining genes were expressed in smaller subsets of cells. For further characterization, the expression profile of each gene in single SCA1^{+}CD31^{-}CD45^{-} cells was compared to each other and grouped using R package clValid, system containing different methods to validate the results obtained from cluster analyses. The resulting outcome was the presence of two large subpopulations inside SCA1^{+}CD31^{-}CD45^{-}, one expressing *Nestin* and *Stat2*, and the other negative for these genes (Figure 23c). The quality of the sorting was validated by immunofluorescence staining. Typical stemness and cardiac progenitor cell markers were chosen, such as ABCG2, GATA4, NANOG, OCT4 and SOX2 to confirm the accuracy of the

sorting (Figure 23d). Expression of ABCG2 was observed in 21.98%, of GATA4 in 16.67%, of NANOG in 0.88%, of OCT4 in 9.58%, and of SOX2 in 25.36% of all analyzed cells.

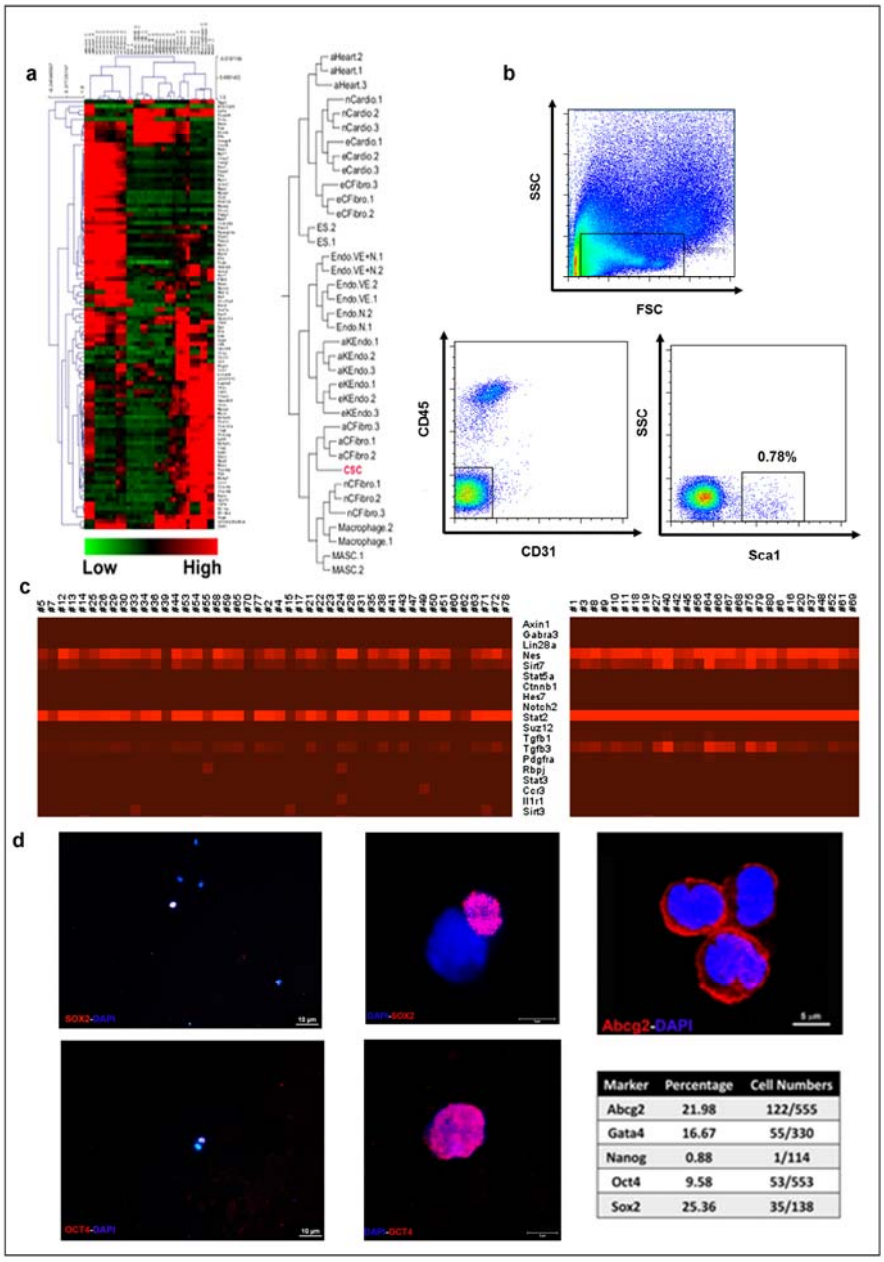

Marker	Percentage	Cell Numbers
Abcg2	21.98	122/555
Gata4	16.67	55/330
Nanog	0.88	1/114
Oct4	9.58	53/553
Sox2	25.36	35/138

Figure 23. Single cells analyses of SCA1-expressing cells and transcriptional profile analyses.
CSC SCA1^{+}-cells were compared with total heart fraction, ES cells, fibroblast, mesenchymal cells and endothelial cells. **(a)** Heat map of the CSCs transcriptional profiles was created using MultiExperiment Viewer (MeV). The higher expression of a gene is indicated in red, a lower expression in green. The CSCs transcriptomic profile was clustered together with data derived from the positive controls (cardiac fibroblasts, MASC, ES, etc.). The hierarchical tree map shows how CSCs (in red), are close to cardiac fibroblasts. **(b)** FACS strategy used to sort single SCA1^{+}CD31^{-}CD45^{-} CSCs. First the isolated cells were selected on the basis of forward and side scatter. In the first plot the gate indicates the cardiac stem cell population selected. In the second plot are indicated the cardiac stem cells negative for CD31 and CD45 (gate bottom left). From these cardiac stem cells, the cells positive for SCA1 were then selected (third plot, gate in the right side). In total the percentage of the cells SCA1^{+}CD31^{-}CD45^{-} were 0.78%.**(c)** Representative heat map of SCA1^{+}CD31^{-}CD45^{-} CSCs single cells, emphasizing the expression of certain genes (e.g. *Nestin, Stat2* and *Tgfb3*) able to mark a division inside this population. Each column represents a single cell and each line a specific gene. The brighter shade of red indicates the high expression of the gene in that particular cell. **(d)** Representative images of cytospin, SCA1^{+}CD31^{-}CD45^{-} CSCs stained with OCT4, SOX2 and ABCG2 antibodies. The percentage of positive CSCs is shown in the table.

6.2 Identification and analyses of resident cell populations in the skeletal muscle and their contribution to muscle regeneration

6.2.1 Sca1 progenitor cells contribute to myofiber formation during aging and after injury

The results obtained in the lineage tracing experiments, lead to the conclusion that these resident stem cells constitute a source of resident stem cells in the heart. Due to these observations, it was speculated that *Sca1*-progenitor cells could also play a role in the maintenance and regeneration of the skeletal muscle. *Sca1*-tTA//LC1-Cre//Z/AP mouse strain was used to address these questions. This mouse represents a perfect model to trace the fate of *Sca1*-derived cells and to reveal the ability of these cells to be committed to myogenic lineage. Furthermore, these investigations could help to answer whether, beside the well characterized unipotent skeletal muscle resident stem cells (satellite cells), other sources of progenitor cells exist and contribute to muscle regeneration. Two different conditions were considered in this study to observe *Sca1*-derived cells behavior in skeletal muscle tissue: aging and muscle regeneration. Aging and the consequent accumulation of fibrotic tissue are known to affect the ability of resident stem cells to differentiate and generate myofibers[137]. Mice at the ages of 3, 6, 18 and 24 months were chosen to determine if *Sca1* progenitor cells are involved in myofiber formation and whether aging could affect their contribution. These ages are used in the literature to define young, adult, old and very old mice respectively[137]. Cardiotoxin injections were performed which well characterized model for studying muscle regeneration. Cardiotoxin is a snake venom able to disrupt the plasma membrane of muscle cells leading to myonecrosis[138]. The damage induces the activation of resident stem cells and leads to their differentiation and subsequent formation of new myofibers[139-141]. In this study, the general procedure was to inject the cardiotoxin in the left leg (left anterior tibialis muscle "TAL") and leave the right one (right anterior tibialis muscle "TAR") uninjured. The TAR was used as negative control. Following this scheme one mouse was suitable for following the behavior of *Sca1*-derived cells both during aging (considering the TAR) and during muscle regeneration (considering the TAL).

Immunofluorescence staining against human placental alkaline phosphatase (AP antibody) in combination with anti-laminin antibody was performed in muscle sections to verify the presence of *Sca1*-derived cells. As shown in Figure 24c some AP^+-cells seemed to be located underneath the basal lamina, which is the typical localization of satellite cells[41]. Furthermore, the presence of AP^+-muscle fibers was observed in tissue sections, suggesting a possible contribution of *Sca1*-precursor cells to muscle fiber formation (Figure 24a & e). The number

of AP^+-fibers was normalized to the total number of fibers presents in an anterior tibialis muscle[115] and the percentage of fibers was derived in order to detect substantial changes in the numbers during aging and regeneration. It was possible to observe a decrease in the number of AP^+-fibers in 3 to 18 month old mice, confirming that aging affects the ability of *Sca1*-derived cells to give rise to myofibers (3 month old mice: 0.21±0.00% in TAR; in 6 month old mice: 0.10±0.01% in TAR; in 18 month old mice: 0.05±0.01% in TAR). Concerning muscle regeneration, the preliminary experiment involving only one cardiotoxin injection revealed that one injury was not sufficient to promote the differentiation of *Sca1*-derived cells. In fact the number of AP^+-fiber was not significantly affected as compared to the contralateral muscle (Figure 24a&b). In this respect, it was speculated that repeated damage could better stimulate *Sca1*-derived cells enhancing their participation in muscle regeneration (Figure 24 b & f). Upon three cardiotoxin injections, a slight decrease in the numbers of AP^+-cells was observed in young and very old mice (in 3 month old mice: 5.37±0.04 cells/mm^2 in TAR and 4.85±0.03 cells/mm^2 in TAL; in 24 month old mice: 4.80±0.25 cells/mm^2 in TAR and 2.91±0.13 in cells/mm^2 TAL) whereas an increase was recorded in adults and old animals (in 6 month old mice: 11.24±0.17 cells/mm^2 in TAR and 12.58±0.21 cells/mm^2 in TAL; 18 month old mice: 5.14±0.49 cells/mm^2 in TAR and 25.20±0.51 cells/mm^2 in TAL) (Figure 24d). However, the fluctuations in the number of AP^+-cells do not directly reflect the number of AP^+-fibers and consequently the potential of *Sca1*-derived cells to contribute to muscle regeneration. Statistically significant increases in the percentage of AP^+-fibers was recorded for young and middle aged mice upon injuries (in 3 month old mice: 0.21±0.00% in TAR and 0.45±0.02% in TAL; in 6 month old mice: 0.10±0.01% in TAR and 0.35±0.04% in TAL) no difference was observed in old age (in 18 month old mice: 0.05±0.01% in TAR and 0.06±0.02% in TAL) (Figure 24f). Furthermore, in very old mice the contribution of *Sca1*-derived cells in muscle regeneration was lower as suggested by the diminished number of AP^+-fibers in the injected muscle as compared to the control (in 24 month old mice: 0.13±0.01% in TAR and 0.07±0.01% in TAL) (Figure 24f).

These data suggest that aging can affect the ability of *Sca1*-derived cells to be involved in myofiber formation and multiple damage can increase their stimulation and participation to muscle regeneration.

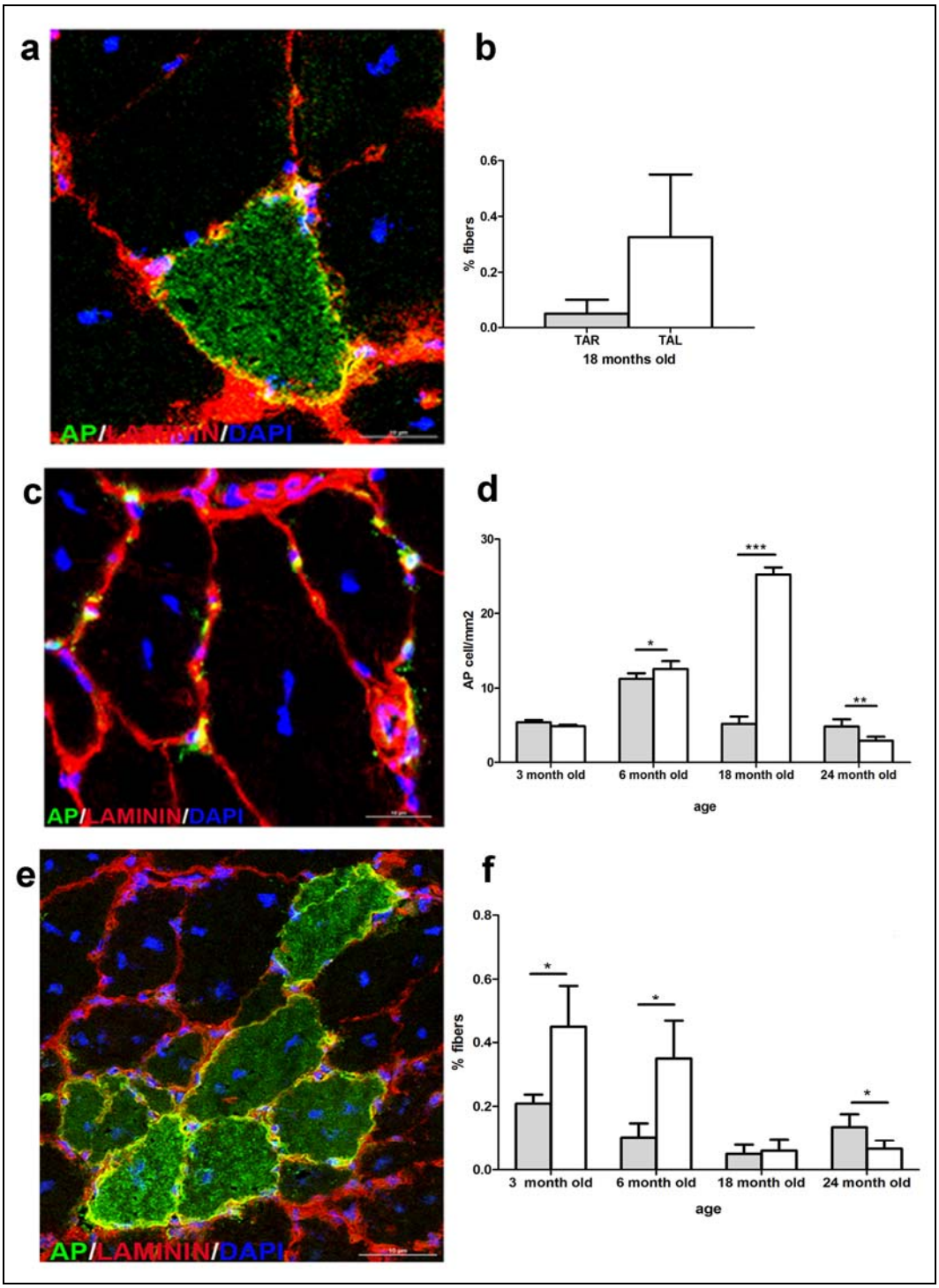

Figure 24. Contribution of *Sca1* progenitor cells to muscle fibers formation during aging and muscle regeneration in the *Sca1*-tTA//LC1-Cre//Z/AP mouse model.
Sca1-tTA//LC1-Cre//Z/AP mouse was used to lineage trace *Sca1* progenitor cells in skeletal muscle *in vivo*. The mice were injected each month with cardiotoxin (a total period of three months) to induce muscle regeneration. The presence of AP^+-cells (stained with anti-hPLAP antibody) and AP^+-fibers was detected. Different mouse ages were considered: 3, 6, 18 and 24 months old. **(a)** Representative image of cross-section of the anterior tibialis muscle injured only one time with cardiotoxin showing one AP^+-fiber. **(b)** Quantification of the number of AP^+-fiber after a single cardiotoxin injection. **(c)** Representative image of cross-section of the anterior tibialis muscle (injured) showing the presence of AP^+-cells presumably located under the basal lamina similarly to satellite cells. **(d)** Quantification of the number of AP^+-cells/mm^2 in mice at different ages. **(e)** Representative image of cross-section of the anterior tibialis muscle (injured) showing the presence of AP^+-fibers. **(f)** Quantification of the number of AP^+-fibers during aging. In all the graphs the grey bar represents the not injured muscle, whereas the white bar represents the injected muscle.

6.2.2 Sca1 progenitors cells contribute to the formation of myofibers in a model of Duchenne muscular dystrophy

To understand if *Sca1* progenitor cells are able to contribute to muscle regeneration in pathological conditions, the triple transgenic mouse system described above (*Sca1*-tTA//LC1-Cre//Z/AP) was crossed with the *mdx* mouse line, which represents a model for Duchenne muscular dystrophy[110] (Figure 25a).

In order to observe the contribution of *Sca1* progenitor cells, 3 and 6 months old *Sca1*-tTA//LC1-Cre//Z/AP//*mdx*$^{(-/-)}$ mice were injected with cardiotoxin as previously described in section 6.2.1. One injection per month was performed for a total period of three months. As shown in Figure 25c, the quantification of the number of AP$^+$-cells was higher in the injured muscle (TAL) compared to the control (TAR) in both ages considered (in 3 month old mice: 13.34±0.59 cells/mm^2 in TAR and 24.06±0.55 in TAL; in 6 month old mice: 17.64±0.68 in TAR and 27.26±1.13 in TAL). Furthermore, when the percentage of AP$^+$-fibers was examined in 3 month old mice, an increased number of AP$^+$-fibers was observed in the injured muscle compared to the control (0.11±0.0034% in TAR and 0.18±0.0037% in TAL) (Figure 25e). However, in contrast to the analysis of *Sca1*-tTA//LC1-Cre//Z/AP mice (section 6.2.1), a decrease in the percentage of AP$^+$-fibers was observed upon injuries in 6 months old mice (0.15±0.0033% in TAR and 0.10±0.0019% in TAL). The presence of AP$^+$-fibers in *Sca1*-tTA//LC1-Cre//Z/AP//*mdx*$^{(-/-)}$ confirm a role for *Sca1* progenitor cells in contributing to muscle regeneration under pathological conditions. This contribution is higher in young animals compared to old ones. However, although the diminished number of AP+-fibers in 6 month old mice after 3 cardiotoxin injections, it was still possible to find newly formed AP$^+$-fibers as indicated by the central position of the nucleus, where usually in pre-existing myofibers the nuclei are located in the periphery[142].

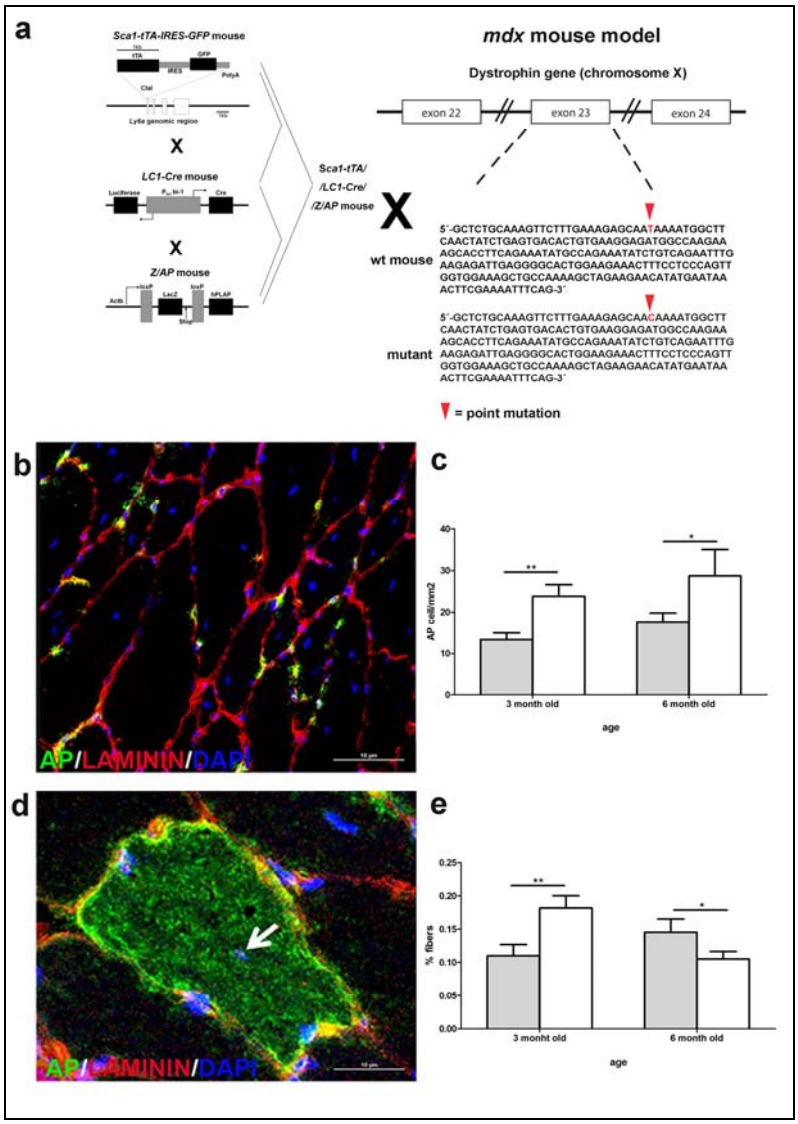

Figure 25. Contribution of *Sca1* progenitor cells after ijury in *mdx* mice.
(a) *Sca1*-tTA//LC1-Cre//Z/AP mice were crossed with "*mdx*" mice, a mouse model of Duchenne muscular dystrophy. For the injury model, the same scheme described in section 6.2.1 was used and two different age groups were considered: 3 and 6 months old. **(b)** Representative image of cross-section of the anterior tibialis muscle (injured) showing the presence of AP^+-cells. **(c)** Quantification of the number of AP^+-cells/mm^2 under pathological condition.
(d) Representative image of cross-section of the anterior tibialis muscle (injured) showing the presence of center nucleated AP^+-fiber, indication of newly regenerated fiber.
(e) Quantification of the number of AP^+-fibers under pathological condition. In the graphs the grey bar represents the not injured muscle, whereas the white bar represents the injected muscle.

6.2.3 Sca1 progenitors cells could differentiate into muscle tissue following different pathways

The results from sections 6.2.1 and 6.2.2 strongly suggest that *Sca1* progenitor cells can contribute to muscle regeneration during aging, upon injury, and under pathological conditions. Myogenic cell differentiation has been described as being regulated by specific myogenic factors such as Pax7, MyoD, Myf5, MRF4 and Myogenin[143]. Pax7, transcription factor, is known to be a marker for satellite cells and it is expressed during the earlier stages of myogenic commitment[143]. Even if it was observed that *Sca1* progenitor cells give rise to myogenic fibers, it still remains unclear whether they follow the "canonical" myogenic expression pathway or not. In order to elucidate if *Sca1* progenitor cells require the expression of *Pax7* to be active and differentiate, *Sca1*-tTA//LC1-Cre//Z/AP mice were crossed with conditional *Pax7* mice ($Pax7^{loxPGu/loxPGu}$). In the $Pax7^{loxPGu/loxPGu}$ mice the DNA binding domain of *Pax7* is flanked by *loxP*-sites[111] (Figure 26a). In *Sca1*-tTA//LC1-

Cre//Z/AP//*Pax7*$^{loxPGu/loxPGu}$ mice, the expression of *Sca1* leads to the expression of Cre-recombinase present in the LC1-Cre allele. The Cre-recombinase recombines the *loxP* of *Pax7* allele with consequent excision of exon I-III of *Pax7* gene inactivating its expression. The same Cre-recombinase will also excise the lacZ-stop cassette present in the Z/AP reporter line, mediating the expression of alkaline phosphatase instead of lacZ. In this mouse model, the cells that express *Sca1* at least once in their life will be positive for alkaline phosphatase (AP) and will not express a functional *Pax7*, whereas cells that will express Pax7 (e.g. satellite cells) will not be labeled and consequently not traced. The presence of AP$^+$-fibers in 3 and 6 month old *Sca1*-tTA//LC1-Cre//Z/AP//*Pax7*$^{loxPGu/loxPGu}$ mice under physiological conditions and after injury (i.e. cardiotoxin injection), confirmed the presence of a subpopulation of *Sca1*$^+$-cells able to contribute to myofiber formation without the expression of *Pax7* (Figure 26b). This subpopulation seems to be more active in muscle regeneration in younger mice, as indicated by the increased number of AP$^+$-fibers in 3 months old mice as compared to 6 month old animals (in 3 month old mice: 0.08±0.0053% in TAR and 0.26±0.16% in TAL; in 6 month old mice: 0.13±0.0038% in TAR and 0.04±0.0021% in TAL) (Figure 26c). This discrepancy might be due to some crucial transcription factors that are normally present during young stages whereas in the adult they are not significantly expressed. This idea is supported by the data already described in literature concerning the difference between embryonic and adult myogenesis[144]. In particular, Lepper *et al.* demonstrated that *Pax7* expression is crucial during myogenic commitment up to twenty-one days after birth (P21). Using a tamoxifen-inducible mouse model to lineage trace *Pax7*-expressing cells (*Pax7(CE)*)[144], they were able to show that 21 days after birth, adult satellite cells do not need the expression of *Pax7* to differentiate into myofibers.

Based on these results and due to the fact that the subpopulation of *Sca1* progenitor cells not expressing *Pax7* are more active in muscle regeneration in younger mice, *Sca1*-tTA//LC1-Cre//Z/AP//*Pax7*$^{loxPGu/loxPGu}$ mice were used to observe whether the involvement of these cells might be pronounced in younger mice. The tibialis anterior muscles from 17 day old pups (P17) were examined and the presence of AP$^+$-fibers was identified under normal physiological conditions both in longitudinal and cross sections (Figure 27). In order to check if muscle injury could activate this *Sca1*$^+$ subpopulation during earlier stage, cardiotoxin was injected in the anterior tibialis muscle of 14 day old pups (P14) and the pups were sacrificed at 21 days after birth (P21). Both anterior tibialis muscles (injected and control) were collected and alkaline phosphatase staining was performed. The higher number of AP$^+$-fibers

in the section suggested an increased contribution of the subpopulation of *Sca1* progenitor cells not expressing *Pax7* at the earlier stages after damage (Figure 27).

These data suggest that a subpopulation of *Sca1* progenitor cells does not seem to need the expression of *Pax7* to participate in muscle regeneration. Furthermore the contribution of this population is almost negligible at young and adult stages during physiological conditions, whereas their involvement increases after injury and even more at earlier stages as before P21.

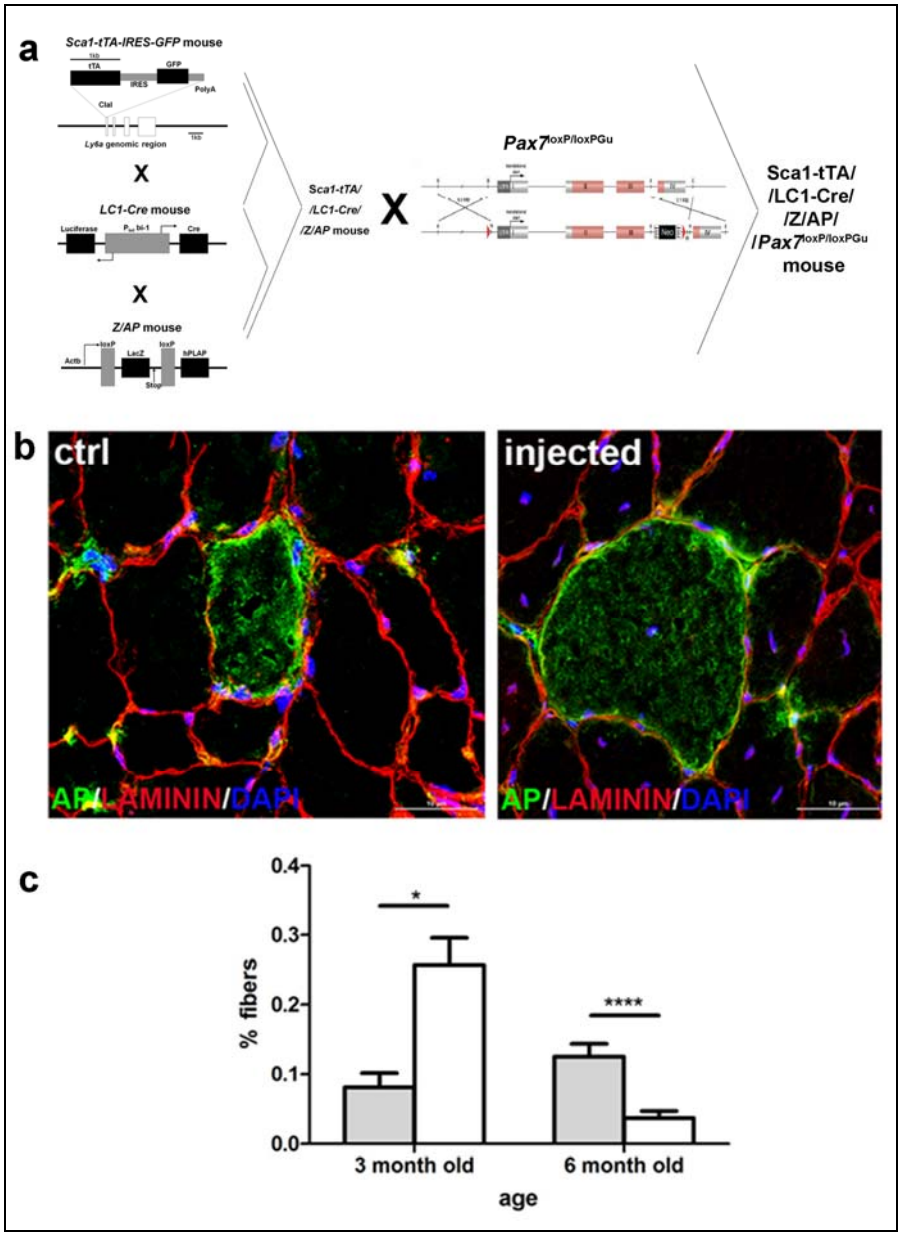

Figure 26. Presence of a subpopulation of *Sca1* progenitor cells in skeletal muscle involved in myogenesis independently from *Pax7* expression.
(a) *Sca1*-tTA//LC1-Cre//Z/AP//*Pax7*$^{loxPGu/loxPGu}$ mouse model scheme. In this mouse model, the expression of *Sca*1 activates tTA and transcribes for Cre-recombinase. Cre-recombinase allows the expression of alkaline phosphatase in Z/AP mouse and at the same time excises exon 1, 2 and 3 from *Pax7* floxed gene. **(b)** Representative images of cross sections of left anterior tibialis muscle of 3 months old mice before and after damage induced by cardiotoxin injection. **(c)** Quantification of the number of AP^+-fibers. Three month old mice show an increased number of AP^+-fibers in response to cardiotoxin injection, whereas in 6 month old mice the number is reduced. In the graph the grey bar represents the not injured muscle, whereas the white bar represents the injected muscle.

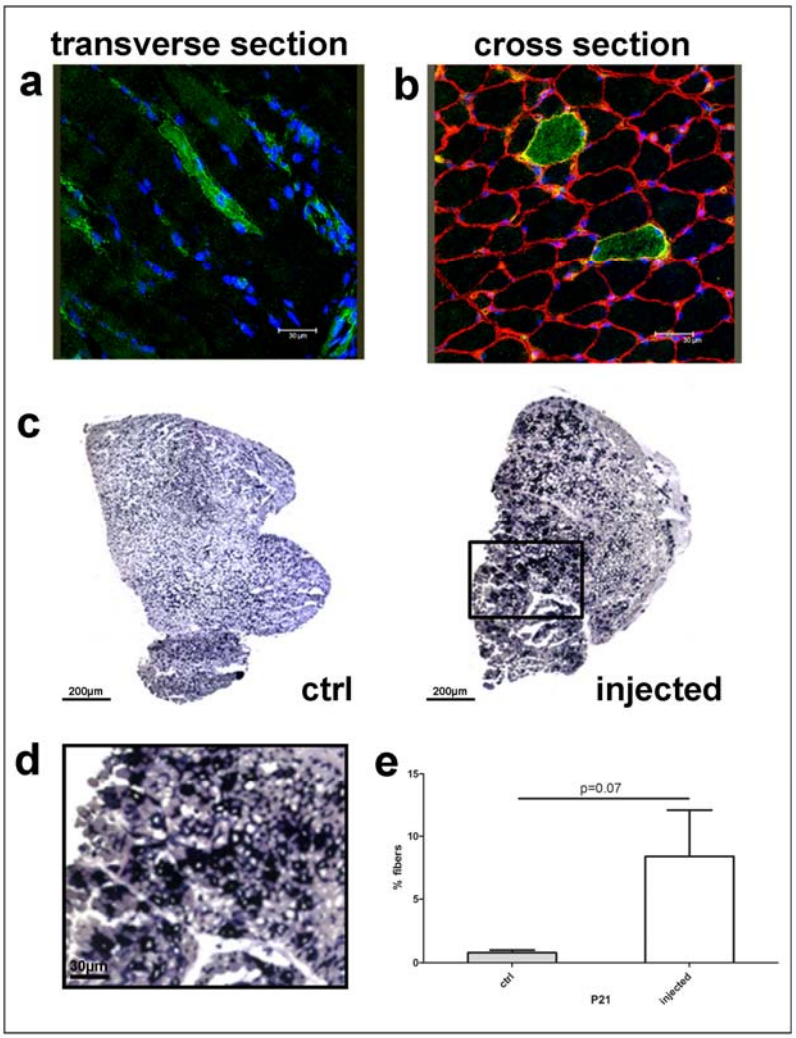

Figure 27. Presence of a subpopulation of *Sca1* progenitor cells that do not express *Pax7* and are involved in myogenesis during early postnatal stages. Contribution of *Sca1* progenitor cells not expressing *Pax7* during earlier stages. **(a & b)** Representative pictures of transverse and cross section of tibialis anterior muscle in P17 mice. Presence of AP^+-fibers was detected. **(c)** Representative images of control and injected anterior tibialis muscle at P21. **(d)** Representative image at higher magnification showing the presence of AP^+-fibers after injection. **(e)** Quantification of the number of AP^+-fibers showing their increase in response to cardiotoxin injection in P21 mice. In the graph the grey bar represents the not injured muscle, whereas the white bar represents the injected muscle.

6.2.4 In vivo Sca1 progenitor cells seem to be multipotent stem cells whereas satellite cells are unipotent

Although *Sca1* progenitor cells could give rise to a certain number of myofibers during aging and pathological conditions, satellite cells remain the major stem cell source for myogenesis. Discovered in 1961, satellite cells are muscle precursor cells that can replenish muscle fibers upon damage[41]. A small percentage (~10%) of these cells possess stem cell-like functions and can expand the pool of resident satellite cells maintaining muscle homeostasis[145]. The potential to easily isolate and culture satellite cells, has increased their use *in vitro* as a model for myogenic differentiation. However, although 50 years have passed since the discovery of satellite cells, the factors that are important in maintaining the stemness of these cells as well as the signaling pathways involved in the control of their proliferation and differentiation still remain poorly understood[146]. It was demonstrated that satellite cells can differentiate into adipocytes and osteoblasts both *in vitro*[147,148] and *ex vivo*[149,57], but it is still not clear whether such differentiation capabilities are retained *in vivo*. In order to address this question the

transgenic mouse *Pax7*-Cre[109] was crossed with a reporter Z/AP mouse line[101] to examine whether satellite cells are unipotent stem cells *in vivo*. In the double transgenic mouse model *Pax7*-Cre//Z/AP, upon expression of the nuclear transcription factor *Pax7* Cre-recombinase is transcribed. The Cre-recombinase recombines the *loxP* sites of the lacZ-stop codon cassette present in the Z/AP reporter mouse activating the transcription of alkaline phosphatase instead of *lacZ* gene. In this mouse model a cell expressing *Pax7* will be permanently labeled with alkaline phosphatase. The *Pax7*-Cre//Z/AP mice were injected with molecules known to be involved *in vivo* in osteoblast (hBMP4)[149]and adipocyte formation (hBMP7)[150]. These molecules were injected either separately or in combination. The injection was performed in the left anterior tibialis muscle whereas the contralateral (right anterior tibialis muscle) was left untreated. The mice were sacrificed one month after the injection and different stainings were performed to validate the possible formation of ectopic tissue and the involvement of satellite cells in this process. Alkaline phosphatase staining was done in order to detect the localization and the contribution of satellite cells after injection. Oil red O, a colorant that forms precipitates in the presence of lipid drops, was used to detect the presence of adipocytes and triglycerides. Furthermore Alizarin red, a dye that forms orange/red precipitates in the presence of calcium, was used to confirm the presence of calcium deposits.

As shown in Figure 28, compared to the injection with hBMP4 alone, the combination of hBMP4/7 showed an increase in Oil Red O stained cells in the injected region as compared to the contralateral muscle. A similar trend was observed in the case of Alizarin red staining. All AP^+-cells were negative for Oil Red O or Alizarin red staining, regardless of the administration of hBMP4 and hBMP7 alone or in combination. These results clearly indicate that, *in vivo*, satellite cell differentiation is restricted to myofibers and they cannot differentiate in either osteoblasts or adipocytes. It has been speculated that this lack of multipotency *in vivo* in satellite cells could be caused by a crosstalk with other cells[65]. For instance, specific cells such as FAPs, fibro/adipocyte progenitor cells, able *in vivo* to give rise to adipocytes and fibroblasts, could balance satellite cell commitment towards a certain lineage rather than another[63,64]. For instance it has been shown that FAPs, by releasing specific interleukins (e.g. IL6), could promote *in vivo* the differentiation of satellite cells into myogenic lineage and suppress their ability to differentiate in other cell types[65]. These FAPs are indeed described to also express *Sca1*[64]. In order to understand if the population of *Sca1* progenitor cells identified in this study shows a multipotent phenotype, the triple transgenic mouse model *Sca1*-tTA//LC1-Cre//Z/AP mouse was again considered (described above in sections 5.1.1 & 6.1.1). Additionally the left tibialis anterior muscle of these mice was

injected with the same set of BMP molecules described above. As shown in Figure 29, alkaline phosphatase staining in combination with Oil red O and Alizarin red revealed the presence of *Sca1*-derived cells in the region of the ectopic tissue formation. These results, indicate the commitment of these cells and their contribution to the ectopic bone and adipose tissue formation, revealing the capability of *Sca1*-derived cells to be committed not only towards a myogenic lineage but also towards the other mesodermal lineages, contrarily to satellite cells.

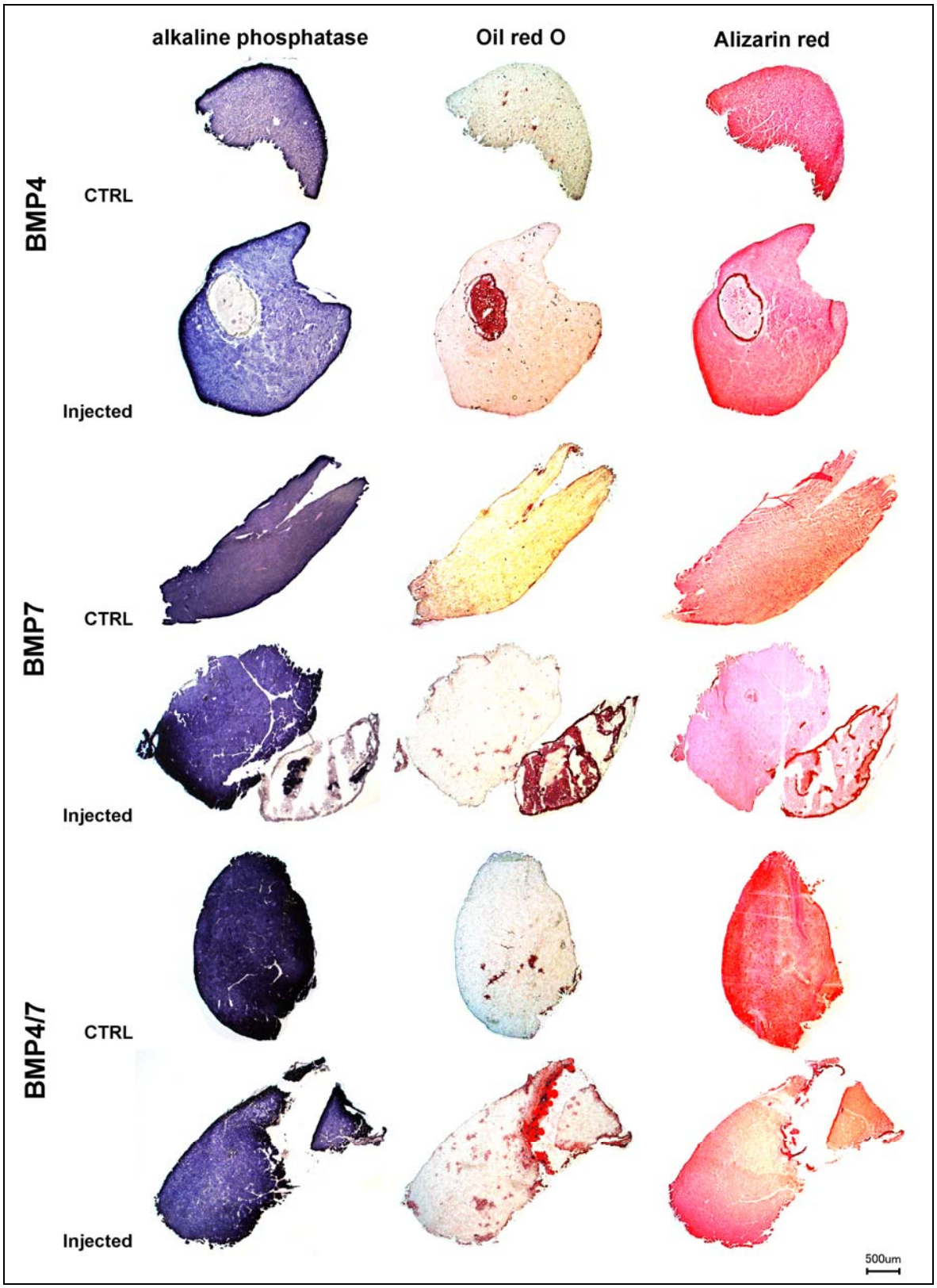

Figure 28. Injections of BMP molecules in *Pax7*-Cre//Z/AP mice.
The muscle anterior tibialis of *Pax7*-Cre//Z/AP mice was injected with different BMP molecules in order to promote the formation of ectopic bone and adipose tissue. Sections of the injected muscle and relative controls were stained with alkaline phosphatase, Oil red O (adipocytes) and Alizarin red (osteoblasts). The absence of alkaline phosphatase positive cells in the region of ectopic formation indicates that satellite cells are not able to differentiate in either adipocytes or osteoblasts.

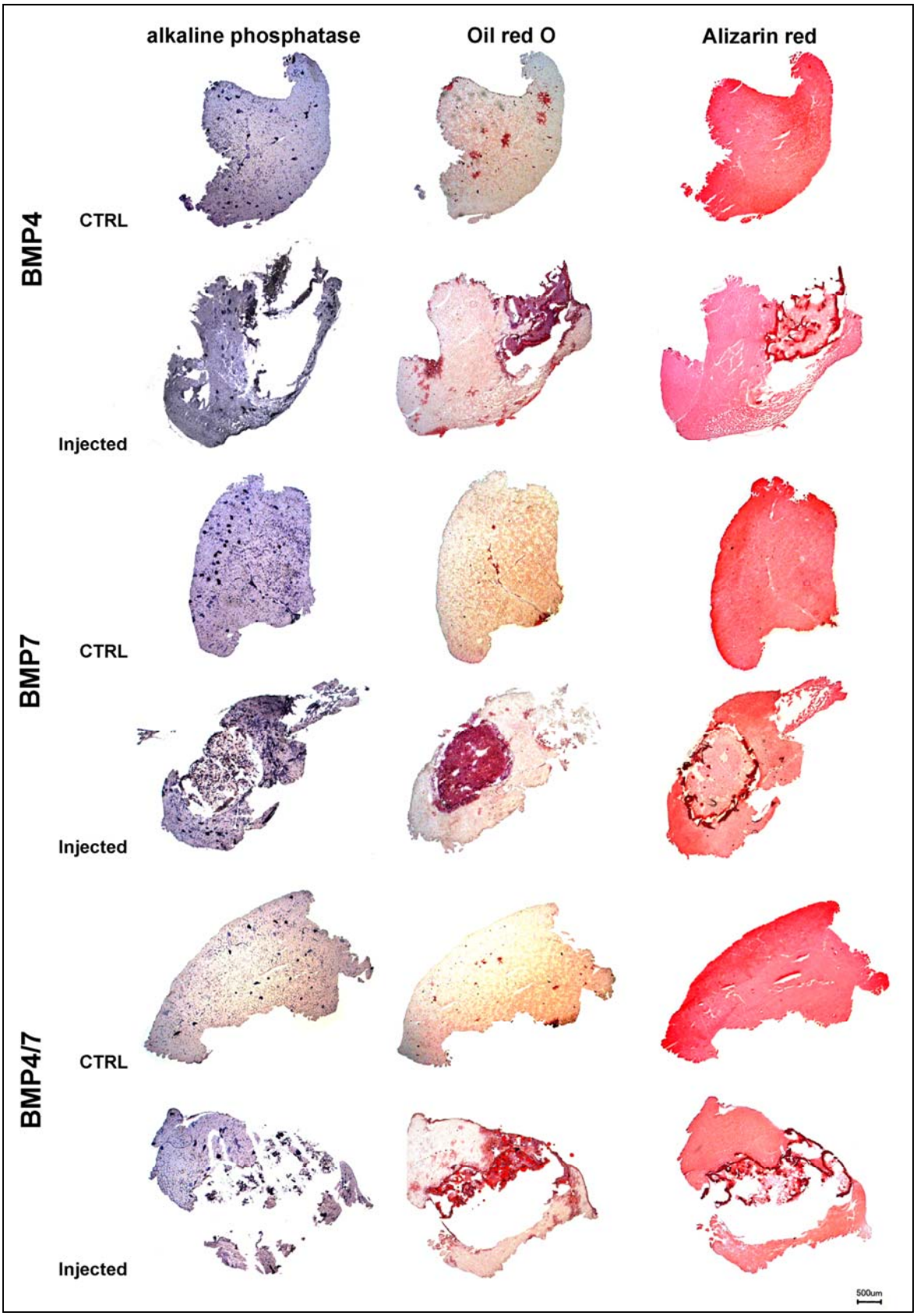

Figure 29. Injections of BMP molecules in *Sca1*-tTA//LC1-Cre//Z/AP mice.
The muscle anterior tibialis of *Sca1*-tTA//LC1-Cre//Z/AP mice were injected with BMP molecules. Different stainings for alkaline phosphatase, Oil red O (adipocytes) and Alizarin red (osteoblasts) were performed to detect the formation of ectopic tissue in the anterior tibialis muscles of the mice. *Sca1*-derived cells are involved and participate in the formation of adipocytes and osteoblasts as confirmed by the positive staining of alkaline phosphatase in the ectopic region.

6.2.5 Sca1 progenitors cells could contribute to adipocytes formation in vivo

The above results strongly support the idea that *Sca1*-derived cells might contribute to the formation of adipocytes and osteoblasts upon injection of BMP molecules. The ability of *Sca1* progenitor cells to form adipocytes *in vivo* was further demonstrated by performing glycerol injection. The glycerol injection model has been reported to induce myogenic cell death by disrupting the cytoplasmic membrane with consequent substitution of muscle tissue with adipose tissue[63]. One source of this lipid formation seems to be FAPs (fibro-adipocyte progenitor cell positive for PDGFRalpha and SCA1)[63]. Therefore the left tibialis anterior muscle of *Sca1*-tTA//LC1-Cre//Z/AP mice was injured with glycerol, whereas the right tibialis anterior muscle was used as a negative control. Oil red O staining was performed to reveal the formation of adipocytes. Large lipid drops were detected throughout all the muscle sections (Figure 30a & b). Furthermore, to identify *Sca1*-derived cells, immunofluorescence staining was performed. Human placental alkaline phosphatase antibody (AP) was used in combination with PERILIPIN, a marker for adipocytes. As shown in Figure 30c, PERILIPIN$^+$ adipocytes are also positive for AP, confirming that *Sca1* progenitor cells are involved in adipocyte formation.

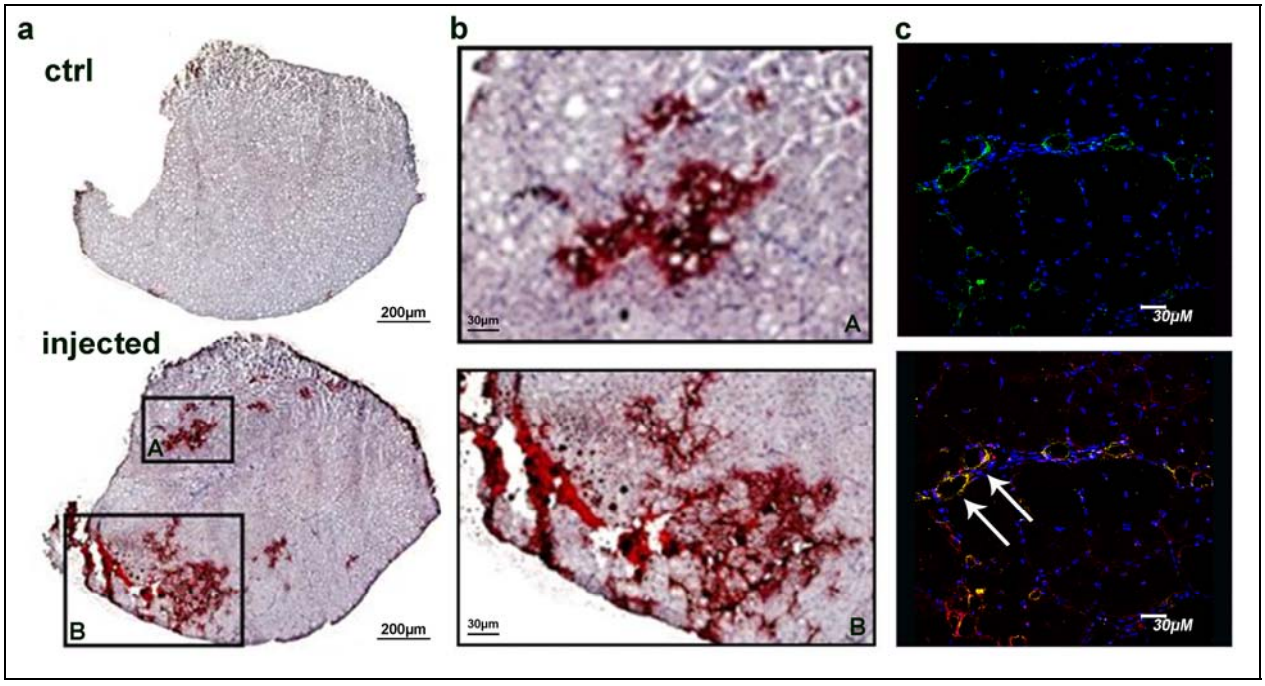

Figure 30. Formation of adipocytes *in vivo*.
Glycerol was injected in tibialis anterior muscle of *Sca1*-tTA//LC1-Cre//Z/AP mice to promote the formation of adipocytes. **(a)** Representative picture of Oil red O staining of the cross section of tibialis anterior muscle. **(b)** Higher magnification of lipid formation after glycerol injection in two different areas of anterior tibialis muscle. **(c)** Immunofluorescence staining using anti-PERILIPIN (for adipocytes, in red) and anti-hPLAP (AP$^+$-cells, in green) antibodies. Nuclei were counterstained with DAPI (in blue). The lower image shows cells double positive for AP and PERILIPIN, confirming the presence of *Sca1*-derived adipocytes (white arrows).

6.2.6 Microarray Analyses of Satellite cells, FAPs and Sca1-expressing progenitor cells

Sca1 progenitor cells traced in this study seem to contribute to all the mesodermal lineages (myogenic, adipogenic, osteogenic) as described in the previous sections. They are able to form myofibers and adipocytes *in vivo* in a similar manner to satellite cells and FAPs respectively. This could be probably due to a common gene expression profile between *Sca1*-expressing cells/satellite cells and *Sca1*-expressing cells/FAPs. In order to confirm this hypothesis, microarray analyses were performed using GeneChip® Mouse Exon 1.0 ST Array (exon arrays) from Affymetrix, Inc., to determine the gene profile of these populations and to provide a better characterization of these cells (Figure 31).

The following populations of cells were isolated by FACS using specific surface markers:

- Satellite cells: SM/C-2.6^{+}CD31^{-}CD45^{-}SCA1^{-}[151];
- FAPs: PDGFRalpha^{+}CD31^{-}CD45^{-}[63,152];
- *Sca1*-expressing cells: SCA1^{+}CD31^{-}CD45^{-}SM/C-2.6^{-}.

SM/C-2.6 is an antibody developed by Fukada and colleagues[153] to isolate quiescent satellite cells. PDGFRalpha was used as a marker for FAPs[63,152]. In all three populations, the cells were gated to be negative for CD31 (endothelial marker) and CD45 (hematopoietic marker). Furthermore, the three populations were analyzed under two conditions: quiescence (physiological condition) and activated state. The activation was obtained by cardiotoxin injection and cells were collected two days after injury. The microarray data were analyzed using "Exon Array Analyzer" (EAA)[119]. The up-regulation (both in quiescence and activate state) of myogenic genes in satellite cells and of fibro-adipogenic genes in FAPs, confirmed their specific lineage commitment observed *in vivo*. The up-regulation of myogenic, fibrogenic, adipogenic genes mainly upon activation in *Sca1*-expressing cells sustained their multipotency *in vivo*. The ability of *Sca1*-expressing cells to give rise to osteoblasts has been shown in the previous sections it was shown that genes known to be involved in osteogenesis were indeed up-regulated in *Sca1*-expressing cells in quiescent state, highlighting their intrinsic osteogenic potency. However upon activation, the same genes were down-regulated, likely due to the specificity of cardiotoxin damage in activating the myogenic program. These data confirm the ability of *Sca1*-expressing cells *in vivo* to differentiate towards other mesodermal lineages besides the myogenic one (as described in sections 6.2.4 & 6.2.5) and cardiotoxin damage seems to activate the myogenic, adipogenic and fibrogenic marker expression but does not induce the osteogenic one.

Although from the microarray data it was possible to find genes commonly expressed in satellite cells and *Sca1*-expressing cells upon activation (Table 6), two particular genes highlighted a clear separation between these two populations: *Bmp1* and *IL6*. These two genes are known to be involved in the regulation of muscle growth. *Bmp1* (Bone morphogenic protein 1, belonging to the tolloid-like metalloproteinases family) has been shown to be highly regulated in quiescent satellite cells[154]. *Il6* (Interleukin 6) has been described to be involved in satellite cell-mediated muscle hypertrophy and induction of muscle growth[155]. According to these data, *Sca1*-expressing cells express high level of *Bmp1* in the quiescent state, whereas upon activation the level of *Il6* increases. These genes could be a key to understand the regulation of quiescence and activation state of *Sca1*-expressing cells. The high level of *Bmp1* in normal physiological conditions could keep these *Sca1*-expressing cells in a quiescent state, which may explain why, although presenting myogenic potential, their contribution to myofibers formation *in vivo* is low compared to satellite cells.

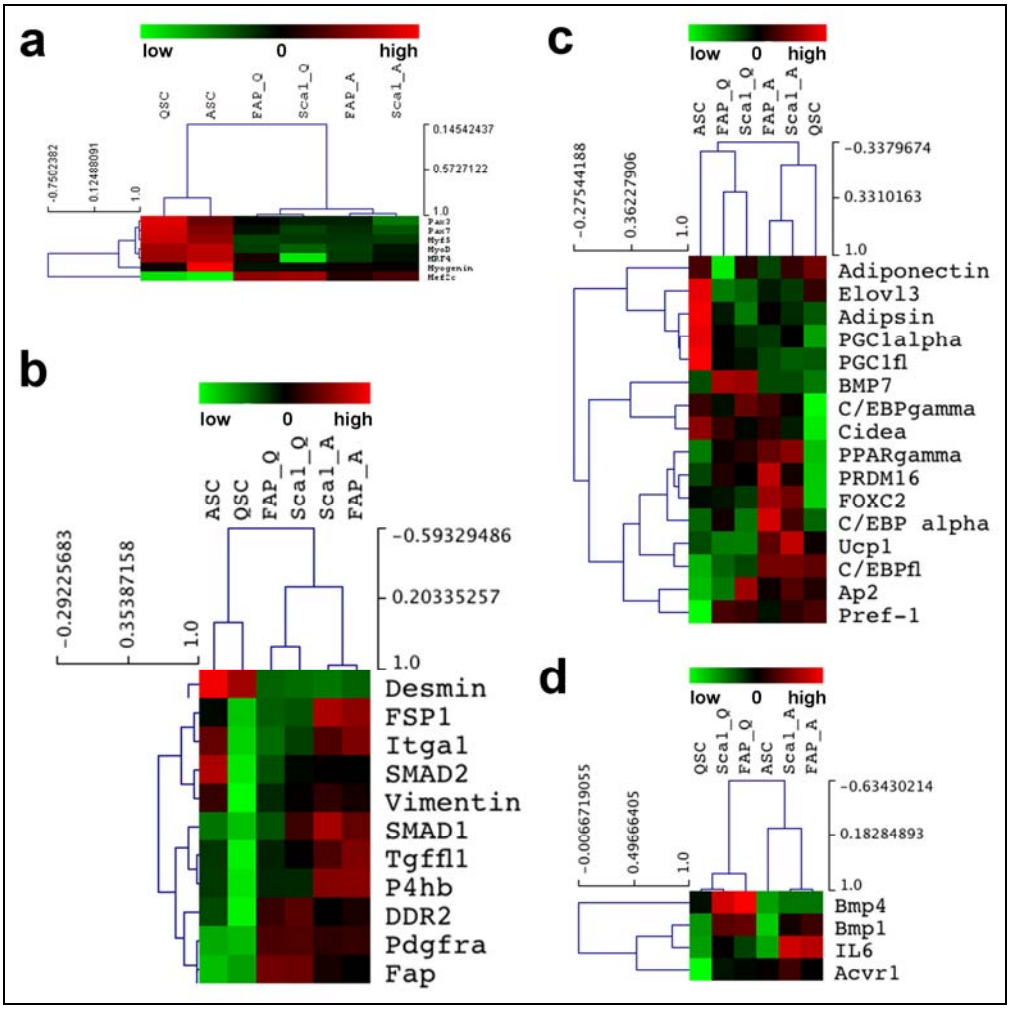

Figure 31. Microarray dataset.
(a) Myogenic array. **(b)** Fibrogenic array. **(c)** Adipogenic array. **(d)** *Bmp4*, *Bmp1*, *Il6*, *Acvr1* genes expression array

A.

		Lineage			
		Fibrogenic	**Adipogenic**	**Osteogenic**	**Other**
QUIESCENT STATE	**SCA1⁺ cells**	*Ddr2, Pdgfralpha, Fap*	*Bmp7, C/ebp gamma, Cidea, PPRgamma*	*Bmp4*	*Bmp1*
	FAPs				

B.

			Lineage		
		Myogenic	**Fibrogenic**	**Adipogenic**	**Other**
ACTIVATE STATE	**SATELLITE cells**	*Pax7,Myf5, MyoD, MRF4, Myogenin*			
	SCA1⁺ cells		*Fsp1, Itgalpha, Smad1, P4hb*	*Prdm16, C7ebpalpha, C7ebp beta, Ucp1, Ap2, Pref-1*	*Il6*
	FAPs				

Table 6.Genes highly upregulated in the microarray analyses.
The table summarizes the genes highly up-regulated and commonly express between satellite cells/*Sca1*$^{+}$-cells and *Sca1*$^{+}$-cells/FAPs visualize in the heat maps of the Figure 31. *Sca1*-expressing cells in quiescence state have a profile similar to FAPs and they have a high expression of genes belonging to fibrogenic, adipogenic, osteogenic lineages. The activation induced by cardiotoxin injection increases the expression also of genes belonging to the myogenic lineage and typical for satellite cells.

6.2.7 Single cell transcriptomic analyses of muscle cell

The data described in the previous paragraph suggest that *Sca1*-expressing cells possess a certain gene expression identity common to both satellite cells and FAPs. FAPs are positive for PDGFRalpha[63] but also express SCA1[64]. This could possibly explain the similarity of the transcriptomic profile between *Sca1*-expressing cells and FAPs. Satellite cells are commonly defined as a population characterized by the expression of the transcriptional factor *Pax7* although they represent a heterogeneous population composed of cells with different biochemical and functional features[156]. Due to this heterogeneity and the similarity found between satellite cells and *Sca1*-expressing cells at the gene expression level upon cardiotoxin injection, it was speculated whether a certain number of satellite cells could possibly express *Sca1* and this expression could mark a specific subpopulation. In order to investigate the cellular heterogeneity of satellite cells and the possible different characteristics of the *Sca1*$^{+}$ *and Sca1*$^{-}$ populations, the same markers used for the microarray analyses (section 6.2.6) were used as well as SM/C2.6 for sorting as the equivalent marker for satellite cells[153] instead of *Pax7*. The following six populations were isolated (Figure 32a):

- FAPS : PDGFRalpha^{+}SCA1^{-} & PDGFRalpha^{+}SCA1^{+},
- Satellite cells: SM/C2.6^{+}SCA1^{-}& SM/C2.6^{+}SCA1^{+};
- Sca1-expressing cells: SCA1^{+}PDGFRalpha^{-} & SCA1^{+}SM/C2.6^{-}.

All the populations were negatively gated for the expression of CD31 and CD45. Single cells were sorted from each population. The transcription level of *Sca1 (Ly6a), Pdgfralpha* and *Pax7* genes was tested using RT-qPCR for the single cells of the six populations mentioned above to examine the accuracy of the sorting. Only the single cells expressing the markers specific for the population they belong to, were chosen for single cell gene expression analyses. The single cell gene data profile of the samples was generated using Fluidigm Dynamic Arrays technology (BioMarkTM HD System). This technology allows performing several distinct single RT-qPCR reactions together, at the same time, using a specific microarray chip card.

From the six different populations, the number of single cells able to pass the quality test and suitable for the next analyses resulted to be 182 and was divided as follows: SM-C2.6^{+}SCA1^{+}CD31^{-}CD45^{-} (32 cells), SM-C2.6^{+}SCA1^{-}CD31^{-}CD45^{-} (32 cells), PDGFRalpha^{+}SCA1^{+}CD31^{-}CD45^{-} (31 cells), PDGFRalpha^{+}SCA1^{-}CD31^{-}CD45^{-} (23 cells). Two samples were created using all the cells mentioned above together with C2C12 and ES cells as internal positive controls (Figure 32b). The samples were analyzed for the expression of 288 genes specific for cell signaling (e.g. BMP, Notch, Wnt), cell cycle, chemokines, growth factors and stem cell markers. For each sample four different microarrays were performed using the primers mentioned above. In order to be able to further analyze the microarray data obtained, the *beta-actin* expression value of the four arrays were compared using Pearson correlation. Pearson correlation defines how well different data sets are related and the linear relationship existing between them. The Pearson coefficient range is defined to be from −1 to 1, where 1 represents a positive linear correlation between the values. As shown in Figure 32c, the comparison of the data generated by Fludigm technology presented a Pearson coefficient close to 1, confirming that the data obtained from the four arrays had high correlation and allowing further analyses.

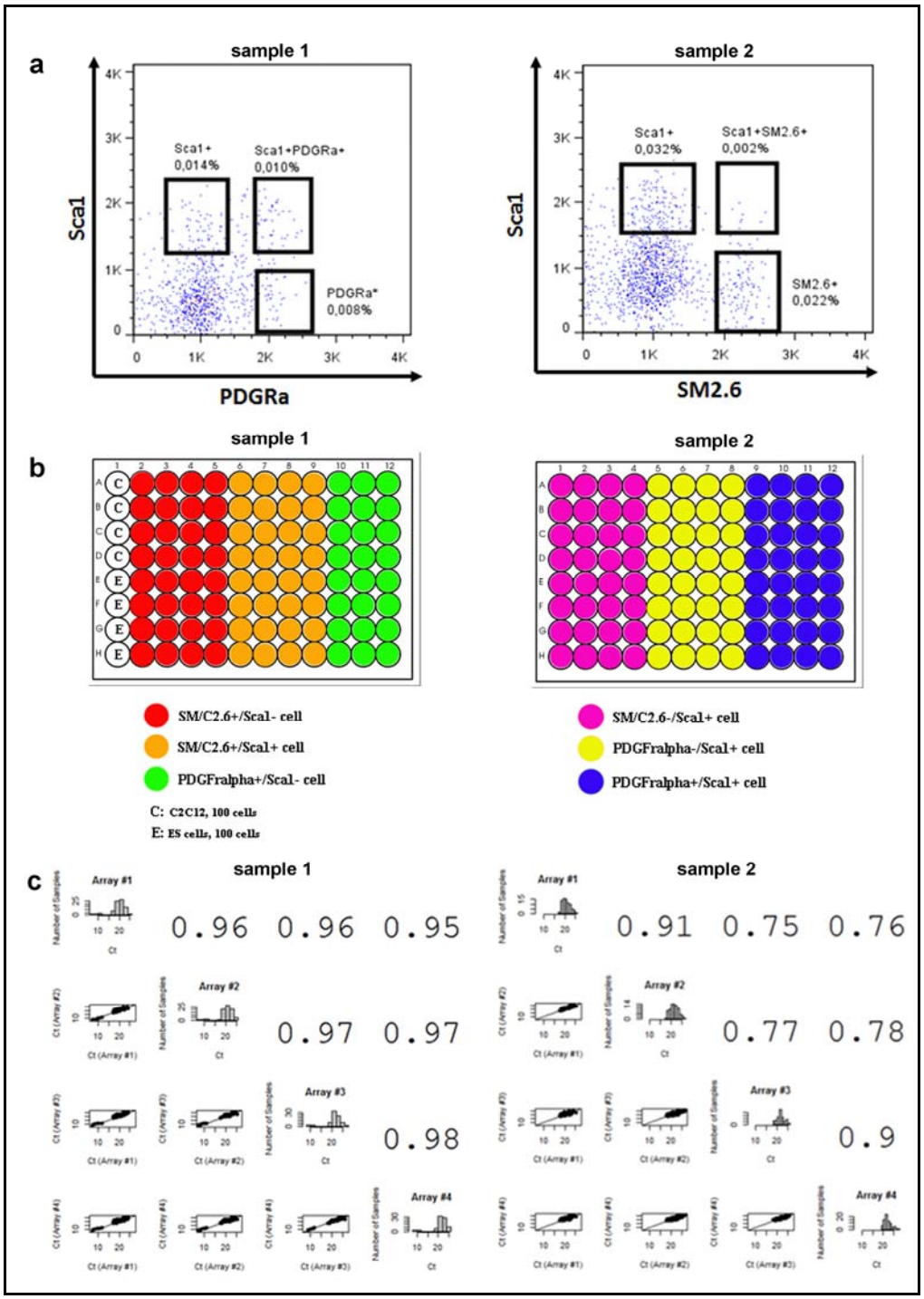

Figure 32. Transcriptomic analyses of different populations of muscle cells.
(a) Six different populations of cells were isolated from the skeletal muscle: $SCA1^{+}PDGFRalpha^{-}$; $SCA1^{+}PDGFRalpha^{+}$; $PDGFRalpha^{+}SCA1^{-}$; $SCA1^{+}SM/C2.6^{-}$; $SCA1^{+}SM/C2.6^{+}$; $SM/C2.6^{+}SCA1^{-}$. Representative images of dot plots and FACS gates used to isolate the six populations. **(b)** Representation of single cells of each population plated in 96-well plates. Two samples were created. The first sample contains the following cell types: in column number one the positive controls, consisting of 4 wells of 100 C2C12 cells and 4 wells of 100 ES cells; 32 cells of the $SM/C2.6^{+}SCA1^{-}$ population (satellite cells-$Sca1^{-}$); 32 cells of the $SM/C2.6^{+}SCA1^{+}$ population (satellite cells-$Sca1^{+}$); 23 cells of the $PDGFRalpha^{+}SCA1^{-}$ population (FAPs-$Sca1^{-}$). In the second plate: 32 cells of the $SM/C2.6^{-}SCA1^{+}$ population ($Sca1^{+}$cells- $SM/C2.6^{-}$); 32 cells of the $PDGFRalpha^{-}SCA1^{+}$ population ($Sca1^{+}$cells-$PDGFRalpha^{-}$); and 31 cells of the $PDGFRalpha^{+}SCA1^{+}$(FAPs-$Sca1^{+}$) population. In both sample plates, the last well was left empty (without sample) as an internal negative control **(c)** Pearson correlations of Ct values of *beta-actin* across experiments. Pearson correlation defines the relation among the different data obtained from the four arrays. A value near one reflects a high correlation. The high correlation obtained among the four arrays reflects the accuracy of each assay and allow comparing the data.

Based on the Fluidigm data, a heatmap was created to visualize the expression variance of the genes in single cells belonging to FAPs cells (PDGFRalpha^{+}Sca1^{-} and PDGFRalpha^{+}Sca1^{+}populations) and satellite cells (SM/C2.6^{+}Sca1^{-} and SM/C2.6^{+}Sca1^{+} populations) (Figure 33a & 34a). The results were then clustered using the R package clValid (as described before in section 5.9.2), in order to group cells presenting the same gene expression (Figure 33b & 34b). However, also after the clustering it was not possible to visualize a common unique gene profile for FAPs and satellite single cells. Although the cells were sorted for the same markers, at a single cell level FAPs and satellite cells reveal a high gene expression variance.

The clustering did not identify any difference in FAPs and satellite cells populations in the presence or the absence of *Sca1*. In order to reveal some distinct features, Student t-Test was performed in satellite cells (SM/C2.6^{+}Sca1^{-} population versus SM/C2.6^{+}Sca1^{+} population) and FAPS (PDGFRalpha^{+}Sca1^{-} population versus PDGFRalpha^{+}Sca1^{+} population). Based on the t-Test significance, in absence or presence of *Sca1* some genes resulted to be significant (Figure 33c & 34c).

In FAPs not expressing *Sca1* (PDGFRalpha^{+}Sca1^{-}), the following genes were highly expressed:

- *Bmp1* (Bone morphogenic protein 1),
- *Hey2* (Hairy/enhancer-of-split related with YRPW motif protein 2, also known as cardiovascular helix-loop-helix factor 1 (CHF1)),
- *Pdgfbeta* (Platelet-derived growth factor subunit beta),
- *Vegfc* (Vascular endothelial growth factor C).

The subpopulation of FAPs expressing *Sca1* (PDGFRalpha^{+}Sca1^{+}) was in contrast characterized by the expression of:

- *Lmna* (Lamin A/C),
- *Il6st* (Interleukin 6 signal transducer or gp130, or Oncostatin M receptor),
- *Stat6* (Signal transducer and activator of transcription 6),
- *Bmp4* (Bone morphogenic protein 4).

Satellite cells (SM/C2.6^{+}SCA1^{-} versus SM/C2.6^{+}SCA1^{+} population) instead of FAPs present a different trend. In the subpopulation of satellite cells expressing *Sca1* (SM/C2.6^{+}SCA1^{+}) the following genes were higher expressed (Figure 34c):

- *Bmp1* (Bone morphogenic protein 1),
- *Pax7* (Paired box gene 7),
- *Cxcl9* (Chemokine (C-X-C motif) ligand 9),

- *Eltd1* (EGF, Latrophilin seven transmembrane domain containing 1).

In the satellite cell fraction not expressing *Sca1* (SM/C2.6^{+}SCA1^{-}), other genes were highly expressed:

- *Il6st*,
- *Hes1* (Hairy and enhancer of split 1 (Drosophila)),
- *Kit* (c-kit, CD117, belly spot, steel factor receptor),
- *Numbl* (Numb-like).

Interestingly, as already observed in the microarray data for the *Sca1*-expressing cell population, also in satellite cells respectively in the presence and absence of *Sca1*, the expression of *Bmp1* and *Il6* was detected. It has been speculated that the presence of *Bmp1* in *Sca1*-expressing cells is involved in maintaining their quiescence, whereas the *Il6* expression promote their myogenic commitment. In this regard the presence of *Bmp1* in SM/C2.6^{+}SCA1^{+} population could mark a quiescent subpopulation, probably the actual cells able to replenish the stem cell pool after damage. On the other hand, the high level of *Il6* in satellite cells not expressing *Sca1* could reflect their tendency to be more prone to differentiation.

These data demonstrate that at a single cell level it is possible to observe a high heterogeneity in both satellite cells and FAPs population. Furthermore, the presence of *Sca1* in satellite cells seems to mark a subpopulation with higher quiescent characteristics.

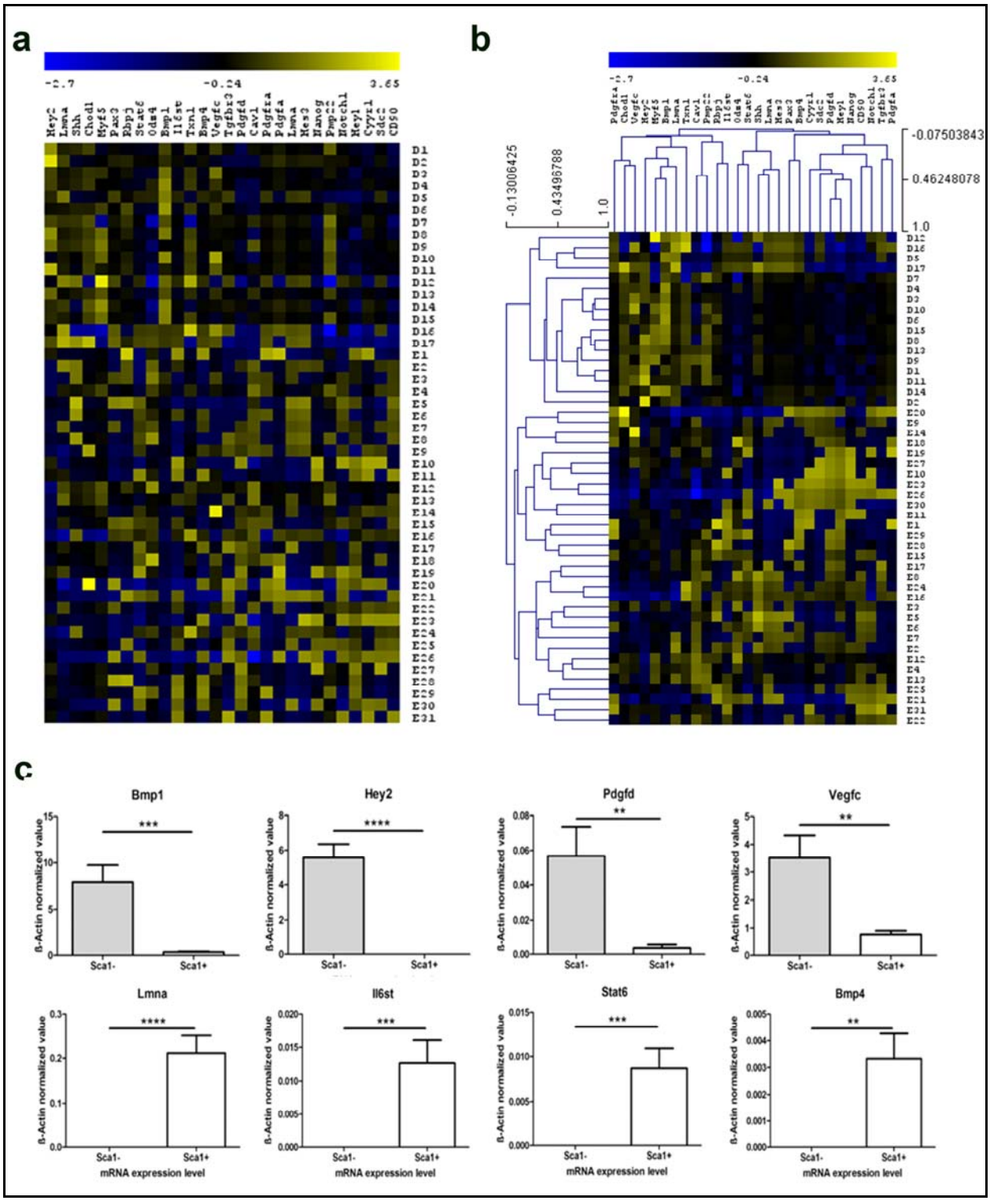

Figure 33. Profiling of fibro-adipocyte progenitor cells (FAPs).
PDGFRalpha^{-}SCA1^{+} and PDGFRalpha^{+}SCA1^{-} were compared. **(a)** Representative image of a heat map highlighting the genes expressed in single cells from PDGFRalpha^{+}Sca1^{-} and PDGFRalpha^{+}Sca1^{+}populations. The gene profile data were obtained by Fluidigm single cell RT-qPCR. In the heat map the yellow spots indicate a high expression and the blue ones a low expression. **(b)** A result of hierarchical clustering performed by Rpackage clValid in order to group cells presenting the same gene expression in FAPs population. **(c)** Representative graphs of genes significantly up or downregulated in the population not expressing (grey bar) or expressing *Sca1* (white bar). After performing Student t-Test between PDGFRalpha^{-}SCA1^{+} and PDGFRalpha^{+}SCA1^{-} the following genes resulted to be relevant: *Bmp1*, *Hey2*, *Pdgfd*, *Vegfc*, *Lmna*, *Il6st*, *Stat6*, *Bmp4*.

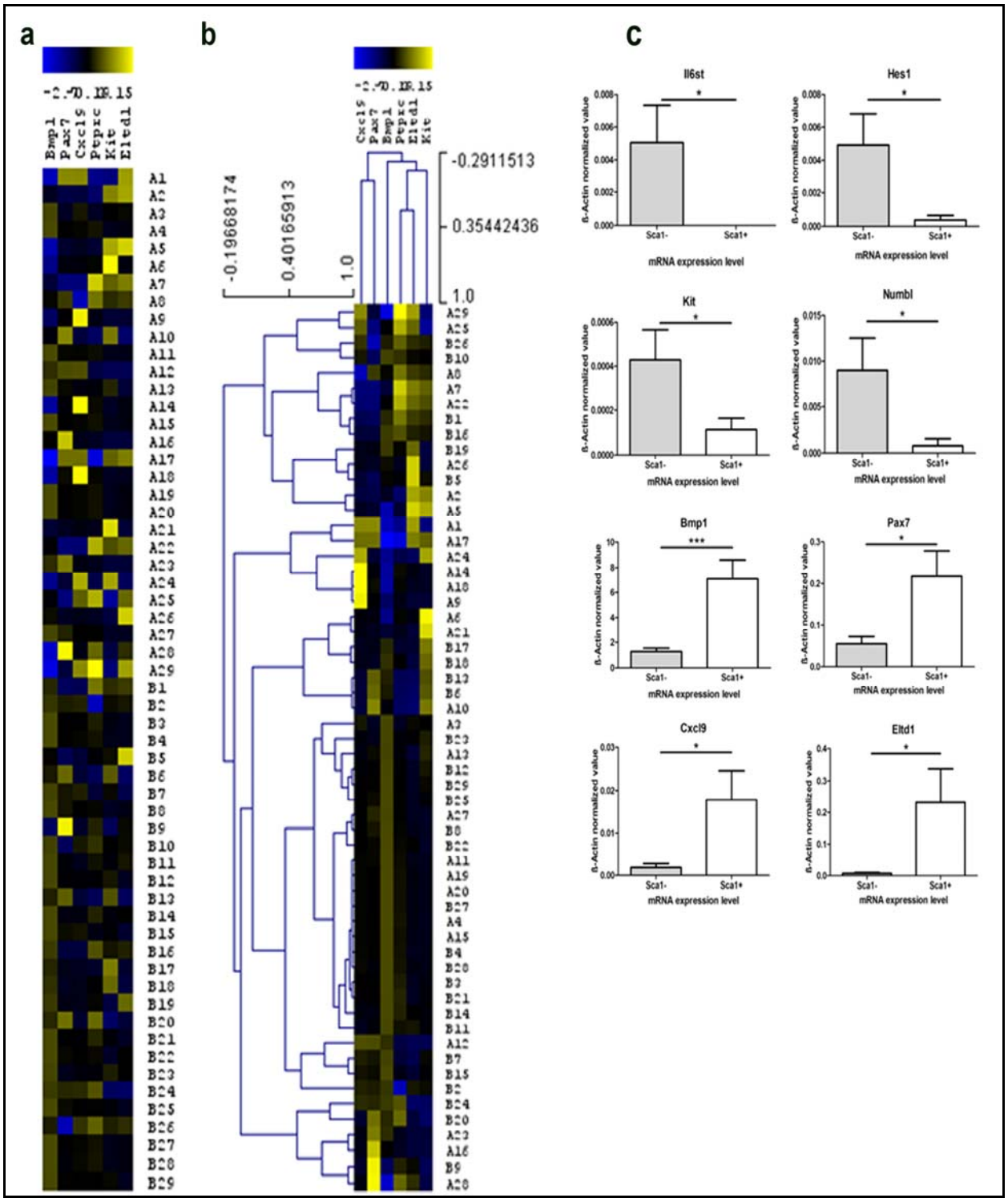

Figure 34. Profiling of satellite cells.
SM/C2.6^{-}SCA1^{+} and SM/C.6^{+}SCA1^{-} were compared. **(a)** Representative image of a heat map highlighting the genes expressed in single cells of SM/C2.6^{-}SCA1^{+} and SM/C.6^{+}SCA1^{-} populations. The gene profile data were obtained by Fluidigm single cell RT-qPCR. In the heat map the yellow spotsr indicate a high expression and the blue ones a low expression. **(b)** A result of hierarchical clustering performed by Rpackage clValid in order to group cells presenting the same gene expression in satellite cells population. **(c)** Representative graphs of genes significant highly up or down regulated in the population not expressing (grey bar) or expressing *Sca1* (white bar). After performing Student t-Test between SM/C2.6^{-}SCA1^{+} and SM/C.6^{+}SCA1^{-} the following genes resulted to be relevant: *Il6st, Hes1, Kit, Numbl, Bmp1, Pax7, Cxcl9, Eltd1*.

7 DISCUSSION

7.1 Evidence of the presence of *Sca1*-expressing cardiac stem cells in the heart

Heart failure and myocardial infarction are the most common cause of death in the western world. Although the human lifespan has increased due to better health care conditions, heart failure still affects 2-3% of the adult population and this percentage increases with age reaching 20-30% in people older than 70 years[157]. The raise of heart diseases affects not only the medical sphere, but also public welfare. The costs related to the treatment of patients affected by heart failure, for instance, have increased exponentially in recent years. Therefore, the need to prevent and cure heart disease has acquired a great importance, not only for the amelioration of health care conditions, but also from social and economic aspects.

It is known from the literature that species such as amphibians and fish possess a high capacity to regenerate damaged organs[158-160]. This remarkable capacity has been lost throughout evolution since mammals have a rather limited regenerative ability compared to lower species. This evolutionary loss is particularly evident in the adult mammalian heart that has been considered for a long time to be a post mitotic organ not able to self-renew[161]. Despite this evidence, recent studies show that murine neonatal hearts are able to regenerate after apical resection through cardiomyocyte proliferation[162,163]. Unfortunately, this remarkable ability of cardiomyocytes is lost within one week after birth, as more mature cardiomyocytes do not proliferate to regenerate the apical dissected heart. However, recent reports in human[49,164] and mouse[48] indicate that even the adult mammalian heart is able to regenerate upon damage. Moreover, it has been shown that the myocardial compartment, including cardiomyocytes, can also be renewed during aging to maintain the homeostasis of the heart[49]. These reports suggest that the heart, rather than a post mitotic organ, is a more dynamic system than previously thought. This concept opens up new perspectives in cardiovascular research that could be used for future therapeutic approaches.

Even though the concept of heart as a dynamic organ has been generally accepted by the scientific community, the cellular source responsible for cardiac self-renewal is far from clear. Some studies suggest that heart regeneration depends on the presence of common resident precursor or stem cells ("cardiac progenitor/stem cells (CSCs)")[130-132], whereas other propose that existing cardiomyocytes contribute to this process by re-entering the cell cycle and dividing again [133,134]. Both possibilities are currently investigated in the field of cardiovascular research. One hypothesis does not necessarily exclude the other and depending on the

condition (e.g. aging or pathological conditions), one source of renewal could be predominant over the other[23].

For instance, in 2007, using the MerCreMer-Z/EG mouse strain, Hsieh and collaborators could show that a pool of resident progenitor cells can differentiate into cardiomyocytes only in response to myocardial infarction, while under normal conditions these cells do not show any contribution[48]. This double transgenic mouse was obtained by mating the mouse strain line B6129-Tg(*Myh6*-Cre/Esr1)1Jmk/J (called αMHC-MerCreMer)[48] with the Z/EG reporter strain. The αMHC-MerCreMer transgenic mouse is a tamoxifen inducible Cre-recombinase (Cre-ERT) strain, in which CreERT expression is under the cardiac-specific alpha myosin heavy chain promoter (*Myh6*). The Z/EG reporter mouse, instead, carries the lacZ gene fused with a stop codon flanked by two *loxP* sites, upstream of the GFP reporter (Figure 11). In the double transgenic mouse αMHC-MerCreMer-Z/EG, in the absence of tamoxifen, cardiomyocytes are positive for lacZ and do not express GFP. Upon tamoxifen injection, Cre-ERT translocates into the nucleus and promotes the excision of the lacZ-stop codon cassette leading to the expression of GFP in cardiomyocytes. Using this mouse the group showed that during normal aging the number of GFP-labeled cardiomyocytes does not change. However, upon myocardial injury, the pool of the GFP-labeled cardiomyocytes is diminished. The authors speculated that this decrease is due to the existence of a pool of progenitor cells that are able to contribute to heart regeneration differentiating in cardiomyocytes which, in this case are negative for GFP. In contrast, under normal physiological conditions, the unchanged number of GFP-labeled cardiomyocytes leading the authors to conclude that cardiomyocyte turnover from the progenitor population does not take place.

On the other hand, Bergmann *et al.*[49] could show that cardiomyocyte renewal occurs even in adult human hearts during aging. The authors, by monitoring the incorporation of Carbon-14 (^{14}C) in the DNA of proliferating cells could prove that cardiomyocytes can be generated postnatally. They calculated that the percentage of cardiomyocyte turnover is approximately 1% every year in individuals aged 25 year old, while this rate declines over time and is around 0.45% in hearts from 75 year olds. In contrast to this low percentage, Kajstura *et al.*[165], estimated that the human heart is completely replaced up to eight times during the human lifespan and this process seems to depend on *C-kit*$^{+}$CSCs.

The data described above support the hypothesis that CSCs are the cells contributing to cardiac regeneration. However, other studies demonstrated that, instead, adult cardiomyocytes re-enter the cell cycle and could be the real source for mammalian heart renewal. Two distinct research groups, focusing on the rate of cardiomyocyte DNA synthesis, found that myocyte

turnover under physiological conditions is present, although it was either really low (0.76%)[134] or almost negligible (0.0006%)[166]. These differences in percentage could depend on the technique employed by the authors to score DNA synthesis. Nevertheless, this percentage increases up to 3.2%[134] upon myocardial infarction. Independently from the conditions, the authors were able to show that this turnover is based on the division of pre-existing cardiomyocytes. In order to do this, Senyo *et al.* took advantage of the MerCreMer-Z/EG mouse strain described above[48]. Using [^{15}N]thymidine, a base analogue that can be incorporated in the newly synthetized DNA during replication, they observed the presence of proliferating cardiomyocytes ($^{15}N^{+}$) positive for GFP. The presence of mononucleated $^{15}N^{+}$-GFP cardiomyocytes suggested that this fraction could only derive from the division of pre-existing GFP^{+}-cardiomyocytes[134].

Malliaras *et al.*[167] reported that based on the conditions, both pre-existing cardiomyocytes and precursor cells do contribute to the regeneration of the heart. Under normal physiological conditions, the murine adult cardiomyocytes re-enter the cell cycle, divide and give rise to new cardiomyocytes at a rate of ~1.3-4% per year. However under pathological conditions, they found that the regenerated cardiomyocytes derive mainly from CSCs. Although the findings of Senyo *et al.*[134] and Malliara *et al.*[167] are intriguing, the results obtained in this thesis suggest a different scenario. The lineage tracing experiments performed in this study show that, in accordance with what has been observed in humans by Bergmann *et al.*, in the murine heart, self-renewal also occurs under physiological conditions and the possible source of this renewal is represented by *Sca1*$^{+}$CSCs. *Sca1* is a specific marker for stem cells, including cardiac stem cells (CSCs)[71,72,129], that is not expressed in mature cardiomyocytes. SCA1 immunostaining in isolated cardiomyocytes highlights that only a pool of small round cells attached to cardiomyocytes that express this marker (Figure 21). Using *Sca1*-tTA//LC1-Cre//Z/AP mice, it was possible to observe that *Sca1*-expressing cells are able to contribute to the self-renewal of the major components of the myocardial compartment, including postnatal cardiomyocytes (Figure 17). In this mouse model, both the cells expressing *Sca1* and *Sca1*-derived cells are labeled with alkaline phosphatase (AP^{+}, as described in section 6.1.1). Using this approach it was possible to identify, cardiomyocytes expressing alkaline phosphatase under physiological conditions, therefore demonstrating the existence of cardiomyocytes derived from *Sca1*-expressing cells. In particular, a fraction of AP^{+} mononucleated cardiomyocytes was constantly present regardless of the age (Figure 20). Cardiomyocytes are mature cells characterized by polyploidy (multiple sets of chromosomes), a phenomenon that usually occurs in cells in response to fusion events, aging or stress[136]. FISH (Fluorescence *in*

situ hybridization) experiments, performed in male *Sca1*-tTA//LC1-Cre//Z/AP mice, revealed that the pool of AP^+ mononucleated cardiomyocytes presents only one Y-chromosome in the nucleus. This result confirms that these cells could not be derived from a fusion event of pre-existing cardiomyocytes with *Sca1*-expressing AP^+-cells. This evidence suggests the hypothesis that these cardiomyocytes could be derived from $Sca1^+$-progenitor cells rather than from existing differentiated cardiomyocytes. Based on these data, the contribution of $Sca1^+$-cells to the physiological turnover of the heart was evaluated. It was shown, using mice of different ages (2 to 18 months old), that the absolute number of AP^+-cardiomyocytes increases exponentially. This confirms a certain role of *Sca1*-derived cells in the maintenance of heart homeostasis during aging. However, as mentioned before, it has been published that CSCs contribute to heart regeneration only after damage, while no contribution under physiological conditions was observed[48]. Based on these results, the contribution of *Sca1*-derived cells was analyzed using two different cardiac damage models: transverse aortic constriction (TAC) and myocardial infarction. Upon damage, the contribution of the *Sca1*-expressing population was prominent as compared to the physiological conditions, confirming the study published by Hsieh and colleagues[48]. Moreover, it was observed that different types of damage influence the fate decisions of *Sca1*-derived cells towards one lineage rather than the other (Figure 18). TAC, for instance, is a model which leads to pressure overload-induced cardiac hypertrophy. The response to this damage consists of an enhancement of cardiac contractility that after a long period causes cardiac dilatation and heart failure. In this model, it was observed that *Sca1*-expressing cells differentiate more towards the cardiomyocyte lineage as compared to the other lineages. Independently from the time points studied (one or five months after the operation), the number of AP^+-cardiomyocytes was approximately two times higher than in the control mice (Figure 18). Myocardial infarction, in contrast to TAC, does not affect the heart dimension. In this model, the damage is based on the permanent ligation of the left anterior descending artery (LAD) that leads to myocardial ischemia. The insufficient blood flow and therefore the low oxygen supply cause a loss of myocardial tissue resulting in scar formation. In this scenario no AP^+-labeled cells, including cardiomyocytes, were detected either in the scar or in the border regions (Figure 18). However, a significant number of AP^+-labeled endothelial cells were found in the septum area (Table 5). These observations support the idea that *Sca1*-expressing cells are resident stem cells able to differentiate into the cell types needed following cardiac remodeling, for example in response to myocardial infarction. In this regard, the external stimuli have a major influence in determining the differentiation fate of these precursor cells. In conditions where the oxygen

supply needs to be properly restored (e.g. myocardial infarction), the *Sca1*-expressing CSCs differentiate more into endothelial and smooth muscle cells rather than into cardiomyocytes, therefore increasing the number of vessels in the scar area. On the other hand, in the TAC model, *Sca1*-expressing CSCs give rise mainly to cardiomyocytes that might contribute to hypertrophy and higher cardiac contractility. Taken together, these data confirm the presence of a pool of progenitor cells, positive for *Sca1*, able to contribute to cardiomyocyte renewal under physiological and pathological conditions. However, the previous studies showed that under physiological conditions, heart renewal is achieved only by the proliferation of pre-existing cardiomyocytes which re-enter the cell cycle and divide again, while no contribution of progenitor cells was reported[167]. The data examined so far in this thesis could support the idea that a population of CSCs expressing *Sca1* is instead, involved in cardiomyocyte renewal during aging. This discrepancy could depend on the lineage tracing methods chosen and their relative limitations. For instance, since *Sca1* is never expressed in adult mature cardiomyocytes, the role of pre-existing cardiomyocytes in heart renewal could not be analyzed in this thesis. On the other hand, in the previous investigations, the authors only focused on the contribution of cardiomyocytes not following the fate of precursor stem cells[134]. In both cases, the studies trace either pre-existing cardiomyocytes or CSCs, not taking into account the possible contribution of an alternative source for heart renewal. It is therefore important to evaluate at the same time, the contribution of CSCs and pre-existing cardiomyocytes during heart regeneration. In order to achieve this, one could cross the *Sca1*-tTA//LC1-Cre//Z/AP mouse used in this thesis with the MerCreMer-ZEG mouse strain used by the other groups described above[48,134,167]. In the penta-transgenic mouse *Sca1*-tTA//LC1-Cre//Z/AP//αMHC-MerCreMer-ZEG, the presence of cardiomyocytes labeled with alkaline phosphatase (i.e. derived from *Sca1*-expressing cells) but negative for GFP after tamoxifen induction would prove that these cells are derived from *Sca1*-expressing CSCs, rather than from the pre-existing cardiomyocytes. Furthermore, it would be possible to follow at the same time the turnover of GFP-labeled cardiomyocytes and the fate of *Sca1*-derived cells by comparing their contribution to heart regeneration. This approach would better elucidate the reason for the differences found between this thesis and the previous studies and might lead to a better understanding of the role of these two different sources in cardiac renewal.

If CSCs do play a major role in regulation of the heart turnover and regeneration, so far these cells have not been well characterized. Besides SCA1[71,72,129], other different CSCs markers, such as ISL1[168] and C-KIT[130], have been identified. However, it is more likely that, rather than only one, a combination of different markers could define the CSCs population. Using

the *Sca1*-tTA//LC1-Cre//*R26R-Confetti* mouse strain it was possible to confirm that *Sca1*-expressing cells represent a heterogeneous population consistent with previous work[169] (Figure 22). In *Sca1*-tTA//LC1-Cre//*R26R-Confetti* mice, Cre expression is under the control of the *Sca1* promoter. In this mouse, Cre promotes the excision of the *loxP* sites present in the *R26R-Confetti* reporter mouse. The recombination removes the roadblock cassette resulting in individual *Sca1*-expressing cells labeled with the fluorescent protein presents right after the roadblock and randomly selected among the four proteins presented in the construct, such as: nGFP (nuclear green fluorescent protein); YFP (monomeric enhanced yellow fluorescent protein); RFP (red fluorescent protein); and mCFP (mCerulean cyan fluorescent protein) (as described in section 6.1.6). The fluorescent protein is retained by the daughter cells, therefore, the resulting clonal population will express the identical fluorescent tag. It was observed in this thesis that one color was not specific for a cell lineage, but each clone (color) was able to give rise to different cell lineages. For instance, yellow smooth muscle cells were detected as well as yellow cardiomyocytes. Furthermore, the analysis of different regions of the heart of *Sca1*-tTA//LC1-Cre//*R26R-Confetti* mice, revealed an unequal contribution of different *Sca1*-expressing clones (characterized by different colors) within the same lineage. Moreover it has been observed that the ratio of cardiomyocytes and other cells types was not constant (Figure 22e). These data could indicate that different *Sca1*-expressing clones may have differences in their potential to become mature cell types.

Although lineage tracing using *Sca1*-tTA//LC1-Cre//*R26R-Confetti* mouse strain reveals certain heterogeneity of the *Sca1*-expressing CSCs, a further characterization of these cells is necessary. The identification of a pure population of CSCs will ensure an easier isolation of these cells for *in vitro* and *in vivo* studies as well as for their potential application in the clinical field. Currently, the most common method utilized to isolate cells is FACS (Fluorescence Activated Cell Sorting). FACS is a technique that allows separating distinct cell populations according to their cell surface markers. In order to specifically characterize CSCs, these cells were first isolated from the total fraction of the adult murine heart and their transcriptomic profile was analyzed using microarrays. The output was compared to microarray data of other cell types (e.g. murine embryonic stem cells, endothelial cells). The obtained CSCs transcriptome was more similar to cardiac fibroblasts than to that of other cells types (Figure 23). The microarray data of cardiac fibroblasts were obtained from fibroblasts successful reprogrammed into cardiac stem cells[170-171]. The similarity found between the CSCs and cardiac fibroblasts confirmed the potential plasticity of these cells, the same normally acquired by reprogrammed cells. However, these data are related to a fraction of

CSCs not completely pure for *Sca1*. The CSCs were isolated using a Millipore kit that guarantees purity up to 50% in the SCA1-expressing cells. In respect to identifying a unique expression profile for pure *Sca1*-expressing CSCs, these cells were individually sorted using SCA1 as a surface marker, while populations expressing CD31 (marker for endothelial cells) and CD45 (marker for hematopoietic cells) were excluded. Immunostaining against transcription factors considered typical for stem cells (Figure 23d) revealed that not all *Sca1*$^{+}$CSCs cells possess the same expression level of typical stem cell markers such as ABCG2, SOX2 and NANOG. The majority of them are positive for ABCG2 and SOX2 (32%), whereas only a small number of cells express NANOG (0.88%). These data further confirm the heterogeneity of *Sca1*$^{+}$CSCs cells. It is known that although cells isolated by FACS present the same specific cell surface marker, this does not guarantee the homogeneity of the population. Indeed, cells belonging to the same population at the single cell level might not have a unique molecular signature because the gene expression may not reflect the level of the corresponding protein[172-175]. This is due to the fact that transcription and translation are stochastic events, leading to a content of mRNA and proteins that differs from cell to cell[176]. To uncover such cell to cell variability, new techniques have been developed in recent years[176,177]. One of them is a method developed by Fluidigm Corporation[178] consisted of high-throughput real-time single cells PCR. This method take advantage of specific chip cards that are composed of different microfluidic chambers and channels in which individuals PCR reactions occur at the same time. In particular, using this method the selected primers are loaded in one side of the chip, whereas the samples are located in the other one. The solutions are, then, primed together and pressurized inside the micro-channels, where the real time PCR reaction is performed using a real time PCR machine (BioMark^{TM}HD Reader). In order to set up multiple reactions, the strategy of this technique is that all the reactions are run using the same melting temperature (60°C) and as a consequence, all the primers considered have to be designed following this specific criterion. In this dissertation this technique was utilized to try to define a specific and homogenous profile for *Sca1*-expressing CSCs at single cell gene level.

Although the heterogeneity of the sorted SCA1^{+}CD31^{-}CD45^{-} CSCs remained high, the analyses of single-cell transcriptomic data generated through BioMark^{TM}HD System revealed a clear and defined common signature of *Sca1*$^{+}$CSCs. Among all the different genes considered in the analyses and known to be related to the heart and stem cell field, three of them were highly expressed in all the single *Sca1*$^{+}$CSCs studied: *Nestin*, *Tgfb3* and *Stat2*. *Nestin* and *Tgfb3* have already been described in literature to be involved in heart

regeneration. *Nestin* has been identified as a marker for CSCs by a number of researchers in the past[179,180], while a point mutations of *Tgfb3* have been causally linked to arrhythmogenic right ventricular cardiomyopathy (ARVC) disease, possibly due to defects in cardiac progenitor cells[181]. *Stat2* has been shown to have a role in regulating myogenic differentiation in satellite cell derived myoblasts[182] but so far, it has never been reported to be associated with cardiomyocytes and cardiomyocyte progenitor cells. These data lead to the conclusion that based on the presence of *Stat2*, *Nestin* and *Tgfb3* genes, within *Sca1*$^{+}$CSCs it is possible to identify a subpopulation of cell presenting a common gene expression profile.

The heterogeneity observed *in vivo* using *R26R-Confetti* mice and in the single cell transcriptional profiling of CSCs could give a possible explanation for the differences in terms of number and contribution of these cells in the heart turnover observed by distinct research groups. Based on the labeled population, it could be that only a small fraction of CSCs were analyzed, while a complete overview of the regenerative capability of CSCs is still missing. In this perspective, the data shown in this thesis have their own limitations. On one side, in the lineage tracing approach used in the present work, only CSCs cell expressing *Sca1* were analyzed and characterized, while the contribution of other CSCs cells that might not express *Sca1* was not considered. On the other hand, although *Sca1*$^{+}$CSCs could represent a very interesting source of cardiac stem cells to be further investigated in order to be used in the clinic, Sca1 does not seem to be a good marker for isolation of CSCs from human patients. Although some groups were able to isolate cardiac progenitor cells from human fetal and adult hearts using anti-murine SCA1 antibody[183], the human ortholog of *Sca1* has not been identified so far[76]. To overcome this problem, instead of using Sca1 as a marker to isolate human CSCs, one possibility could be to consider other markers that in this study have shown high significance at single cell transcriptomic level. Nevertheless, even with of these restrictions it was possible to define a unique population of CSCs in this thesis. Another important goal would be to find a way to manipulate these cells in order to stimulate their differentiation toward particular cell types (e.g. in the heart into cardiomyocytes), that would make these cells particularly attractive also for clinical purposes. In particular, it will be interesting to understand the molecular pathway that regulates the differentiation process of *Sca1*$^{+}$CSCs toward the different mature cell types. In this regard the experiments performed in this study could be helpful to find certain substances that could be used as possible drugs to stimulate the differentiation *Sca1*$^{+}$CSC. Following this idea, the mouse model used in this thesis could be considered a good tool to screen *in vivo* which substances are more effective. The *Sca1*-tTA//LC1-Cre//Z/AP mouse is under the control of the Tet-off system meaning that

in the presence of doxycycline tTA is not able to bind the operator and the transcription of Cre-recombinase is repressed. In the absence of Cre the cells expressing *Sca1* will be positive for lacZ whereas alkaline phosphatase labeling will not occur. One possible idea could be to administer doxycycline and suppress the AP-labeling of the cells until the administration of inhibitors for instance. After the drugs injection, the administration of doxycycline will be removed and the cells expressing *Sca1* will start to express alkaline phosphatase. In this context, if the substance chosen could stimulate *Sca1*$^{+}$CSCs differentiation, it could be possible to find an increased number of AP^{+}-cardiomyocytes compared to the untreated control. Another possible read out of the efficiency of the substances chosen could be to test them *in vitro*. During this study, several attempts were made to culture the isolated *Sca1*-expressing CSCs but unfortunately these cells quickly became senescent and no further experiments were possible. However, it was observed that *in vitro*, *Sca1*-expressing cells are normally attached to the cardiomyocytes and specifically located under the basal lamina of cardiomyocytes, which in this dissertation has been proposed to be the possible niche for CSCs (Figure 21). Taken these results into account, a possible way to cultivate these cells would be to isolate cardiomyocytes together with the attached CSCs and co-culture them. For this purpose, it might be useful to utilize the *Sca1*-GFP mouse line already considered in this thesis to identify the niche of *Sca1*-expressing cells. In this mouse, the expression of GFP is controlled by *Sca1* gene regulatory sequence. In particular, *Sca1*-expressing cells are labeled by GFP, since GFP is under the endogenous promoter of *Sca1*, however after their commitment towards mature cells types (e.g. cardiomyocyte) the GFP signal is lost due to the fact that the differentiated cells do not express *Sca1* any longer, as previously mentioned. It has been observed in this thesis that in normal culture conditions *Sca1*-positive cells preferably remains quiescent and do not spontaneously differentiate. As a consequence, if the substances chosen could specifically stimulate only *Sca1*-expressing cells to differentiate towards cardiomyocytes lineages *in vitro* for instance, the GFP signal in these cells should be lost and performing a counterstain with cardiac marker specific (e.g. alpha myosin heavy chain, dystrophin, phalloidin) should reveal an increase number of mononucleated cardiomyocytes.

In conclusion, this study demonstrates the existence of resident cardiac progenitor cells expressing *Sca1* in the murine adult heart. They seem to be located in a specific position, attached to cardiomyocytes and under the basal lamina, similarly to satellite cells in the skeletal muscle. It is proposed here that these *Sca1*$^{+}$-cells can give rise to different mature cell types upon differentiation. These mature cell types include cardiomyocytes, which can be

replenished during the normal aging process to maintain the homeostasis of the heart, albeit in a limited manner. Furthermore, these cells are directed to a certain lineage upon external stimuli caused by myocardial damages (Figure 35). Further work based on this study is essential to further characterize these cells and identify the molecular mechanisms that control their behavior in response to specific drug treatment, in order to understand if *Sca1*$^{+}$-cells could be a possible choice as source of stem cells to be used therapeutically.

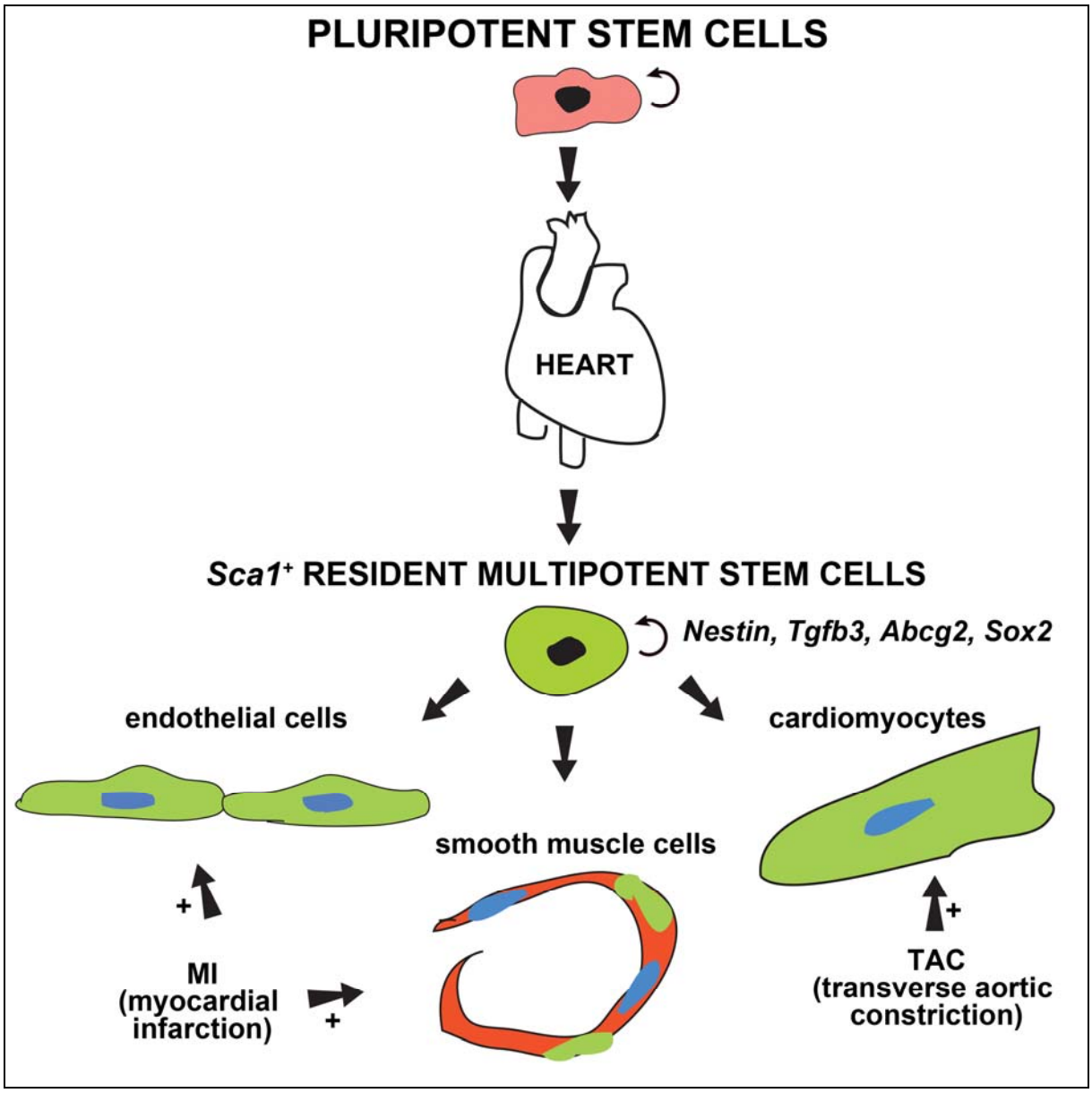

Figure 35. Possible scheme showing the contribution of *Sca1*-derived cells in the heart regeneration.

7.2 Evidence that *Sca1*-expressing cells are a source of skeletal muscle renewal and regeneration

In the skeletal muscle, the contribution of resident stem cells to regeneration of muscle fibers has been studied in more detail as compared to the heart.

The classical "dogma" in skeletal muscle research is that only one stem cell type is present, the so called "satellite cells"[59,184]. Since their discovery in 1961[41], satellite cells have been described to be a unique population of stem cells in the muscle that are able to self-renew and are characterized by the expression of protein markers such as C-MET, CD34, M-CADHERIN and the transcriptional factor PAX7. Satellite cells reside underneath the basal lamina and are able to differentiate in mature myofibers maintaining the muscle homeostasis and thereby contribute to skeletal muscle repair. In contrast to the classical definition of stem cells[185-188] which are able to differentiate in multiple lineages (multipotency), satellite cells show only myogenic commitment *in vivo*[189]. Although satellite cells are the muscle stem cell par excellence, in the recent years other stem cell populations have been identified in the skeletal muscle. These include: Fibro-Adipo Progenitors cells (FAPs)[63,64,152], Progenitor Interstitial Cells (PICs)[60,190], pericytes[191], mesangioblasts[192] and Muscle Derived Stem Cells (MDSCs)[66]. Some of them clearly regulate satellite cells quiescence and differentiation to balance the myogenic regeneration (FAPs, PICs), while others show multipotency for example MDSCs (Figure 36). MDSCs are indeed able to self-renew and to differentiate, both *in vitro* and *in vivo*, into distinct lineages and therefore are, among all muscle stem cells the ones showing more features of classical stem cells. It has been shown in addition that transplantation of MDSCs leads to a better regeneration and higher dystrophin delivery in the dystrophic mouse model[193], as compared to satellite cells. Interestingly, a common characteristic among all the muscle stem cells populations described above, beside satellite cells, is the expression of stem cell antigen 1 marker (Sca1).

Using the same mouse model as in the heart lineage tracing studies (*Sca1*-tTA//LC1-Cre//Z/AP) it was also possible to monitor the fate of *Sca1* progenitor cells *in vivo* in the skeletal muscle. In *Sca1*-tTA//LC1-Cre//Z/AP mouse, once a cell expresses *Sca1*, Cre is transcribed and the cell is permanently labelled with alkaline phosphatase. Since alkaline phosphatase has been described in the literature by Cappellari *et al.* to be a marker for pericytes[194], another stem cell population identified in the skeletal muscle, one could argue that the lineage tracing performed in this thesis simply traced their fate. However, since the Z/AP allele produces human Placental Alkaline Phosphatase (hPLAP), using a specific antibody for hPLAP (AP) and the described mouse model, it was possible to rule out the simple tracing of pericytes and discriminate them from the cells expressing hPLAP. The *in vivo* data shown in section 6.2.1 demonstrate that a *Sca1*-expressing cell population is able to

partially contribute to muscle regeneration under normal physiological conditions. In fact in 3 to 18 month old mice it was possible to detect AP^+-fibers, although their number decreased from younger to older mice confirming how aging affects the ability of *Sca1*-derived cells to give rise to myofibers. Since the number of AP^+-fibers detected in cross-sections of the skeletal muscle in these conditions was extremely low, muscle damage was induced in *Sca1*-tTA//LC1-Cre//Z/AP mice to examine if the subsequent muscle regeneration could stimulate *Sca1*-expressing cells to differentiate more into the myogenic lineage. As a first approach, the regeneration was monitored, in response to muscle damage induced by a single cardiotoxin injection (snake venom able to destroy myofibers), according to the literature[195]. Although, after damage, a slight increase in the number of AP^+-fibers was detected, this was not significant compared to the physiological condition (Figure 24 a & b). This result might be due to the fact that one cardiotoxin injection represents soft damage, not sufficient to properly activate *Sca1*-expressing cells. Therefore severe damage conditions were used by performing one cardiotoxin injection every month for a total period of three months (Figure 24). Although the contribution to muscle regeneration of *Sca1*-expressing cells remained less than satellite cells, a slight increase in the number of labeled myofibers after three injections was observed as compared to mice injected only once. This behavior seems to be similar to the hematopoietic "dormant" stem cells[196], described in the literature as a quiescent cell population not able to participate in normal hematopoiesis. However, upon severe damage (e.g. bone marrow injury), these dormant stem cells proliferate and differentiate in all blood cell types. These data confirmed that, although satellite cells still represent the major source of muscle regeneration, *Sca1*-expressing cells might function as a reservoir of stem cells upon severe damage. One hypothesis might be that the regeneration process sustained by satellite cells upon repetitive injury seems to be insufficient and as such other types of stem cells, normally dormant (i.e. *Sca1*-expressing cells), start to differentiate and assist satellite cells in myofiber formation. Furthermore, it was speculated that *Sca1*-expressing cells show higher myogenic contribution in an environment where a continuous regeneration occurs thereby promoting continuous stem cell differentiation. An example of such an environment could be represented by degenerative disorders leading to skeletal muscle wasting, such as muscular dystrophies[197]. Duchenne dystrophy is one of the most common muscular dystrophies which affects 1 in 3500 male birth in the world. It is a recessive X-linked disease characterized by a total absence or a defect (usually a point mutation) in the dystrophin gene. Dystrophin is a cytoskeletal protein present in the myofiber sarcolemma, involved on the linkage between the cytoskeleton and the extracellular matrix[198]. A defect in the dystrophin protein leads to muscle

membrane abnormalities which influence myofiber functionality. Although satellite cells in this disease are perfectly functional, the constant muscle damage, continuously stimulates satellite cells to enter the cell cycle and differentiate into new fibers leading to impoverishment of the stem cell reservoir[199]. Gene therapy, exon skipping and cell therapies are the common approaches under investigation to treat this pathology, even if the clinical results still remain disappointing[200]. In the research field, the *mdx* (X-linked muscular dystrophy) mouse represents the experimental Duchenne dystrophy model. The *mdx* mouse is a modified genetic strain in which the exon 23 of the dystrophin gene carries a non-sense point mutation that causes abnormal dystrophin production and consequent progressive degeneration of the skeletal muscle[201]. However, in *mdx* mice spontaneous somatic reversion of the mutation occurs, generating a limited number of dystrophin positive fibers called "revertant" fibers[202], able to promote partial muscle regeneration. Furthermore it has been described that presence of longer telomere as well as normal telomerase activity in mice[203] are the reason of lifespan prolongation in the *mdx* mice as compared to humans. A patient affected by Duchenne dystrophy, in fact, can survive a maximum of 35 years; while *mdx* mice normally die when they are around 15-19 months old. Although *mdx* mice show some features different from the human Duchenne dystrophy, they can be considered as a good animal model for both genetic and biological studies[204]. Different studies have shown that although *ex vivo* transplantation of satellite cells obtained from healthy donor mice into *mdx* host mice increases the level of functional dystrophin positive fibers, in general their contribution turned out to be poorly efficient and did not lead to any significant benefits[205,206]. A possible explanation of the low efficiency of satellite cells in a degenerative environment might be that, in this situation, satellite cells are not able alone to rescue skeletal muscle regeneration but they rather need the support of other stem cells. In this study, the contribution of *Sca1*-expressing cells in myofiber formation was investigated in *mdx* mice as model mimicking a condition of extreme muscle damage. *Sca1*-tTA//LC1-Cre//Z/AP mice were crossed with *mdx* mice and injected each month with cardiotoxin for a total of three times. In this context, it was found that in young mice the number of *Sca1*-derived myofibers increased as compared to the not injected contralateral muscle (TAR), therefore used as a control (3 months old: 0.11±0.0034% in TAR and 0.18±0.0037% in TAL). Contrarily, in the older mice (6 months old) this number was decreased slightly, even though newly regenerated fibers (center-nucleated) were detectable (Figure 25d). This approach demonstrates that *Sca1*-expressing cells have a higher contribution in muscle fiber regeneration under pathological conditions. These data could support the hypothesis that *Sca1*-expressing cells are dormant stem cells

able to be properly activated only in extreme adverse environments. As mentioned above, the repetitive cycles of regeneration occurring in *mdx* mice lead to a constant activation and differentiation of the satellite cells impoverishing their pool. In this respect, *Sca1*-expressing stem cells could represent a possible source of stem cells able to be recruited to replenish the stem cell pool[184] and contribute to muscle regeneration.

The involvement of *Sca1*-expressing cells in muscle regeneration under both physiological and pathological conditions, do not however clarify the question whether these cells are a population of stem cells distinct from satellite cells or not. In 2013, a population of muscle stem cells which express SCA1 and the satellite marker PAX7[207] was identified. In this regard the *in vivo* results showed in this study may be a mere observation of a subset satellite cells expressing SCA1. However, the presence of alkaline phosphatase labeled myofibers in the *Sca1*-tTA//LC1-Cre//Z/AP//*Pax7*$^{loxPGu/loxPGu}$ mouse model rebuts this point. In this mouse model, when a cell expresses *Sca1*, Cre is transcribed and recombines the *loxP* present in both Z/AP and *Pax7*$^{loxPGu/loxPGu}$ strains. The recombination leads to the permanent labelling of *Sca1*-expressing cells with alkaline phosphatase and to the excision of the exons 1-3 from *Pax7* gene resulting in a loss of expression of Pax7 (Figure 26a). Pax7 is a transcription factor which belongs to the family of paired-box proteins. It is involved in different developmental processes and is one of the most common markers specific for quiescent satellite cells. When the satellite cells start to differentiate, the expression of this marker is shut down[208]. Although the function of *Pax7* has been shown to be required for the myogenic determination of satellite cells during embryonic stages, it is still not clear if it is also necessary on adulthood[144]. Accordingly Seale *et al.*[209] demonstrated that, although in *Pax7* deficient mice (*Pax7*$^{-/-}$) satellite cells are completely absent, another distinct type of muscle stem cells exists that does not express *Pax7*. In the absence of PAX7 expression, this population showed high *in vitro* hematopoietic potential, whereas when they express the PAX7 their potency is limited to satellite cells commitment. In contrast with these results, Sambasivan *et al.*[210] demonstrated that the role of PAX7^{+} satellite cells is also fundamental for the regeneration of muscle fibers in adult stages. More recently, Günther *et al.*[111], developed the mouse model *Pax7*$^{loxPGu/loxPGu}$ (used also in this thesis) and confirmed the importance of *Pax7* in the myogenic commitment of stem cells during adult stages. In particular, the authors showed that the deletion of *Pax7* gene in adult Pax7^{+} and Myf5^{+} cells population leads to respectively completely satellite cell loss and in impaired muscle regeneration. The debate concerning the role of satellite cells in adult stage and the presence of other source of stem cells remains open. The results obtained in this thesis using *Sca1*-tTA//LC1-Cre//Z/AP//*Pax7*$^{loxPGu/loxPGu}$ mouse model, suggest the idea

of the presence of a population of stem cells distinct from satellite cells. Normally a muscle stem cell requires to sequentially express *Pax7*, *Myf5*, *MyoD* and *Myogenin* to become a fiber[211], however the presence of AP^+-labeled myofibers in *Sca1*-tTA//LC1-Cre//Z/AP//*Pax7*$^{loxPGu/loxPGu}$ mouse (Figure 26) confirmed the existence of *Sca1*-expressing cells that are able to differentiate towards the myogenic lineage without the requirement of *Pax7* expression. This contribution to muscle regeneration was rather limited both under normal physiological and after cardiotoxin damage. Based on the data showed by Lepper *et al.* [144], supporting the idea that during the muscle regeneration *Pax7* expression is not required after postnatal day 21 (P21), *Sca1*-expressing cell contribution was also investigated before P21. An increased number of labeled fibers was present in *Sca1*-tTA//LC1-Cre//Z/AP//*Pax7*$^{loxPGu/loxPGu}$ mice at P21 (Figure 27) injected with cardiotoxin at P14, as compared to the uninjected control mice. These observations lead to the conclusion that a subpopulation of *Sca1*-expressing cells is able to differentiate into myofibers independent of *Pax7* expression in neonatal stages. The increased number of AP^+-myofibers detected in the neonatal mice as compared to the adult stage suggest that, in a young environment, *Sca1*-expressing cells are more active. However, one should take into account that Günther *et al.* [111], using the inducible Cre *Pax7*$^{CE/loxPGu}$ transgenic mice, showed that upon tamoxifen (TAM) injection the subsequent deletion of *Pax7* does not immediately lead to the loss of all satellite cells. Instead there is an almost complete deletion only after 30 days post TAM injection. Based on these data, the presence of more AP^+-fibers during neonatal stages in *Sca1*-tTA//LC1-Cre//Z/AP//*Pax7*$^{loxPGu/loxPGu}$ model, could depend on the presence of a subpopulation of satellite cells expressing *Sca1*. However as described by Gunther *et al.*[111] after 14 days after birth, time point chosen in this thesis to induce muscle damage, the satellite cells presence is almost negligible ensuring that the *Sca1*-expressing cells contributing to muscle regeneration are the one that already lost satellite cell characteristics. These data propose that, in a small population of *Sca*1-expressing muscle resident stem cells, the function of *Pax7* seems not to be crucial, although it remains indisputable that satellite cells are the myogenic precursor population with the higher contribution in muscle regeneration.

As previously reported[189], satellite cells lack the ability to differentiate into cell types other than myofibers *in vivo*, whereas cells expressing *Sca1* and positive also either for PDGFRalpha-positive[63] or alpha7INTEGRIN[64], namely FAPS[63,64], are multipotent. FAPs have been reported to be a cell population completely distinct from satellite cells, that is able to differentiate into fibrotic and adipose tissues. They seem to play a major role in balancing the muscle regeneration and fibro-adipose tissue content under physiological conditions and

in response to damage through the release of chemokine (e.g. IL6). Interestingly, it has been recently shown that the expression of SCA1 and PDGFRalpha in PICs, another muscle stem cells population, could define a subpopulation also able to give rise to fibroblast and adipocytes. PICs have been defined by Mitchell *et al.*[60] to be positive for nuclear protein PW1 (PEG3) and able to give rise to myofibers only in the presence of satellite cells. Furthermore, within PICs, Pannérec *et al.*[190] have identified three subpopulations defined as follows: (1) $SCA1^-$ PICs, positive either for NG2/AP or for *Pax7* that are able to differentiate into myofibers; (2) $SCA1^+$ PICs, that do not need the expression of *Pax7* to differentiate into myofibers; (3) $SCA1^+$/$PDGFRalpha^+$ PICs, that are able to give rise to adipocytes.

In this thesis, the capability of *Sca1*-derived cells to differentiate into other mesodermal lineages beside the myogenic one was confirmed by injections of BMP4 and BMP7 into the tibialis anterior muscle of *Sca1*-tTA//LC1-Cre//Z/AP and *Pax7*-Cre/Z/AP mice . These BMPs molecules are known to promote the formation of bone[149] and fat[150] respectively. The administration of BMP4 and BMP7 in combination or alone in *Sca1*-tTA//LC1-Cre//Z/AP suggested a contribution of *Sca1*-expressing cells in the formation ectopic bone and fat, confirming the potential of *Sca1*-derived cells committed into different cell lineages (Figure 25). Satellite cells, contrarily, do not participate to this process. In this work the fate of satellite cells and their contribution to fat and bone formation was traced using the transgenic mouse model *Pax7*-Cre/Z/AP. In this mouse the Cre expression is under the control of *Pax7* promoter therefore in the cells expressing *Pax7* (satellite cells) the Cre expression recombine the *loxP* in the Z/AP reporter locus, leading to permanent labeling these cells with alkaline phosphatase. In this mouse in response to BMP molecule treatment, performed as mentioned above, it was shown that satellite cells do not contribute to the ectopic tissue formation (Figure 28). These data clarified that satellite cells *in vivo* are unable to give rise to either osteoblasts or adipocytes, opposite of what has been shown previously by Asakura *et al.*[149] using isolated satellite cells. In this work the authors could show that *in vitro* satellite cells, after treatment with BMP4 and BMP7, are able to differentiate into other lineages different from the myogenic one, indicating that probably some other cell populations could inhibit *in vivo* the differentiation of satellite cells. In this dissertation, it was shown that a population of stem cells expressing *Sca1* exists, which is able to contribute to ectopic tissue formation *in vivo*. In particular, *Sca1*-expressing cells differentiate *in vivo* into the three mesordermal lineages (myogenic, adipogenic and osteogenic lineages) whereas the differentiation potential of satellite cells *in vivo* is only myogenic. The possible explanation of the differences in the plasticity of these two populations could be due to differences in the gene profile of these

cells. Transcriptomic analyses of three different muscle populations (i.e. satellite cells, FAPs and *Sca1*-expressing cells) in both quiescence and activated state, highlighted the possible reason for the different behavior of the satellite cells and *Sca1*-expressing cells observed *in vivo*. Satellite cells, both in quiescence and activated state, showed mainly an up regulation of the genes involved in myogenesis (e.g. *Pax7*, *Myf5*, *MyoD*), whereas *Sca1*-expressing cells, after activation, presented an up regulation also of genes specific for fibrogenesis (e.g. *Fsp1*, *Itga*, *Smad1*, *P4hb*), adipogenesis (e.g. *Bmp7,C/ebp gamma, Cidea*, *PPRgamma*) and osteogenesis (*Bmp4)* (Table 6). Regarding the adipogenic pathway an interesting gene was identified and namely *Prdm16*. PRDM16 has been shown to be involved in the transdifferentiation of C2C12 into brown adipocytes through PPRgamma binding regulation[212]. The microarray analyses showed that *Sca1*-expressing cells present a low expression of *Prdm16,* whereas *PPRgamma* is up regulated (Figure 31c). This high expression could probably be sufficient to stimulate the adipogenic commitment of these stem cells. On the other hand, in satellite cells, both *Prdm16* and *PPRgamma* genes show a low expression level. These results could possibly explain why, although the high expression of other adipogenic genes (e.g *Adiponectin*, *Elovl3*, *Adipsin*, *Cidea*), satellite cells are not able to form adipose tissue *in vivo*. The administration of BMP molecules performed in this study showed an involvement of *Sca1*-expressing cells not only in the adipogenesis but also in osteogenesis. To dissect this observation more carefully, the expression of genes related to the osteogenic pathway was examined. *Acvr1*[213] and *Bmp4*[214] are upregulated in quiescent *Sca1*-expressing cells, but their expression level decreased after activation. These data support the hypothesis that *Sca1*-expressing cells have the potential to be committed towards osteogenic lineage although cardiotoxin injection does not activate this pathway (Figure 31d). Furthermore, in the gene array dataset, two genes clearly marked a division between satellite cells and *Sca1*-expressing-FAPs cells (Figure 31d), such as *Bmp1* and *Il6*. *Bmp1* is known to be involved in the activation of latent myostatin, a negative regulator of muscle growth[215] and it has also been shown to be involved in cartilage formation[216]. *Bmp1* is expressed in *Sca1*-expressing cells and FAPs, whereas in satellite cells its expression is quite low, both in quiescence and activated state. Satellite cells are important in muscle formation and repair and it has already been shown that myostatin inhibits satellite cell renewal and activation[217]. The low expression level of *Bmp1* in satellite cells population could determine the inactivation of myostatin explaining the higher ability of satellite cells to participate to muscle formation and repair. Contrarily, the high expression level of *Bmp1* in quiescent *Sca1*-expressing cells and FAPs suggests that the differentiation ability of *Sca1*-expressing cells towards myofibers

could be inhibited by the expression of this gene. This is in accordance with the fact that *Bmp1* has a really low expression after activation, when the *Sca1*-expressing cells probably activate their myogenic pattern. As mentioned above *Bmp1* is also involved in cartilage and bone formation. Thus, another possible explanation of the high level of *Bmp1* in *Sca1*-expressing cells might be that these cells are able to differentiate also into cartilage. On the other hand *Il6* is known to be involved in satellite cells-mediated muscle hypertrophy and induction of muscle growth[155]. Furthermore, the importance of *Il6* as a released factor that is able to regulate the quiescence and activated state of satellite cells has already been shown by other groups[64]. Taken together this evidence, it might allow one to hypothesize that the high expression level of *Il6* in *Sca1*-expressing cells after activation could be a key regulator in the promotion of the myogenic commitment of these cells.

The different expression levels of *Bmp1* and *Il6* seem to be a possible regulator of the different myogenic potential observed in satellite cells and *Sca1*-expressing cells. Interestingly, a specific profile of these two genes also emerged at the single cell level in satellite cells and FAPs either in presence or absence of *Sca1* expression. FAPs are described in the literature to be positive also for *Sca1* so the presence of a subpopulation expressing this marker within the population sorted for PDGFRalpha is not surprisingly. Regarding satellite cells, although they have been described as a heterogeneous population, composed of different subpopulations containing cells that differ from each other to a certain level[156], the existence of a subpopulation of satellite cells positive for *Sca1* has not been so far clearly defined. For instance, in 2009, Olwin and colleagues[218] identified a population distinct from satellite cells but with myogenic characteristics similar to them. They describe this population to be positive for Syndecan4, Syndecan3, Pax7, the SP marker ABCG2 and Sca1. The authors proved that this population has high quiescent capability and enhanced stem cell characteristics. These characteristics might be derived from the presence of *Sca1*. The single cell analyses performed in this thesis show that satellite cells in the presence of *Sca1* express low level of *IL6-st* (IL6 receptor subunit beta) and high expression level of *Bmp1*. Based on the fact that *Il6* has been described to promote muscle differentiation[155], whereas *Bmp1* inhibits this process[215], these results might explain the role of the two genes in the maintenance of the quiescent state in the subpopulation of satellite cells expressing *Sca1* (Figure 34). To test such hypothesis, one possible experiment would be to isolate $SCA1^+$ and $SCA1^-$ satellite cells by FACS. Both cell types are then treated with a BMP1 inhibitor to score for their differentiation capability *in vitro* upon myogenesis induction. Furthermore, based on the arrays data, either Western blot or ELISA (Enzyme-linked immunosorbent assay) could be

performed to determine whether IL6-st is also present at the protein level in these populations. Once the presence of the receptor *in vitro* is established, it will be possible to monitor the behavior of the two sorted cell populations cultured with different concentrations of IL6.

In conclusion, this study provides evidence that *Sca1*-expressing cells could be considered as muscle stem cells. Using lineage tracing approaches, it has been shown that *Sca1*-expressing cells are multipotent and are able to differentiate into other mesodermal lineages (i.e. adipose and osteogenic tissue), although their contribution to myofibers is rather limited compared satellite cells. The transcriptomic profile of *Sca1*-expressing cells highlighted the difference between this population and satellite cells, entertaining the idea of a possible distinct muscle stem cell population that expresses *Sca1* and is highly quiescent (Figure 37). A source of stem cells more plastic and multipotent (i.e. *Sca1*-expressing cells) could be an advantage in clinical treatment of skeletal muscle disease since satellite cells alone have not been shown to be sufficient after stem cell transplantation. It will be therefore important to refine the *Sca1*-expressing cells isolation and elucidate possible methods to expand this population. A possible combination of transplanted satellite cells and *Sca1*-expressing cells could be, indeed, a better solution in terms of engraftment and repair in skeletal muscle pathologies.

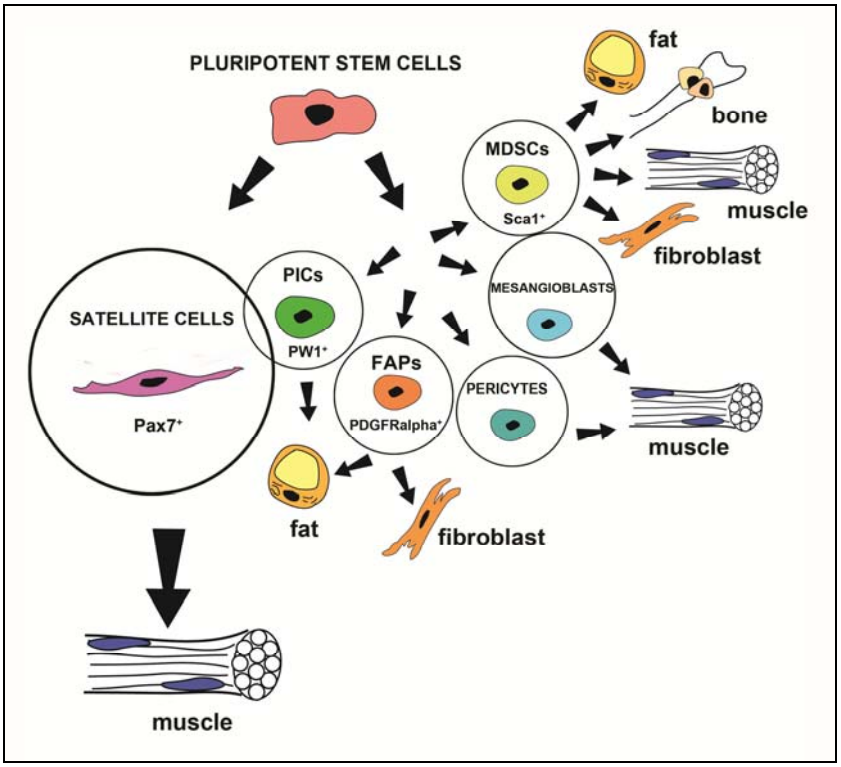

Figure 36. Classical overview of stem cell contribution in the skeletal muscle.

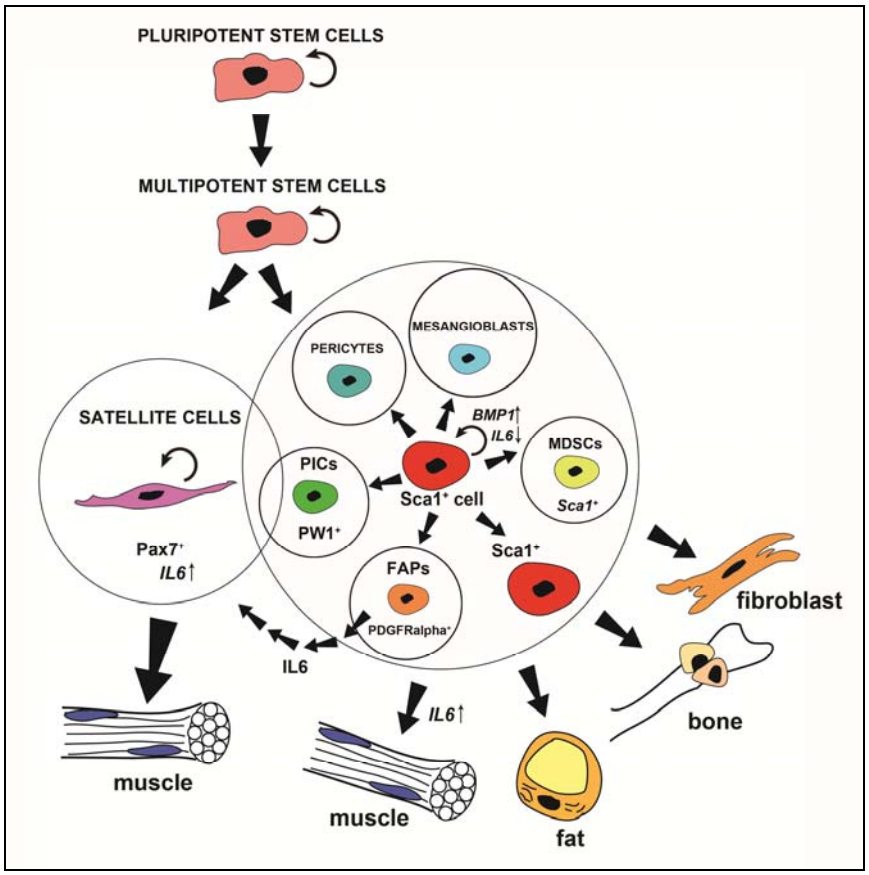

Figure 37. New possible scheme illustrating the muscle stem cells contribution in skeletal muscle.
The cartoon summarizes and links all the possible sources of stem cells in the skeletal muscle and their possible contribution during the regeneration event.

8 ABBREVIATIONS

µl	microliter
µM	microMolar
^{14}C	Carbon 14
4-OHT	4-hydroxy-tamoxifen
Abcg2	ATP-binding cassette sub-family G member 2
aCFibro	murine adult cardiomyocytes
Actbeta	beta actin
Acvr1	Activin receptor type 1
AFP	alpha fetoprotein
aHeart	murine adult heart
Airn	Antisense of IGF2R Non-Protein Coding RNA
aKEndo	glomerular endothelial cells from adult Tie2-GFP mice
alphaMHC	alpha Myosin Heavy Chain
alphaSMactin	alpha smooth muscle actin
AP	Alkaline phosphatase
aP2	adipocyte protein 2
BCIP	5-Bromo-4-chloro-8-indolilphosphate
BD	Becton Dickinson
BEX1	Brain-expressed X-linked protein 1
BMCs	Bone Marrow Cells
BM-MASCs	Adult bone marrow-derived multipotent mesenchymal stem cells
BMP(1,4,7,9)	Bone Morphogenic Protein
BS-1	bandeira simplicifolia 1
C/EBPalpha/beta/gamma	enhancer-binding protein alpha/beta/gamma
C	Cytosine
$CaCl_2$	Calcium chloride
cc	cubic centimeter
CD(31,34, 45,79a etc)	Claster of Differentiation
cDNA	complementary Deoxyribonucleic acid
CFP	cyan fluorescence protein
Cidea	cell death activator
C-KIT	proto-oncogene c-Kit or tyrosine-protein kinase Kit or CD117 or Mast/stem cell growth factor receptor (SCFR)
CLARA	a sampling-based algorithm, implementation of PAM
CMV	cytomegalovirus
CPs	Cardiac progenitor cells

Crabp2a	cellular retinoic acid-binding protein 2
Cre	Causes or Cyclization recombinase
CSCs	Cardiac Stem Cells
Ct	threshold cycle
CX43/45	Connexin 43/45
Cxcl9	Chemokine (C-X-C motif) ligand 9
CY2/3	Cyanine 2/3
DAPI	4',6-Diamidino-2-Phenylindole, Dihydrochloride
ddCt	delta delta threshold cycle
ddH_2O	double-distilled water
DDR2	Discoidin Domain Receptor 2
DIANA	DNA Intelligent Analysis, divisive hierarchical approach to clustering
Dil	1,1'-dioctadecyl-3,3,3',3'-tetramethylindocarbocyanine
Dio	3,3´ -dioctadecyloxacarbocyanine
DMEM	Dulbecco´s modified eagle medium
DNA	Deoxyribonucleic acid
EAA	Exon Array Analyzer
EGFP	enhanced fluorescence protein
Elovl3	elongation of very long chain fatty acids
Eltd1	EGF, latrophilin seven transmembrane domain containing 1
Emsd	eomesodermin
Endo.N.	endothelial cell lines derived from murine embryonic stem cells expressing N-cadherin
Endo.VE.	endothelial cell lines derived from murine embryonic stem cells expressing VE-cadherin
Endo.VE+N	endothelial cell lines derived from murine embryonic stem cells expressing both N-cadherin and VE-cadherin
ER	Estrogen Receptor
ERT	estrogen receptor responsive element
ESs	Embryonic Stem cells
FACS	Fluorescence-Activated Cells Sorting
FANNY	algorithm performs fuzzy clustering
Fap	Fibroblast Activation Protein
FAPs	Fibro-adipogenic precursor cells
FCS	Fetal Calf Serum
FGFR-4	Fibroblast growth factor receptor
FISH	Fluorescence *in situ* hybridization
FITC	fluorescein isothiocyanate

Flk-1	Fetal Liver Kinase 1, a receptor for vascular endothelial growth factor (VEGF)
FoxC2/D3	Forkhead box protein
FSP1	Intermediate-Filament-associate Protein
GAA	Gene Array Analyzer
Gapdh	glyceraldehyde-3-phosphate dehydrogenase
GATA4	protein binding the GATA DNA region
GEO	Gene Expression Omnibus
GFP	green fluorescence protein
GLUT-1	glucose transporter 1
H_2O	water
HAND1	Heart- and neural crest derivatives-expressed protein 1
hBMP	human bone morphogenetic proteins
HCl	hydrocloric acid
HEB	helix-loop-helix protein bindinf to E2A and ITF2 proteins
Hes1 /3	Hairy and enhancer of split 1/3
Hey2	Hairy/enhancer-of-split related with YRPW motif protein 2, also known as cardiovascular helix-loop-helix factor 1 (CHF1)
HGF	hepatocyte growth factor
HIF-1b	hypoxia inducible factor
HRP	horseradish peroxidase
HSCs	hematopoietic stem cells
HSPs	hot shock proteins
IL6	interleuchin 6
Il6st	Interleuchin 6 signal transducer or, gp130, or oncostatin M receptor
Ilr1	IAA-amino acid hydrolase
iPSs	induced pluripotent stem cells
Itgα1	Integrin alpha 1
IU	international unit
KCl	potassium chloride
KH_2PO_4	potassium dihydrogen phosphate
$KHCO_3$	potassium bicarbonate
Kit	c-kit, CD117, belly spot, steel factor receptor
KRTL-14	keratin 14
LacZ	betagalactosidase gene
LAD	left anterior descending coronary arteries
LC1	Luciferase (luc) and the CRE recombinase (cre) *gene* under the control of a bidirectional minimal promoter (Ptetbi-1)

LIF	leukemia inhibitor factor
Lin28a	microRNA-binding protein binding the IGF-2 (insulin-like growth factor 2
Lmna	Lamin A/C
LoxP	lox sequences derived from bacteriophage P1
Ly6	lymphocyte activation protein 6
mCFP	mouse cyan fluorescence protein
Mclust	model-based clustering
MDSCs:	muscle derived stem cells
Mdx	X chromosome-linked muscular dystrophy
MEF	murine embryonic fibroblast
Mef2c	Myocyte-specific enhancer factor 2C
MeV	MultiExperiment Viewer
mg	milligram
$MgSO_4$	magnesium sulfate
MI	myocardial infarction
ml	milliliter
mm	millimeter
mM	milliMolar
MNF	myocyte nuclear factor
MRF4	myogenic factor 6 (herculin)
mRNA	messenger Ribonucleic acid
MSCs	Mesenchymal Stem Cells
Myf5	myogenic factor 5
MyoD	myogenic differentiation 1
Na_2HPO_4	Disodium hydrogen phosphate or sodium phosphate dibasic
NaCl	sodium chloride
$NaHCO_3$	sodium bicarbonate
Nanog	homeobox Transcription Factor Nanog
NBT	nitroblue tetrazolium
nCardio	murine neonatal cardiomyocytes
ncRNA	non coding RNA
nGFP	nuclear green fluorescence protein
Nkx2.5	Cardiac-Specific Homeo Box NK2 Transcription Factor Related, Locus 5
NTMT	Alkaline phosphatase buffer (5 M NaCl, 1 M Tris-Cl (pH 9.5), 1 M $MgCl_2$, Tween 20)
Numbl	Numb-like

OCT	Optimum Cutting Temperature
Oct-4	Octamer binding protein 4
OrO	Oil red O
P(14/17/21)	14/17/21 post natal days
P/S	Penicillin/Streptomycin
P4hb	Prolyl4-hydroxylase
PAM	Partitioning Around Medoids
Pax7	paired box transcription factor 7
PBS	Phosphate Buffered Saline
PCR	Polymerase Chain Reaction
Pdgfalpha/beta	Platelet-derived growth factor subunit alpha/beta
Pdgfralpha/beta	Platelet-derived growth factor receptor alpha/ beta
PE	phycoerythrin
PFA	Paraformaldehyde
PGC1alpha/beta	Peroxisome proliferator-activated receptor gamma coactivator 1-alpha/beta
PICs	progenitor interstitial cells
PLAP	alkaline phosphatase placental
PPRgamma	peroxisome proliferator-activated receptors
PRDM16	PR domain containing 16
Pref-1	Preadipocyte factor 1
pTet	tetracycline promoter
PW1/PEG3	Paternally express 3
R26R	Rosa26 locus
REX1	or ZFP42, acidic zinc finger protein
RFP	red fluorescence protein
RMA	Multi-Array Average
RNA	Ribonucleic acid
rpm	rounds per minutes
RT-PCR	Real Time Polymerase Chain Reaction
Sca1	Stem Cell Antigen 1
SEM	Standard Error of the Mean
SER	Smooth Endoplasmic Reticulum
Sirt7	Sirtuin 7
SM/C-2.6	monoclonal antibody specific for satellite cells
SMAD1	Mothers against decapentaplegic homolog 1
SOM	Self-Organizing Maps

SOTA	Self-Organizing Tree Algorithm
SOX2	SRY, sex determining region Y-box 2
SSC	Saline Sodium-Citrate Buffer
SSEA1/3/4	Stage Specific Embryonic Antigens1/4
STA-RT	Reverse Transcription (RT)-Specific Target Amplification (STA)
Stat2/5a/6	Signal transducer and activator of transcription 2/5a/6
SYBR green	N',N'-dimethyl-N-[4-[(E)-(3-methyl-1,3-benzothiazol-2-ylidene)methyl]-1-phenylquinolin-1-ium-2-yl]-N-propylpropane-1,3-diamine T: timine
TA	transit amplifying
TAC	transverse aortic constriction
TAL	tibialis anterior left
TAR	tibialis anterior right
Tbx5	T-box transcription factor 5
TerR	tetracycline repressor
TERT	telomerase reverse transcriptase
TetO	tetracycline operator
Tgfb3	Transforming growth factor beta-3
Tra-1-60/Tra-1-81	Tumor rejection antigen 1-60/1-81
TRE	Tetracycline Response Element
TRF-1/-2	Telomeric Repeat-Binding Factor *1/2*
Tris-HCl	tris(hydroxymethyl)aminomethane-hydrocloric acid
TRITC	tetramethylrhodamine isothiocyanate
TRIzol	TRIzol® Invitrogen Life Technologies
tTA	tetracycline transactivator protein
Ucp1	uncoupling protein 1
UV	ultra violet
v/v	volume/ volume
Vegfc	Vascular endothelial growth factor C
VP16	or Herpes simplex virus protein vmw65 or α-TIF (Trans Inducing Factor
vs	versus
YFP	yellow fluorescence protein
Z/AP	LacZ/ Alkaline Phosphatase
Z/EG	LacZ/enhanced green fluorescence protein

9 LIST OF FIGURES AND TABLES

9.1 Figures

Figure 1. Symmetric and asymmetric cell division. 6

Figure 2. The potency of stem cells. 7

Figure 3. Pluripotency of embryonic stem cells. 9

Figure 4. Scheme of potential regeneration and cellular turnover of different organs and tissues. 11

Figure 5. An example of classical hierarchy of adult stem cells in epithelial cells. 12

Figure 6. *Sca1* as a stem cell marker. 17

Figure 7. How to choose an appropriate lineage tracing strategy. 19

Figure 8. Cre-recombinase and *loxP* sites. 21

Figure 9. Tet-Off and Tet-On systems. 22

Figure 10. Cre-ERT system. 23

Figure 11. An example of a reporter mouse. 24

Figure 12. Mouse transgenic constructs. 25

Figure 13. *Sca1*-GFP transgenic mouse. 26

Figure 14. *Pax7*-Cre//Z/AP transgenic mouse. 26

Figure 15. *Sca1*-tTA//LC1-Cre//Z/AP//*mdx* transgenic mouse. 27

Figure 16. Sca1-tTA//LC1-Cre//Z/AP//$Pax7^{loxPGu/loxPGu}$ scheme. 28

Figure 17. *Sca1* progenitor cells *in vivo*. 42

Figure 18. *Sca1* progenitor cells contribution *in vivo* under pathological conditions (myocardial infarction and transverse aortic constriction). 44

Figure 19. Number of nuclei in cardiomyocytes. 46

Figure 20. Cardiomyocyte regeneration and polyploidy. 47

Figure 21. Possible niche of CSCs. 48

Figure 22. Heterogeneity of *Sca1*-derived progenitor cells *in vivo*. 50

Figure 23. Single cells analyses of SCA1-expressing cells and transcriptional profile analyses. 52

Figure 24. Contribution of *Sca1* progenitor cells to muscle fibers formation during aging and muscle regeneration in the *Sca1*-tTA//LC1-Cre//Z/AP mouse model. 55

Figure 25. Contribution of *Sca1* progenitor cells after ijury in *mdx* mice. 57

Figure 26. Presence of a subpopulation of *Sca1* progenitor cells in skeletal muscle involved in myogenesis independently from *Pax7* expression. 59

Figure 27. Presence of a subpopulation of *Sca1* progenitor cells that do not express *Pax7* and are involved in myogenesis during early postnatal stages. 60

Figure 28. Injections of BMP molecules in *Pax7*-Cre//Z/AP mice. 63
Figure 29. Injections of BMP molecules in *Sca1*-tTA//LC1-Cre//Z/AP mice. 64
Figure 30. Formation of adipocytes *in vivo*. 65
Figure 31. Microarray dataset. 67
Figure 32. Transcriptomic analyses of different populations of muscle cells. 70
Figure 33. Profiling of fibro-adipocyte progenitor cells (FAPs). 73
Figure 34. Profiling of satellite cells. 74
Figure 35. Possible scheme showing the contribution of *Sca1*-derived cells in the heart regeneration. 84
Figure 36. Classical overview of stem cell contribution in the skeletal muscle. 94
Figure 37. New possible scheme illustrating the muscle stem cells contribution in skeletal muscle. 94

9.2 Tables

Table 1. Markers for human and murine ES cells. 9
Table 2. List of mouse and human resident CSCs based on the different markers expression. 14
Table 3. List of Primers used for genotyping. 28
Table 4. Table of antibodies. 35
Table 5. Distribution of labeled cells after myocardial infarction. 44
Table 6. Genes highly upregulated in the microarray analyses. 68

10 REFERENCES

1 Wikipedia. <http://en.wikipedia.org/wiki/Stem_cell>

2 A., C. Stem Cell Bioengineering. *The Science Creative Quarterly* (2004).

3 Adewumi, O. *et al.* Characterization of human embryonic stem cell lines by the International Stem Cell Initiative. *Nature biotechnology* **25**, 803-816 (2007).

4 Ginis, I. *et al.* Differences between human and mouse embryonic stem cells. *Developmental biology* **269**, 360-380 (2004).

5 Amit, M. *et al.* Clonally derived human embryonic stem cell lines maintain pluripotency and proliferative potential for prolonged periods of culture. *Developmental biology* **227**, 271-278 (2000).

6 Savatier, P., Lapillonne, H., van Grunsven, L. A., Rudkin, B. B. & Samarut, J. Withdrawal of differentiation inhibitory activity/leukemia inhibitory factor up-regulates D-type cyclins and cyclin-dependent kinase inhibitors in mouse embryonic stem cells. *Oncogene* **12**, 309-322 (1996).

7 Prelle, K., Vassiliev, I. M., Vassilieva, S. G., Wolf, E. & Wobus, A. M. Establishment of pluripotent cell lines from vertebrate species--present status and future prospects. *Cells, tissues, organs* **165**, 220-236 (1999).

8 Thomson, J. A. *et al.* Embryonic stem cell lines derived from human blastocysts. *Science* **282**, 1145-1147 (1998).

9 Lindvall, O., Kokaia, Z. & Martinez-Serrano, A. Stem cell therapy for human neurodegenerative disorders-how to make it work. *Nat Med* **10 Suppl**, S42-50 (2004).

10 Syed, B. A. & Evans, J. B. Stem cell therapy market. *Nature reviews. Drug discovery* **12**, 185-186 (2013).

11 Wobus, A. M. Potential of embryonic stem cells. *Molecular aspects of medicine* **22**, 149-164 (2001).

12 Lanza, R. P. *et al.* Generation of histocompatible tissues using nuclear transplantation. *Nature biotechnology* **20**, 689-696 (2002).

13 Takahashi, K. & Yamanaka, S. Induction of pluripotent stem cells from mouse embryonic and adult fibroblast cultures by defined factors. *Cell* **126**, 663-676 (2006).

14 Okano, H. *et al.* Steps toward safe cell therapy using induced pluripotent stem cells. *Circulation research* **112**, 523-533 (2013).

15 Bartel, R. L. *et al.* From Bench to Bedside: Review of Gene and Cell-Based Therapies and the Slow Advancement into Phase 3 Clinical Trials, with a Focus on Aastrom's Ixmyelocel-T. *Stem cell reviews* (2013).

16 Grounds, M. D., White, J. D., Rosenthal, N. & Bogoyevitch, M. A. The role of stem cells in skeletal and cardiac muscle repair. *The journal of histochemistry and cytochemistry : official journal of the Histochemistry Society* **50**, 589-610 (2002).

17 Balami, J. S., Fricker, R. A. & Chen, R. Stem cell therapy for ischaemic stroke: translation from preclinical studies to clinical treatment. *CNS & neurological disorders drug targets* (2013).

18 Kang, K. S. *et al.* A 37-year-old spinal cord-injured female patient, transplanted of multipotent stem cells from human UC blood, with improved sensory perception and mobility, both functionally and morphologically: a case study. *Cytotherapy* **7**, 368-373 (2005).

19 Dominguez-Bendala, J. & Ricordi, C. Present and future cell therapies for pancreatic beta cell replenishment. *World journal of gastroenterology : WJG* **18**, 6876-6884 (2012).

20 Bjorklund, A. & Kordower, J. H. Cell therapy for Parkinson's disease: what next? *Movement disorders : official journal of the Movement Disorder Society* **28**, 110-115 (2013).

21 Asakawa, K. *et al.* Hair organ regeneration via the bioengineered hair follicular unit transplantation. *Scientific reports* **2**, 424 (2012).

22 Melville, H., Carpiniello, M., Hollis, K., Staffaroni, A. & Golestaneh, N. Stem cells: a new paradigm for disease modeling and developing therapies for age-related macular degeneration. *Journal of translational medicine* **11**, 53 (2013).

23 Garbern, J. C. & Lee, R. T. Cardiac stem cell therapy and the promise of heart regeneration. *Cell stem cell* **12**, 689-698 (2013).

24 Sohn, R. L. & Gussoni, E. Stem cell therapy for muscular dystrophy. *Expert opinion on biological therapy* **4**, 1-9 (2004).

25 O'Donoghue, K. & Fisk, N. M. Fetal stem cells. *Best Pract Res Clin Obstet Gynaecol* **18**, 853-875 (2004).

26 Secco, M. *et al.* Multipotent stem cells from umbilical cord: cord is richer than blood! *Stem cells* **26**, 146-150 (2008).

27 Ottersbach, K. & Dzierzak, E. The murine placenta contains hematopoietic stem cells within the vascular labyrinth region. *Developmental cell* **8**, 377-387 (2005).

28 Parolini, O. *et al.* Concise review: isolation and characterization of cells from human term placenta: outcome of the first international Workshop on Placenta Derived Stem Cells. *Stem cells* **26**, 300-311 (2008).

29 Mellor, A. L. & Munn, D. H. Immunology at the maternal-fetal interface: Lessons for T cell tolerance and suppression. *Annu Rev Immunol* **18**, 367-391 (2000).

30 In 't Anker, P. S. *et al.* Amniotic fluid as a novel source of mesenchymal stem cells for therapeutic transplantation. *Blood* **102**, 1548-1549 (2003).

31 Prusa, A. R., Marton, E., Rosner, M., Bernaschek, G. & Hengstschlager, M. Oct-4-expressing cells in human amniotic fluid: a new source for stem cell research? *Hum Reprod* **18**, 1489-1493 (2003).

32 Tsai, M. S., Lee, J. L., Chang, Y. J. & Hwang, S. M. Isolation of human multipotent mesenchymal stem cells from second-trimester amniotic fluid using a novel two-stage culture protocol. *Hum Reprod* **19**, 1450-1456 (2004).

33 De Coppi, P. *et al.* Isolation of amniotic stem cell lines with potential for therapy. *Nature biotechnology* **25**, 100-106 (2007).

34 Dexter, T. M. Introduction to the haemopoietic system. *Cancer surveys* **9**, 1-5 (1990).

35 Woodbury, D., Reynolds, K. & Black, I. B. Adult bone marrow stromal stem cells express germline, ectodermal, endodermal, and mesodermal genes prior to neurogenesis. *Journal of neuroscience research* **69**, 908-917 (2002).

36 Rando, T. A. Stem cells, ageing and the quest for immortality. *Nature* **441**, 1080-1086 (2006).

37 Fuchs, E., Tumbar, T. & Guasch, G. Socializing with the neighbors: stem cells and their niche. *Cell* **116**, 769-778 (2004).

38 Moore, K. A. & Lemischka, I. R. Stem cells and their niches. *Science* **311**, 1880-1885 (2006).

39 Rawlins, E. L. & Hogan, B. L. Epithelial stem cells of the lung: privileged few or opportunities for many? *Development* **133**, 2455-2465 (2006).

40 Weglarz, T. C. & Sandgren, E. P. Timing of hepatocyte entry into DNA synthesis after partial hepatectomy is cell autonomous. *Proc Natl Acad Sci U S A* **97**, 12595-12600 (2000).

41 Mauro, A. Satellite cell of skeletal muscle fibers. *The Journal of biophysical and biochemical cytology* **9**, 493-495 (1961).

42 Banerjee, I., Fuseler, J. W., Price, R. L., Borg, T. K. & Baudino, T. A. Determination of cell types and numbers during cardiac development in the neonatal and adult rat and mouse. *American journal of physiology. Heart and circulatory physiology* **293**, H1883-1891 (2007).

43 Nag, A. C. Study of non-muscle cells of the adult mammalian heart: a fine structural analysis and distribution. *Cytobios* **28**, 41-61 (1980).

44 Rubart, M. & Field, L. J. Cardiac regeneration: repopulating the heart. *Annual review of physiology* **68**, 29-49 (2006).

45 Kawamata, M. & Ochiya, T. Gene-manipulated embryonic stem cells for rat transgenesis. *Cellular and molecular life sciences : CMLS* **68**, 1911-1915 (2011).

46 Carvalho, A. B. & de Carvalho, A. C. Heart regeneration: Past, present and future. *World journal of cardiology* **2**, 107-111 (2010).

47 Karsner, H. T., Saphir, O. & Todd, T. W. The State of the Cardiac Muscle in Hypertrophy and Atrophy. *The American journal of pathology* **1**, 351-372 351 (1925).

48 Hsieh, P. C. *et al.* Evidence from a genetic fate-mapping study that stem cells refresh adult mammalian cardiomyocytes after injury. *Nat Med* **13**, 970-974 (2007).

49 Bergmann, O. *et al.* Evidence for cardiomyocyte renewal in humans. *Science* **324**, 98-102 (2009).

50 Nygren, J. M. *et al.* Bone marrow-derived hematopoietic cells generate cardiomyocytes at a low frequency through cell fusion, but not transdifferentiation. *Nat Med* **10**, 494-501 (2004).

51 Toma, C., Pittenger, M. F., Cahill, K. S., Byrne, B. J. & Kessler, P. D. Human mesenchymal stem cells differentiate to a cardiomyocyte phenotype in the adult murine heart. *Circulation* **105**, 93-98 (2002).

52 Makino, S. *et al.* Cardiomyocytes can be generated from marrow stromal cells in vitro. *The Journal of clinical investigation* **103**, 697-705 (1999).

53 Smits, A. M., van Vliet, P., Hassink, R. J., Goumans, M. J. & Doevendans, P. A. The role of stem cells in cardiac regeneration. *Journal of cellular and molecular medicine* **9**, 25-36 (2005).

54 Stamm, C., Choi, Y. H., Nasseri, B. & Hetzer, R. A heart full of stem cells: the spectrum of myocardial progenitor cells in the postnatal heart. *Therapeutic advances in cardiovascular disease* **3**, 215-229 (2009).

55 Uchida S., D. G. P., Braun T. in *Stem cell in clininc and research* (ed InTech) (2011).

56 Otto, A., Collins-Hooper, H. & Patel, K. The origin, molecular regulation and therapeutic potential of myogenic stem cell populations. *Journal of anatomy* **215**, 477-497 (2009).

57 Brack, A. S. *et al.* Increased Wnt signaling during aging alters muscle stem cell fate and increases fibrosis. *Science* **317**, 807-810 (2007).

58 Taylor-Jones, J. M. *et al.* Activation of an adipogenic program in adult myoblasts with age. *Mechanisms of ageing and development* **123**, 649-661 (2002).

59 Charge, S. B. & Rudnicki, M. A. Cellular and molecular regulation of muscle regeneration. *Physiological reviews* **84**, 209-238 (2004).

60 Mitchell, K. J. *et al.* Identification and characterization of a non-satellite cell muscle resident progenitor during postnatal development. *Nature cell biology* **12**, 257-266 (2010).

61 Cossu, G. & Bianco, P. Mesoangioblasts--vascular progenitors for extravascular mesodermal tissues. *Current opinion in genetics & development* **13**, 537-542 (2003).

62 Dellavalle, A. *et al.* Pericytes of human skeletal muscle are myogenic precursors distinct from satellite cells. *Nature cell biology* **9**, 255-267 (2007).

63 Uezumi, A., Fukada, S., Yamamoto, N., Takeda, S. & Tsuchida, K. Mesenchymal progenitors distinct from satellite cells contribute to ectopic fat cell formation in skeletal muscle. *Nature cell biology* **12**, 143-152 (2010).

64 Joe, A. W. *et al.* Muscle injury activates resident fibro/adipogenic progenitors that facilitate myogenesis. *Nature cell biology* **12**, 153-163 (2010).

65 Rodeheffer, M. S. Tipping the scale: muscle versus fat. *Nature cell biology* **12**, 102-104 (2010).

66 Huard, J., Cao, B. & Qu-Petersen, Z. Muscle-derived stem cells: potential for muscle regeneration. *Birth defects research. Part C, Embryo today : reviews* **69**, 230-237 (2003).

67 Deasy, B. M., Jankowski, R. J. & Huard, J. Muscle-derived stem cells: characterization and potential for cell-mediated therapy. *Blood cells, molecules & diseases* **27**, 924-933 (2001).

68 Miles, C., Sanchez, M. J., Sinclair, A. & Dzierzak, E. Expression of the Ly-6E.1 (Sca-1) transgene in adult hematopoietic stem cells and the developing mouse embryo. *Development* **124**, 537-547 (1997).

69 Trevisan, M. & Iscove, N. N. Phenotypic analysis of murine long-term hemopoietic reconstituting cells quantitated competitively in vivo and comparison with more advanced colony-forming progeny. *The Journal of experimental medicine* **181**, 93-103 (1995).

70 Kondo, M., Weissman, I. L. & Akashi, K. Identification of clonogenic common lymphoid progenitors in mouse bone marrow. *Cell* **91**, 661-672 (1997).

71 Oh, H. *et al.* Cardiac progenitor cells from adult myocardium: homing, differentiation, and fusion after infarction. *Proc Natl Acad Sci U S A* **100**, 12313-12318 (2003).

72 Wang, X. *et al.* The role of the sca-1+/CD31- cardiac progenitor cell population in postinfarction left ventricular remodeling. *Stem cells* **24**, 1779-1788 (2006).

73 Shen, X. *et al.* Genome-wide examination of myoblast cell cycle withdrawal during differentiation. *Developmental dynamics : an official publication of the American Association of Anatomists* **226**, 128-138 (2003).

74 Epting, C. L. *et al.* Stem cell antigen-1 is necessary for cell-cycle withdrawal and myoblast differentiation in C2C12 cells. *Journal of cell science* **117**, 6185-6195 (2004).

75 Anversa, P. & Nadal-Ginard, B. Myocyte renewal and ventricular remodelling. *Nature* **415**, 240-243 (2002).

76 Holmes, C. & Stanford, W. L. Concise review: stem cell antigen-1: expression, function, and enigma. *Stem cells* **25**, 1339-1347 (2007).

77 Stern, C. D. & Fraser, S. E. Tracing the lineage of tracing cell lineages. *Nature cell biology* **3** (2001).

78 Kretzschmar, K. & Watt, F. M. Lineage tracing. *Cell* **148**, 33-45 (2012).

79 Cepko, C. L., Roberts, B. E. & Mulligan, R. C. Construction and applications of a highly transmissible murine retrovirus shuttle vector. *Cell* **37**, 1053-1062 (1984).

80 Notta, F. *et al.* Isolation of single human hematopoietic stem cells capable of long-term multilineage engraftment. *Science* **333**, 218-221 (2011).

81 Giangreco, A. *et al.* Stem cells are dispensable for lung homeostasis but restore airways after injury. *Proc Natl Acad Sci U S A* **106**, 9286-9291 (2009).

82 Lowell, S., Jones, P., Le Roux, I., Dunne, J. & Watt, F. M. Stimulation of human epidermal differentiation by delta-notch signalling at the boundaries of stem-cell clusters. *Current biology : CB* **10**, 491-500 (2000).

83 Hoess, R. H., Ziese, M. & Sternberg, N. P1 site-specific recombination: nucleotide sequence of the recombining sites. *Proc Natl Acad Sci U S A* **79**, 3398-3402 (1982).

84 Lodish H, B. A., Zipursky SL, et al. *Molecular Cell Biology*. 4th edition edn, (2000).

85 *Cre-LoxP system*, <http://2012.igem.org/Team:Tsinghua-A/Project/Design>

86 Pfannkuche, K. *et al.* Generation of a double-fluorescent double-selectable Cre/loxP indicator vector for monitoring of intracellular recombination events. *Nature protocols* **3**, 1510-1526 (2008).

87 Alcolea, M. P. & Jones, P. H. Tracking cells in their native habitat: lineage tracing in epithelial neoplasia. *Nature reviews. Cancer* **13**, 161-171 (2013).

88 Laboratories, T. J. <http://cre.jax.org/introduction.html>

89 Gossen, M. & Bujard, H. Tight control of gene expression in mammalian cells by tetracycline-responsive promoters. *Proc Natl Acad Sci U S A* **89**, 5547-5551 (1992).

90 Urlinger, S. *et al.* Exploring the sequence space for tetracycline-dependent transcriptional activators: novel mutations yield expanded range and sensitivity. *Proc Natl Acad Sci U S A* **97**, 7963-7968 (2000).

91 Zhou, X., Vink, M., Klaver, B., Berkhout, B. & Das, A. T. Optimization of the Tet-On system for regulated gene expression through viral evolution. *Gene therapy* **13**, 1382-1390 (2006).

92 Branda, C. S. & Dymecki, S. M. Talking about a revolution: The impact of site-specific recombinases on genetic analyses in mice. *Developmental cell* **6**, 7-28 (2004).

93 Metzger, D., Clifford, J., Chiba, H. & Chambon, P. Conditional site-specific recombination in mammalian cells using a ligand-dependent chimeric Cre recombinase. *Proc Natl Acad Sci U S A* **92**, 6991-6995 (1995).

94 Danielian, P. S., Muccino, D., Rowitch, D. H., Michael, S. K. & McMahon, A. P. Modification of gene activity in mouse embryos in utero by a tamoxifen-inducible form of Cre recombinase. *Current biology : CB* **8**, 1323-1326 (1998).

95 Logie, C. & Stewart, A. F. Ligand-regulated site-specific recombination. *Proc Natl Acad Sci U S A* **92**, 5940-5944 (1995).

96 Feil, R., Wagner, J., Metzger, D. & Chambon, P. Regulation of Cre recombinase activity by mutated estrogen receptor ligand-binding domains. *Biochemical and biophysical research communications* **237**, 752-757 (1997).

97 Indra, A. K. *et al.* Temporally-controlled site-specific mutagenesis in the basal layer of the epidermis: comparison of the recombinase activity of the tamoxifen-inducible Cre-ER(T) and Cre-ER(T2) recombinases. *Nucleic acids research* **27**, 4324-4327 (1999).

98 Feil, R. *et al.* Ligand-activated site-specific recombination in mice. *Proc Natl Acad Sci U S A* **93**, 10887-10890 (1996).

99 Leone, D. P. *et al.* Tamoxifen-inducible glia-specific Cre mice for somatic mutagenesis in oligodendrocytes and Schwann cells. *Molecular and cellular neurosciences* **22**, 430-440 (2003).

100 Novak, A., Guo, C., Yang, W., Nagy, A. & Lobe, C. G. Z/EG, a double reporter mouse line that expresses enhanced green fluorescent protein upon Cre-mediated excision. *Genesis* **28**, 147-155 (2000).

101 Lobe, C. G. *et al.* Z/AP, a double reporter for cre-mediated recombination. *Developmental biology* **208**, 281-292 (1999).

102 Vintersten, K. *et al.* Mouse in red: red fluorescent protein expression in mouse ES cells, embryos, and adult animals. *Genesis* **40**, 241-246 (2004).

103 Zong, H., Espinosa, J. S., Su, H. H., Muzumdar, M. D. & Luo, L. Mosaic analysis with double markers in mice. *Cell* **121**, 479-492 (2005).

104 Livet, J. *et al.* Transgenic strategies for combinatorial expression of fluorescent proteins in the nervous system. *Nature* **450**, 56-62 (2007).

105 Snippert, H. J. *et al.* Intestinal crypt homeostasis results from neutral competition between symmetrically dividing Lgr5 stem cells. *Cell* **143**, 134-144 (2010).

106 Sato, T. *et al.* Paneth cells constitute the niche for Lgr5 stem cells in intestinal crypts. *Nature* **469**, 415-418 (2011).

107 Schonig, K., Schwenk, F., Rajewsky, K. & Bujard, H. Stringent doxycycline dependent control of CRE recombinase in vivo. *Nucleic acids research* **30**, e134 (2002).

108 Ma, X., Robin, C., Ottersbach, K. & Dzierzak, E. The Ly-6A (Sca-1) GFP transgene is expressed in all adult mouse hematopoietic stem cells. *Stem cells* **20**, 514-521 (2002).

109 Keller, C., Hansen, M. S., Coffin, C. M. & Capecchi, M. R. Pax3:Fkhr interferes with embryonic Pax3 and Pax7 function: implications for alveolar rhabdomyosarcoma cell of origin. *Genes & development* **18**, 2608-2613 (2004).

110 Bulfield, G., Siller, W. G., Wight, P. A. & Moore, K. J. X chromosome-linked muscular dystrophy (mdx) in the mouse. *Proc Natl Acad Sci U S A* **81**, 1189-1192 (1984).

111 Gunther, S. *et al.* Myf5-Positive Satellite Cells Contribute to Pax7-Dependent Long-Term Maintenance of Adult Muscle Stem Cells. *Cell stem cell* (2013).

112 O'Connell, T. D., Ni, Y., Lin, K. M., Han, H. & Yan, Z. Isolation and culture of adult mouse cardiac myocytes for signaling studies. *AfCS Research Reports* **1**, 1-9 (2003).

113 Belema-Bedada, F., Uchida, S., Martire, A., Kostin, S. & Braun, T. Efficient homing of multipotent adult mesenchymal stem cells depends on FROUNT-mediated clustering of CCR2. *Cell stem cell* **2**, 566-575 (2008).

114 Kreymborg, K. *et al.* Identification of right heart-enriched genes in a murine model of chronic outflow tract obstruction. *J Mol Cell Cardiol* **49**, 598-605 (2010).

115 Hagiwara, Y., Ishii, A., Nonaka, I., Kikuchi, T. & Takeda, S. Fiber-type-dependent expression of adenovirus-mediated transgene in mouse skeletal muscle fibers. *Acta neuropathologica* **96**, 228-232 (1998).

116 Kostin, S., Hein, S., Bauer, E. P. & Schaper, J. Spatiotemporal development and distribution of intercellular junctions in adult rat cardiomyocytes in culture. *Circulation research* **85**, 154-167 (1999).

117 Zheng, B. *et al.* Prospective identification of myogenic endothelial cells in human skeletal muscle. *Nature biotechnology* **25**, 1025-1034 (2007).

118 Gellert, P. *et al.* Gene Array Analyzer: alternative usage of gene arrays to study alternative splicing events. *Nucleic acids research* (2011).

119 Gellert, P., Uchida, S. & Braun, T. Exon Array Analyzer: a web interface for Affymetrix exon array analysis. *Bioinformatics (Oxford, England)* **25**, 3323-3324 (2009).

120 Irizarry, R. A. *et al.* Exploration, normalization, and summaries of high density oligonucleotide array probe level data. *Biostatistics (Oxford, England)* **4**, 249-264 (2003).

121 Saeed, A. I. *et al.* TM4 microarray software suite. *Methods in enzymology* **411**, 134-193 (2006).

122 Stover, B. C. & Muller, K. F. TreeGraph 2: combining and visualizing evidence from different phylogenetic analyses. *BMC bioinformatics* **11**, 7 (2010).

123 Ieda, M. *et al.* Cardiac fibroblasts regulate myocardial proliferation through beta1 integrin signaling. *Developmental cell* **16**, 233-244 (2009).

124 Brunskill, E. W. & Potter, S. S. Gene expression programs of mouse endothelial cells in kidney development and disease. *PloS one* **5**, e12034 (2010).

125 Ieda, M. *et al.* Direct reprogramming of fibroblasts into functional cardiomyocytes by defined factors. *Cell* **142**, 375-386 (2010).

126 Giampietro, C. *et al.* Overlapping and divergent signaling pathways of N-cadherin and VE-cadherin in endothelial cells. *Blood* **119**, 2159-2170 (2012).

127 Uchida, S., Fuke, S. & Tsukahara, T. Upregulations of Gata4 and oxytocin receptor are important in cardiomyocyte differentiation processes of P19CL6 cells. *Journal of cellular biochemistry* **100**, 629-641 (2007).

128 Guo, G. *et al.* Resolution of cell fate decisions revealed by single-cell gene expression analysis from zygote to blastocyst. *Developmental cell* **18**, 675-685 (2010).

129 Tateishi, K. *et al.* Clonally amplified cardiac stem cells are regulated by Sca-1 signaling for efficient cardiovascular regeneration. *Journal of cell science* **120**, 1791-1800 (2007).

130 Beltrami, A. P. *et al.* Adult cardiac stem cells are multipotent and support myocardial regeneration. *Cell* **114**, 763-776 (2003).

131 Messina, E. *et al.* Isolation and expansion of adult cardiac stem cells from human and murine heart. *Circulation research* **95**, 911-921 (2004).

132 Cai, C. L. *et al.* Isl1 identifies a cardiac progenitor population that proliferates prior to differentiation and contributes a majority of cells to the heart. *Developmental cell* **5**, 877-889 (2003).

133 Bersell, K., Arab, S., Haring, B. & Kuhn, B. Neuregulin1/ErbB4 signaling induces cardiomyocyte proliferation and repair of heart injury. *Cell* **138**, 257-270 (2009).

134 Senyo, S. E. *et al.* Mammalian heart renewal by pre-existing cardiomyocytes. *Nature* **493**, 433-436 (2013).

135 Naqvi, N., Li, M., Yahiro, E., Graham, R. M. & Husain, A. Insights into the characteristics of mammalian cardiomyocyte terminal differentiation shown through the study of mice with a dysfunctional c-kit. *Pediatric cardiology* **30**, 651-658 (2009).

136 Vitale, I. *et al.* Illicit survival of cancer cells during polyploidization and depolyploidization. *Cell death and differentiation* **18**, 1403-1413 (2011).

137 Conboy, I. M., Conboy, M. J., Smythe, G. M. & Rando, T. A. Notch-mediated restoration of regenerative potential to aged muscle. *Science* **302**, 1575-1577 (2003).

138 Ownby, C. L., Fletcher, J. E. & Colberg, T. R. Cardiotoxin 1 from cobra (Naja naja atra) venom causes necrosis of skeletal muscle in vivo. *Toxicon : official journal of the International Society on Toxinology* **31**, 697-709 (1993).

139 d'Albis, A., Couteaux, R., Janmot, C., Roulet, A. & Mira, J. C. Regeneration after cardiotoxin injury of innervated and denervated slow and fast muscles of mammals. Myosin isoform analysis. *European journal of biochemistry / FEBS* **174**, 103-110 (1988).

140 Hosaka, Y. *et al.* Alpha1-syntrophin-deficient skeletal muscle exhibits hypertrophy and aberrant formation of neuromuscular junctions during regeneration. *The Journal of cell biology* **158**, 1097-1107 (2002).

141 Terada, M. *et al.* Effects of mechanical over-loading on the properties of soleus muscle fibers, with or without damage, in wild type and mdx mice. *PloS one* **7**, e34557 (2012).

142 Shi, X. & Garry, D. J. Muscle stem cells in development, regeneration, and disease. *Genes & development* **20**, 1692-1708 (2006).

143 Bentzinger, C. F., Wang, Y. X. & Rudnicki, M. A. Building muscle: molecular regulation of myogenesis. *Cold Spring Harbor perspectives in biology* **4** (2012).

144 Lepper, C., Conway, S. J. & Fan, C. M. Adult satellite cells and embryonic muscle progenitors have distinct genetic requirements. *Nature* **460**, 627-631 (2009).

145 Brack, A. S. & Rando, T. A. Tissue-specific stem cells: lessons from the skeletal muscle satellite cell. *Cell stem cell* **10**, 504-514 (2012).

146 Scharner, J. & Zammit, P. S. The muscle satellite cell at 50: the formative years. *Skeletal muscle* **1**, 28 (2011).

147 Hu, E., Tontonoz, P. & Spiegelman, B. M. Transdifferentiation of myoblasts by the adipogenic transcription factors PPAR gamma and C/EBP alpha. *Proc Natl Acad Sci U S A* **92**, 9856-9860 (1995).

148 Yeow, K. *et al.* Inhibition of myogenesis enables adipogenic trans-differentiation in the C2C12 myogenic cell line. *FEBS letters* **506**, 157-162 (2001).

149 Asakura, A., Komaki, M. & Rudnicki, M. Muscle satellite cells are multipotential stem cells that exhibit myogenic, osteogenic, and adipogenic differentiation. *Differentiation; research in biological diversity* **68**, 245-253 (2001).
150 Tseng, Y. H. *et al.* New role of bone morphogenetic protein 7 in brown adipogenesis and energy expenditure. *Nature* **454**, 1000-1004 (2008).
151 Fukada, S. *et al.* Molecular signature of quiescent satellite cells in adult skeletal muscle. *Stem cells* **25**, 2448-2459 (2007).
152 Uezumi, A. *et al.* Fibrosis and adipogenesis originate from a common mesenchymal progenitor in skeletal muscle. *Journal of cell science* **124**, 3654-3664 (2011).
153 Fukada, S. *et al.* Purification and cell-surface marker characterization of quiescent satellite cells from murine skeletal muscle by a novel monoclonal antibody. *Experimental cell research* **296**, 245-255 (2004).
154 Liu, L. *et al.* Chromatin modifications as determinants of muscle stem cell quiescence and chronological aging. *Cell reports* **4**, 189-204 (2013).
155 Serrano, A. L., Baeza-Raja, B., Perdiguero, E., Jardi, M. & Munoz-Canoves, P. Interleukin-6 is an essential regulator of satellite cell-mediated skeletal muscle hypertrophy. *Cell metabolism* **7**, 33-44 (2008).
156 Biressi, S. & Rando, T. A. Heterogeneity in the muscle satellite cell population. *Seminars in cell & developmental biology* **21**, 845-854 (2010).
157 López-Sendón, J. The heart failure epidemic. *Medicographia* **33** (2011).
158 Oberpriller, J. O. & Oberpriller, J. C. Response of the adult newt ventricle to injury. *The Journal of experimental zoology* **187**, 249-253 (1974).
159 Witman, N., Murtuza, B., Davis, B., Arner, A. & Morrison, J. I. Recapitulation of developmental cardiogenesis governs the morphological and functional regeneration of adult newt hearts following injury. *Developmental biology* **354**, 67-76 (2011).
160 Poss, K. D., Wilson, L. G. & Keating, M. T. Heart regeneration in zebrafish. *Science* **298**, 2188-2190 (2002).
161 Soonpaa, M. H. & Field, L. J. Survey of studies examining mammalian cardiomyocyte DNA synthesis. *Circulation research* **83**, 15-26 (1998).
162 Drenckhahn, J. D. *et al.* Compensatory growth of healthy cardiac cells in the presence of diseased cells restores tissue homeostasis during heart development. *Developmental cell* **15**, 521-533 (2008).
163 Porrello, E. R. *et al.* Transient regenerative potential of the neonatal mouse heart. *Science* **331**, 1078-1080 (2011).
164 Urbanek, K. *et al.* Myocardial regeneration by activation of multipotent cardiac stem cells in ischemic heart failure. *Proc Natl Acad Sci U S A* **102**, 8692-8697 (2005).
165 Kajstura, J. *et al.* Cardiomyogenesis in the aging and failing human heart. *Circulation* **126**, 1869-1881 (2012).
166 Soonpaa, M. H. & Field, L. J. Assessment of cardiomyocyte DNA synthesis in normal and injured adult mouse hearts. *The American journal of physiology* **272**, H220-226 (1997).
167 Malliaras, K. *et al.* Cardiomyocyte proliferation and progenitor cell recruitment underlie therapeutic regeneration after myocardial infarction in the adult mouse heart. *EMBO molecular medicine* **5**, 191-209 (2013).
168 Moretti, A. *et al.* Multipotent embryonic isl1+ progenitor cells lead to cardiac, smooth muscle, and endothelial cell diversification. *Cell* **127**, 1151-1165 (2006).
169 Barile, L., Messina, E., Giacomello, A. & Marban, E. Endogenous cardiac stem cells. *Progress in cardiovascular diseases* **50**, 31-48 (2007).
170 Efe, J. A. *et al.* Conversion of mouse fibroblasts into cardiomyocytes using a direct reprogramming strategy. *Nature cell biology* **13**, 215-222 (2011).

171 Qian, L., Berry, E. C., Fu, J. D., Ieda, M. & Srivastava, D. Reprogramming of mouse fibroblasts into cardiomyocyte-like cells in vitro. *Nature protocols* **8**, 1204-1215 (2013).
172 Schwanhausser, B. *et al.* Global quantification of mammalian gene expression control. *Nature* **473**, 337-342 (2011).
173 de Sousa Abreu, R., Penalva, L. O., Marcotte, E. M. & Vogel, C. Global signatures of protein and mRNA expression levels. *Molecular bioSystems* **5**, 1512-1526 (2009).
174 Maier, T., Guell, M. & Serrano, L. Correlation of mRNA and protein in complex biological samples. *FEBS letters* **583**, 3966-3973 (2009).
175 Vogel, C. *et al.* Sequence signatures and mRNA concentration can explain two-thirds of protein abundance variation in a human cell line. *Molecular systems biology* **6**, 400 (2010).
176 Cai, L., Friedman, N. & Xie, X. S. Stochastic protein expression in individual cells at the single molecule level. *Nature* **440**, 358-362 (2006).
177 Rosenfeld, N., Young, J. W., Alon, U., Swain, P. S. & Elowitz, M. B. Gene regulation at the single-cell level. *Science* **307**, 1962-1965 (2005).
178 Fluidigm. *Single-cell gene expression* <http://www.fluidigm.com/single-cell-gene-expression.html>
179 Scobioala, S. *et al.* Up-regulation of nestin in the infarcted myocardium potentially indicates differentiation of resident cardiac stem cells into various lineages including cardiomyocytes. *FASEB J* **22**, 1021-1031 (2008).
180 Beguin, P. C. *et al.* The phenotype and potential origin of nestin+ cardiac myocyte-like cells following infarction. *Journal of applied physiology* **107**, 1241-1248 (2009).
181 Lombardi, R. & Marian, A. J. Molecular genetics and pathogenesis of arrhythmogenic right ventricular cardiomyopathy: a disease of cardiac stem cells. *Pediatric cardiology* **32**, 360-365 (2011).
182 Wang, K., Wang, C., Xiao, F., Wang, H. & Wu, Z. JAK2/STAT2/STAT3 are required for myogenic differentiation. *The Journal of biological chemistry* **283**, 34029-34036 (2008).
183 Goumans, M. J. *et al.* TGF-beta1 induces efficient differentiation of human cardiomyocyte progenitor cells into functional cardiomyocytes in vitro. *Stem cell research* **1**, 138-149 (2007).
184 Zammit, P. S., Partridge, T. A. & Yablonka-Reuveni, Z. The skeletal muscle satellite cell: the stem cell that came in from the cold. *The journal of histochemistry and cytochemistry : official journal of the Histochemistry Society* **54**, 1177-1191 (2006).
185 Ham R. , V. M. *Mechanisms of development*. (C.V. Mosby company, 1980).
186 Shostak, S. (Re)defining stem cells. *BioEssays : news and reviews in molecular, cellular and developmental biology* **28**, 301-308 (2006).
187 Blau, H. M., Brazelton, T. R. & Weimann, J. M. The evolving concept of a stem cell: entity or function? *Cell* **105**, 829-841 (2001).
188 Seaberg, R. M. & van der Kooy, D. Stem and progenitor cells: the premature desertion of rigorous definitions. *Trends in neurosciences* **26**, 125-131 (2003).
189 Seale, P., Asakura, A. & Rudnicki, M. A. The potential of muscle stem cells. *Developmental cell* **1**, 333-342 (2001).
190 Pannerec, A., Formicola, L., Besson, V., Marazzi, G. & Sassoon, D. A. Defining skeletal muscle resident progenitors and their cell fate potentials. *Development* (2013).
191 Armulik, A., Genove, G. & Betsholtz, C. Pericytes: developmental, physiological, and pathological perspectives, problems, and promises. *Developmental cell* **21**, 193-215 (2011).
192 Sampaolesi, M. *et al.* Mesoangioblast stem cells ameliorate muscle function in dystrophic dogs. *Nature* **444**, 574-579 (2006).

193 Qu-Petersen, Z. *et al.* Identification of a novel population of muscle stem cells in mice: potential for muscle regeneration. *The Journal of cell biology* **157**, 851-864 (2002).
194 Cappellari, O. *et al.* Dll4 and PDGF-BB convert committed skeletal myoblasts to pericytes without erasing their myogenic memory. *Developmental cell* **24**, 586-599 (2013).
195 Couteaux, R., Mira, J. C. & d'Albis, A. Regeneration of muscles after cardiotoxin injury. I. Cytological aspects. *Biology of the cell / under the auspices of the European Cell Biology Organization* **62**, 171-182 (1988).
196 Wilson, A. *et al.* Hematopoietic stem cells reversibly switch from dormancy to self-renewal during homeostasis and repair. *Cell* **135**, 1118-1129 (2008).
197 Cossu, G. & Sampaolesi, M. New therapies for Duchenne muscular dystrophy: challenges, prospects and clinical trials. *Trends in molecular medicine* **13**, 520-526 (2007).
198 Straub, V. & Campbell, K. P. Muscular dystrophies and the dystrophin-glycoprotein complex. *Current opinion in neurology* **10**, 168-175 (1997).
199 Laing, N. G., Davis, M. R., Bayley, K., Fletcher, S. & Wilton, S. D. Molecular diagnosis of duchenne muscular dystrophy: past, present and future in relation to implementing therapies. *The Clinical biochemist. Reviews / Australian Association of Clinical Biochemists* **32**, 129-134 (2011).
200 Rodino-Klapac, L. R., Mendell, J. R. & Sahenk, Z. Update on the treatment of Duchenne muscular dystrophy. *Current neurology and neuroscience reports* **13**, 332 (2013).
201 Rando, T. A., Disatnik, M. H. & Zhou, L. Z. Rescue of dystrophin expression in mdx mouse muscle by RNA/DNA oligonucleotides. *Proc Natl Acad Sci U S A* **97**, 5363-5368 (2000).
202 Hoffman, E. P., Morgan, J. E., Watkins, S. C. & Partridge, T. A. Somatic reversion/suppression of the mouse mdx phenotype in vivo. *Journal of the neurological sciences* **99**, 9-25 (1990).
203 Sacco, A. *et al.* Short telomeres and stem cell exhaustion model Duchenne muscular dystrophy in mdx/mTR mice. *Cell* **143**, 1059-1071 (2010).
204 Chamberlain, J. S., Metzger, J., Reyes, M., Townsend, D. & Faulkner, J. A. Dystrophin-deficient mdx mice display a reduced life span and are susceptible to spontaneous rhabdomyosarcoma. *FASEB J* **21**, 2195-2204 (2007).
205 Rando, T. A. & Blau, H. M. Primary mouse myoblast purification, characterization, and transplantation for cell-mediated gene therapy. *The Journal of cell biology* **125**, 1275-1287 (1994).
206 Fan, Y., Maley, M., Beilharz, M. & Grounds, M. Rapid death of injected myoblasts in myoblast transfer therapy. *Muscle & nerve* **19**, 853-860 (1996).
207 Chapman, M. R. *et al.* Sorting single satellite cells from individual myofibers reveals heterogeneity in cell-surface markers and myogenic capacity. *Integrative biology : quantitative biosciences from nano to macro* **5**, 692-702 (2013).
208 Zammit, P. S. *et al.* Pax7 and myogenic progression in skeletal muscle satellite cells. *Journal of cell science* **119**, 1824-1832 (2006).
209 Seale, P. *et al.* Pax7 is required for the specification of myogenic satellite cells. *Cell* **102**, 777-786 (2000).
210 Sambasivan, R. *et al.* Pax7-expressing satellite cells are indispensable for adult skeletal muscle regeneration. *Development* **138**, 3647-3656 (2011).
211 Hettmer, S. & Wagers, A. J. Muscling in: Uncovering the origins of rhabdomyosarcoma. *Nat Med* **16**, 171-173 (2010).

212 Seale, P. *et al.* PRDM16 controls a brown fat/skeletal muscle switch. *Nature* **454**, 961-967 (2008).
213 Shore, E. M. *et al.* A recurrent mutation in the BMP type I receptor ACVR1 causes inherited and sporadic fibrodysplasia ossificans progressiva. *Nature genetics* **38**, 525-527 (2006).
214 Kan, L., Hu, M., Gomes, W. A. & Kessler, J. A. Transgenic mice overexpressing BMP4 develop a fibrodysplasia ossificans progressiva (FOP)-like phenotype. *The American journal of pathology* **165**, 1107-1115 (2004).
215 Wolfman, N. M. *et al.* Activation of latent myostatin by the BMP-1/tolloid family of metalloproteinases. *Proc Natl Acad Sci U S A* **100**, 15842-15846 (2003).
216 Wozney, J. M. *et al.* Novel regulators of bone formation: molecular clones and activities. *Science* **242**, 1528-1534 (1988).
217 McCroskery, S., Thomas, M., Maxwell, L., Sharma, M. & Kambadur, R. Myostatin negatively regulates satellite cell activation and self-renewal. *The Journal of cell biology* **162**, 1135-1147 (2003).
218 Tanaka, K. K. *et al.* Syndecan-4-expressing muscle progenitor cells in the SP engraft as satellite cells during muscle regeneration. *Cell stem cell* **4**, 217-225 (2009).

11 DECLARATION

"I declare that I have completed this dissertation single-handedly without the unauthorized help of a second party and only with the assistance acknowledged therein. I have appropriately acknowledged and referenced all text passages that are derived literally from or are based on the content of published or unpublished work of others, and all information that relates to verbal communications. I have abided by the principles of good scientific conduct laid down in the charter of the Justus Liebig University of Giessen in carrying out the investigations described in the dissertation."

Date 20-06-14 Piera De Gaspari

12 APPENDIX

12.1 Acknowledgments

I would like to express my gratitude to Prof. Dr. Dr. Thomas Braun for providing me the opportunity to perform this work in his department and Dr. Shizuka Uchida as my mentor, for his continuous support during these years and his help in writing this thesis. I want to thank also Prof Dr. Dorrestejin as my second supervisor in the university

Special thanks are going to all the people I met in these years, supporting and sharing this experience all important in their own way to help me to reach this goal

All my lab members Mizue, Yuliya, Ayca and David, Pascal for his informatic tips and in particular Katharina with whom I shared bench & desk thank you for your support and help in all the situations.

Thanks to all the colleagues of the Max Planck that make working in the lab easier and more fun: Kathy, Dani, Alex, Janine, Judith, Johannes, Tanja, Jian, Ettore, Angelina, Stas, Ting, Mareike, Christian, Polina, Janine, Luca, Akis, Shuici, Stephan, Sonja, Susanne, Katja, Moni, Susanne, Marianne, Peter, Nina

Matthew, Megan and Auntie Angela for having the best English in the world, thank you guys for your help and corrections

André Schneider´s lab in particular Jiwen for using their inconsumable and perfect PUK

Johnny to improve my presentation skills, thanks to your challenges, it was helpful & fun

Isabelle&Birgit thank you girls for all your help with my crazy mice and your support

Krishna for our incomprehensible chats ending always in understanding each other

Dine, Vera, Nikki & Buddy-Michael thank you because you were always there for me and helping me in all most critical moments and of course, without you this thesis had no German abstract

Jennifer to be so great and reliable in her job, you take care of my mice in a wonderful way

Marion for cardiomyocytes isolation and for the nice time spent in S2 lab together laughing about our “Schweiz käse”

Sawa and all my “Mädels” in Groedelhaus: Beate, Brigitte and Renate thanks to be so nice and kind with me and Kerstin for antibodies, FACS support and more

Marina, Elisabetta & Diya to share all troubles and funny moments

Carmen without whom all this thesis was not happening, THANK YOU for sharing with me your knowledge, your time, your positivity and your jokes

Brady-Ale with whom I started this adventure, sharing good and bad moments, THANK YOU to all the effort you put to rewrite this thesis with me, trying to teach me the "comma rule" and "ing" form (no hope), thanks to be how you are and for showing me what means having a real passion for this job

Special thanks to people I met in Giessen and became good friends and important person in my life: Katharina & Peter to be great flatmates and friends, their patience and their help in teaching me the correct German and all the Van Wickeren family. Anna &Frank, Kati for their support. Regi & Antonio and all the Finger-Medebach family, to always help me in all possible situations, take care of me and make me always feel part of the family. My super tipi-topi flatmates Kate (&Römer family) and Corinna you are amazingggg girlssssss
All my "Mädels" in the ballet schüle Tanz A Studio, to make me not think, at least once per week, about work in particular thanks to Andrea and to my teacher Fely Ruytinx to be able to motivate and giving me always good energy and strength.
To all the people that for sure I forgot to mention (Alzheimer is cominggggg), people I met during these years and in their own way they left something in me

I cannot forget all the important people I left in Italy and their precious support
All my friends and all my family THANKS to be always there to give me the motivation to go on, for your support and for listening all my problems, to help me to become the person who I am today. I will never be able with words to express all my gratitude to you guys:
Ly&Ettore, Ire&Matteo, Claudia, Ale&Lux, Elisa-Sisú, my "forever mentor" Alessandra, Ca´, Marty&Luca, Marta&Andrea, Vale, Aly, Elisa Borin, Sara, Marco, Alessandro, Antonia, Vanessa, Laura, Carlotta, Marco&Francesca, my Karolinka, Ely&Carlo. My little ones Nicolo´, Elena, Vittoria, Linda, Arianna to be so cheerful and lovable
My mum Mariella, my dad Marino, my uncle Giampaolo, my uncles and aunties and cousins (Vera, Claudio, Giacomo, Valter, Morena, Ludovica, Gabriella, Andrea, Cristiano……)
My wonderful & incredible brother Cesare always the one giving me the best advice. And finally to my grandparents and Andrea, wherever you are I hope I could make you proud of me.

This work is dedicated to all of you, because all of you contribute to a piece of it!

12.2 Curriculum Vitae

The curriculum vitae was removed from the electronic version of the paper.